Titre: Title:	Development of theory of periodic sequence
Auteur: Author:	Guifu Gong
Date:	2004
Type:	Mémoire ou thèse / Dissertation or Thesis
Référence: Citation:	Gong, G. (2004). Development of theory of periodic sequence [Mémoire de maîtrise, École Polytechnique de Montréal]. PolyPublie. https://publications.polymtl.ca/7389/

UNIVERSITÉ DE MONTRÉAL

DEVELOPMENT OF THEORY OF PERIODIC SEQUENCE

GUIFU GONG
DÉPARTEMENT DE GÉNIE ÉLECTRIQUE
ÉCOLE POLYTECHNIQUE DE MONTRÉAL

MÉMOIRE PRÉSENTÉ
POUR APPROBATION DU SUJET DE RECHERCHE DANS LE CADRE
DU DIPLÔME DE MAÎTRISE ÈS SCIENCES APPLIQUÉES
(GÉNIE ÉLECTRIQUE)
DECEMBRE 2004

Your file Votre référence
ISBN: 0-494-01332-X
Our file Notre référence
ISBN: 0-494-01332-X

UNIVERSITÉ DE MONTRÉAL

ÉCOLE POLYTECHNIQUE DE MONTRÉAL

Ce mémoire intitulé:

DEVELOPMENT OF THEORY OF PERIODIC SEQUENCE

présenté par: Guifu GONG

en vue de l'examen oral pour l'approbation du sujet de recherche

dans le cadre du diplôme de : Maîtrise ès Sciences Appliquées

a été dûment accepté par le jury d'examen constitué de :

M. BOSISO Renato G, M.Sc.A., Président

M. WU Ke, Ph. D., membre et directeur de recherche

M. KASYHAP Raman, Ph. D., membre

To my family and my friends,

Thanks for everything.

ACKNOWLEDGEMENT

First of all, I would like to express my deep gratitude to my director, Professor Ke Wu, for his guidance with my Master's research. His invaluable advice, inspiring ideas and financial support gave me the courage to complete my research and to finish this thesis.

I am very grateful to the members of my committee, Professor Renato G. Bosisio and Professor Raman Kashyap for their suggestions and review of this thesis.

I would like to thank Dr Feng Xu, member of our research group, for his valuable advice and ideas for my research work.

Thanks to all of my professors and my laboratory colleagues for their help and friendship.

Finally, I would like to thank my wife for her support and courage during my research.

RÉSUMÉ

Le présent mémoire démontre les principales facettes de la théorie de séquence périodique proposée par le Professeur Ke Wu. Cette théorie est appliquée à la théorie des champs et à la théorie des circuits pour les calculs numériques. Il s'agit d'une analyse ni dans le domaine temporel, ni dans le domaine fréquentiel. Il s'agit d'une nouvelle théorie et méthode. Les caractéristiques de cette théorie sont les suivantes :

1. Elle donne des solutions analytiques de champs électromagnétiques. Ce sont des solutions analytiques, discrètes et simplement calculables.
2. L'autre caractéristique est que les valeurs propres d'une matrice peuvent décrire des caractéristiques de propagation d'onde.
3. La simulation est simple et précise. L'erreur est petite et contrôlable.

L'idée de base de cette théorie est que la réponse est périodique si l'excitation est périodique dans un système linéaire. Après la discrétisation, la structure périodique peut être exprimée par une matrice. Ensuite, le système devient un système couplé et discret. Il peut être découplé par une transformation. Puis, il devient un système simple et résolvable.

Parmi les applications de la théorie de Ke Wu dans la théorie des champs, ce mémoire étudie les équations de Maxwell sans source. Il dérive les équations d'ondes ou équations de Helmholtz. Il démontre la relation entre le nombre d'onde et les valeurs propres d'une matrice de constantes qui dépendant seulement d'un nombre donné. Il donne aussi l'autre relation entre les valeurs propres et la fréquence de coupure du guide d'ondes rectangulaires. Ces formules démontrent qu'il y a des relations parmi les valeurs propres et les paramètres des micro-ondes. À guise d'exemple, les résultats sont appliqués à des guides d'ondes. Il étudie des ondes de surface de plaques diélectriques (a grounded dielectric slab) en utilisant des conditions différentes. Ces résultats peuvent être appliqués à d'autres guides d'ondes, à des lignes micro rubans, etc.

L'autre application de cette théorie s'applique aux lignes de transmission dans la théorie des circuits. Les cas avec et sans pertes des lignes de transmission sont étudiés séparément. Le cas sans pertes ne peut pas être utilisé dans le cas avec pertes parce qu'ils impliquent des conditions différentes. Dans le cas sans pertes, cette théorie est appliquée aux équations des télégraphistes. Elle donne les solutions analytiques et discrètes de tension et de courant. Les constantes sont déterminées avec des conditions à l'infini. La condition de convergence est donnée. En guise d'exemple, il montre les courbes de la théorie et de la nouvelle méthode.

Dans le cas avec pertes, cette nouvelle théorie est appliquée à des lignes de transmission. Les solutions analytiques et discrètes sont données en utilisant la théorie analytique et algébrique. Des constantes sont déterminées par des conditions différentes. Les conditions de convergence et de signaux complets à la sortie sont données par la longueur de l'intervalle de temps et le nombre de partitions. Par exemple, ils étudient les influences de paramètres tels que le nombre de partitions, la position z, la résistance et la conductance.

Il sera question aussi des les paramètres caractéristiques des lignes de transmission. Les calculs de l'impédance caractéristique, du coefficient de réflexion et de l'impédance d'entrée et VSWR sont présentés. On peut aussi montrer les solutions de la tension et du courant à l'entrée et à la sortie. Les adaptations au générateur et à la charge sont discutées.

Ce mémoire est juste une introduction à la théorie de Ke Wu. Il y a beaucoup de travail à faire afin de poursuivre cette recherche.

Mots Clés : Électromagnétisme, micro-onde, séquence périodique, équation de Maxwell, équation de téléphoniste, équation de Helmholtz, ligne de transmission, computation numérique, valeur propre, guide onde.

ABSTRACT

This thesis presents the development of periodic sequence theory of Ke Wu. This theory is neither in the time domain analysis nor in the frequency domain analysis. This theory and its method can be applied to a very wide domain such as field theory and circuit theory for numerical computations. The characteristics of this theory are as follows:

1. It gives the analytical solutions to problems. These solutions are discrete and simply calculable.
2. Another characteristic is that the eigenvalues of a matrix can describe the characteristics of wave propagation.
3. The simulation is simple and accurate. The error is very small and controllable.

The basic hypothesis of this theory is that the response is periodical if the excitation is periodical and the system is linear. After discretization, this periodic structure can be expressed by a matrix. Thus the system becomes coupled and discrete. It can be decoupled through transformations. It then becomes a decoupled and resolvable system.

As an application of Wu's theory in field theory, this thesis studies the Maxwell equations without source. It derives the wave equations, that is, Helmholtz wave equations. It shows the relation between the traditional wavenumber and the eigenvalues of a constant matrix which only depends on a given number. It also gives another relation between the eigenvalues and the cutoff frequency of a rectangular waveguide. These formulas suggest that there are relations amongst the eigenvalues and the other microwave parameters. As examples, the results are used for a rectangular waveguide and a ground dielectric slab waveguide by setting different boundaries conditions. These results can be applied to other waveguides, to micro-strips, etc.

Another application of this theory is related to transmission lines in circuit theory. The lossless case and lossy case of transmission lines are studied separately. The lossless case can't be used in the lossy case because they have different conditions. In the lossless case, this theory is applied to telegraph equations. It obtains the discrete and

analytic solutions of voltage and current. The constants are determined with the conditions at infinity. The condition of convergence is obtained. As an example, the curves of both the theory and this new method will be shown.

In the second case, this new theory is used for lossy transmission lines. The analytical and discrete solutions are given by using analytic and algebraic theory. The constants are determined by changing conditions at infinity. The conditions of convergence and complete signal output are given by the interval length Δt of partitions on time and the number of partition. As examples, the influences of parameters such as the number of partitions, the point z, the resistance and the conductance are studied.

I shall discuss the characteristic parameters of transmission lines. The calculus of characteristic impedance, deflexion coefficient and input impedance and VSWR are presented. The solutions of voltage and current at input port and load port are also shown. The load matching is discussed.

This thesis is just an introduction to Ke Wu's theory. His ideas and thoughts are so rich that I can only express a small portion of them. Further research will take place in the future.

Key words: Electromagnetism, microwave, Periodic sequence, Maxwell equation, telegraph equation, Helmholtz equation, transmission line, numerical computation, eigenvalue, waveguide

CONDENSÉ EN FRANÇAIS

DÉVELOPPMENT DE THÉORIE DE SEQUENCE PÉRIODIQUE

Ce mémoire présente la théorie de séquence périodique du professeur Ke Wu. Il s'agit d'une nouvelle théorie. Il ne s'agit ni d'une analyse dans le domaine temporel, ni dans le domaine fréquentiel. Cette analyse peut être appliquée à la théorie des champs et à la théorie des circuits pour calculs numériques.

0.1 Applications de la nouvelle théorie à la théorie de champs

L'hypothèse de base de cette théorie est que la réponse est périodique si l'excitation est périodique et le système est linéaire. Le Professeur Ke Wu utilise cette idée pour discrétiser des équations de Maxwell. La séquence périodique correspond à une matrice circulante. Les équations de Maxwell sans source peuvent être approximées par

$$\nabla \times \vec{E} = \frac{\mu}{d} D^t \vec{H} \tag{0.1}$$

$$\nabla \times \vec{H} = \frac{\varepsilon}{d} D \vec{E} \tag{0.2}$$

où D est une matrice de constante. Puis, Ke Wu fait les transformations suivantes

$$\vec{E} = T_e \vec{e} \tag{0.3}$$

$$\vec{H} = T_h \vec{h} \tag{0.4}$$

où T_e et T_h sont les matrices des transformations. Dans le domaine transformé, on a

$$\nabla \times \nabla \times \vec{e} = \frac{\mu\varepsilon}{d^2} M \vec{e} \tag{0.5}$$

$$\nabla \times \nabla \times \vec{h} = \frac{\mu\varepsilon}{d^2} M \vec{h} \tag{0.6}$$

où M est une matrice réelle et symétrique. Les variables sont couplées dans ces équations. En utilisant la théorie algébrique, on peut diagonaliser la matrice M en choisissant T_e et T_h. Et puis, on obtient les équations indépendantes

$$\begin{cases} \nabla\times\nabla\times\vec{e} = \dfrac{\mu\varepsilon}{d^2}\lambda^2\vec{e} \\ \nabla\times\nabla\times\vec{h} = \dfrac{\mu\varepsilon}{d^2}\lambda^2\vec{h} \end{cases} \tag{0.7}$$

où λ est une matrice diagonale. Ce système représente la propagation d'ondes. Ensuite, on peut démontrer que le système d'équations (0.7) correspond aux équations de Helmholtz qui sont indépendantes et ainsi résolvables.

Des équations en composants pour les Modes TM, TE et TEM sont présentés. Les solutions des ondes planaires sont obtenues.

Il aussi présente la relation entre les valeurs propres et le nombre d'onde.

Comme applications de ce système, elles sont appliquées à un guide d'ondes rectangulaire et aussi étudié les ondes surface de plaques diélectriques (grounded dielectric slab).

0.2 Applications de la nouvelle théorie à la théorie de circuits

Une application de la nouvelle théorie est la théorie des circuits. Ce mémoire démontre les applications pour des lignes de transmission. Les cas avec et sans pertes des lignes de transmission sont étudiés séparément. Dans le cas sans pertes, on dérive les équations des télégraphistes en utilisant cette méthode. Et puis, les constantes doivent être déterminées à l'aide des conditions initiales. La condition de convergence est présentée. Les courbes de la théorie et de la nouvelle méthode sont présentées.

Dans le cas avec pertes, les équations des télégraphistes avec pertes sont des équations couplées et discrètes. En utilisant les transformations, elles deviennent découplées et résolvables. Les solutions sont trouvées pour des constantes arbitraires. Les constantes arbitraires sont déterminées par les conditions à l'infini. Les résultats des lignes de transmission sans pertes ne sont pas un cas particulier du cas avec pertes. Ils donnent aussi la condition de convergence. Ils montrent les relations parmi le nombre de partitions ou la longueur de l'intervalle de temps, le point z, la résistance et la conductance. Ils étudient l'effet de la position sur la propagation d'onde, l'effet de

changement de la résistance et de la conductance. Dans tous les cas, on compare les courbes de la nouvelle méthode avec celles de la théorie.

Les paramètres caractéristiques des lignes de transmission sont définis. Les calculs de l'impédance caractéristique, du coefficient de réflexion, de l'impédance d'entrée et du T.O.S. sont présentés. On montre aussi les solutions de la tension et du courant à l'entrée et à la sortie. Les adaptations au générateur et à la charge sont discutées.

La nouvelle méthode est caractérisée par son efficacité, sa simplicité et sa rigueur. L'erreur est très petite et peut être contrôlée. La convergence est rapide par rapport aux méthodes traditionnelles, telles que la méthode spectrale, la méthode du domaine temporel de la différence finie (FDTD), la méthode des moments, etc. Cette théorie aura beaucoup d'applications dans le domaine de micro-ondes et du génie.

Contents

DEDICATION ..... **iv**

ACKNOWLEDGEMENTS ..... **v**

RÉSUMÉ ..... **vi**

ABSTRACT ..... **viii**

CONDENSÉ EN FRANÇAIS ..... **x**

CONTENTS ..... **xiii**

LIST OF FIGURES ..... **xvii**

LIST OF TABLES ..... **xix**

LIST OF SYMBOLS AND ABBREVIATIONS ..... **xix**

Chapter 1 Introduction and Overview 1

1.1 Origin of periodic sequence theory 1

1.2 Theory of periodic sequence 1

1.3 Development of periodical sequence theory 1

1.4 Overview of the computational methods 2

Chapter 2 Applications of Periodic Sequence Theory to Field Theory 9

2.1 Introduction 9

2.2 Theory of Periodic Sequence 9

2.2.1 Discretization 9

2.2.2 Transformations 10

2.2.3 Diagonalization 12

2.3 Standard forms 13

Chapter 3 General TEM, TE and TM Waves 14

3.1 The wave equations 14

3.2 TEM waves 15

3.3 TE waves 16
3.4 TM waves 17
3.5 Solutions of General plane waves 18
3.6 Wavenumber and eigenvalues 22
3.7 Variance of electric field in t 23

Chapter 4. Rectangular Waveguide 24

4.1 Introduction 24
4.2 TM modes 25
4.3 TE modes 26
4.4 Cutoff frequency 27
4.4.1 Elliptical conditions 27
4.4.2 Relation of cutoff frequencies between original fields and transformed fields 28
4.4.3 An example 30
4.4.4 Convergence on N 31

Chapter 5 Applications of Periodic Sequence Theory to Circuit Theory: Lossless Transmission Lines 32

5.1 Introduction 32
5.2 Application of new theory to lossless transmission lines 33
5.3 Solution of telegraph equations 35
5.3.1 The form of solutions 35
5.3.2 The relation between $\vec{a}_k$ and $\vec{b}_k$ 35
5.3.3 Determining $\vec{a}_k$ 36
5.4 Convergence on the number N of partitions 36
5.5 Wave propagation of the lossless transmission lines 37

Chapter 6 Applications of Periodic Sequence Theory to Circuit Theory: Lossy Transmission Lines 39

6.1 Introduction 39

6.2 Applications of new theory to telegraph equations 40

6.3 Solutions of telegraph equations 43

6.4 The relation between complete signals and N 45

6.5 Numeric computations and convergence 52

6.5.1 The lossless case 52

6.5.2 The effect of position z on wave propagation 57

6.5.3 The convergence on N 62

6.5.4 The effect of R and G 65

Chapter 7 Characteristic Parameters of Transmission Lines 73

7.1 Characteristic impedance 73

7.2 Voltage and current expressed by input 74

7.3 Voltage and current expressed by output 74

7.4 Reflection coefficients 75

7.5 Input impedance 76

7.6 Voltage standing-wave ratio (VSWR) 77

7.7 Generator and load matches 77

Chapter 8 Grounded Dielectric Slab Waveguide 79

8.1 Introduction 79

8.2 TM Modes 79

8.3 TE Modes 83

CONCLUTION 88

BIBLIOGRAPHY 89

Appendix A 91

A.1 Linearly polarized waves 91
A.2 Wave shapes 91
A.3 Polarized plane waves 98

LIST OF FIGURES

Figure 4.1 Geometry of rectangular waveguide 24

Figure 4.2 Elliptic conditions of m_p, n_p and λ_p 27

Figure 4.3 Cutoff frequencies vs N 30

Figure 5.1 T-type equivalent circuit model of a lossless transmission line..... 33

Figure 5.2 Curve comparisons between theory and new method for periodic impulse 38

Figure 6.1 T-type equivalent circuit model of a transmission line 40

Figure 6.2 The case of N=20 < 134 46

Figure 6.3 The case of z=50mm and N=100 < 134 47

Figure 6.4 The case of z=50mm and N=150 > 134 48

Figure 6.5 The case of z = 460mm and N=200 <667 49

Figure 6.6 The case of z=460mm and N=400 <667 50

Figure 6.7 The case of z=460mm and N=800 >667 51

Figure 6.8 The wrong use of the solution (6.31) by choosing R=G=0..... 53

Figure 6.9 The case of R= 1 nΩ and G=1nS 54

Figure 6.10 The case of R= 1nΩ and G=0 55

Figure 6.11 The case of R= 0 and G=1nS 56

Figure 6.12 The case of z = 0 and N=500 57

Figure 6.13 The case of z = 70mm and N=500 58

Figure 6.14 The case of z = 260mm and N=500 59

Figure 6.15 The case of z = 540mm and N=500 60

Figure 6.16 The case of z = 850mm and N=500 61

Figure 6.17 The case of N=100 and z=250mm 62

Figure 6.18 The case of N=300 and at point z=250mm 63

Figure 6.19 The case of N=500 at point z=250mm..... 64

Figure 6.20 The case of G=0.08S and $R = 10\Omega$ 65

Figure 6.21 The case of G=0.1S and $R = 10\Omega$ 66

Figure 6.22 The case of G=0.15S and $R = 10\Omega$ 67

Figure 6.23 The case of G=0.2S and $R = 10\Omega$ 68

Figure 6.24 The case of $R = 100\Omega$ and G=0.05S 69

Figure 6.25 The case of $R = 200\Omega$ and G=0.05S 70

Figure 6.26 The case of R=300 Ω and G=0.05S 71

Figure 6.27 The case of R=400 Ω and G=0.05S 72

Figure 7.1 A transmission line terminated by a load impedance Z_L 74

Figure 7.2 Transmission line circuit for mismatched load and generator 77

Figure 8.1 Geometry of a grounded dielectric slab 79

Figure 8.2 Graphical solution of the transcendental equation for the cutoff frequency of a TM mode with d=2mm, i=N/5 82

Figure 8.3 Graphical solution of the transcendental equation for the cutoff frequency of a TM mode with d=5 mm, i=N/2 83

Figure 8.4 Graphical solution of the transcendental equation for the cutoff frequency of a TM mode with d=2 mm, i=N/2 85

Figure 8.5 Graphical solution of the transcendental equation for the cutoff frequency of a TM mode with d=4 mm, i=N/2 85

Figure 8.6 Graphical solution of the transcendental equation for the cutoff frequency of a TM mode with d=8 mm, i=N/2 86

Figure A.1 Sinusoidal wave in E 92

Figure A.2 Another sinusoidal wave in E 93

Figure A.3 Distorted sinusoid I in E 94

Figure A.4 Distorted sinusoid II in E 95

Figure A.5 Distorted sinusoid III in E 96

Figure A.6 Square wave in E (N=10, z=0.001) 97

Figure A.7 Triangular wave E (N=10, z=0.001) 98

Figure A.8 Sinusoidal wave E with $\phi = 45^\circ$ 99

Figure A.9 Circularly polarized wave in E 100

LIST OF TABLES

Table 3.1 Calculation of k and $F(\vec{\Lambda})$ 23

Table 4.1 ..... Comparison of fc between both methods 29

LIST OF SYMBOLS AND ABBREVIATIONS

$\vec{E}$	the electric field intensity
$\vec{H}$	the magnetic field intensity
TE	transverse electric
TEM	transverse electromagnetic
TM	transverse magnetic
ε	the permittivity
μ	the permeability
∇	the gradient $\frac{\partial}{\partial x}\hat{x}+\frac{\partial}{\partial y}\hat{y}+\frac{\partial}{\partial x}\hat{z}$

CHAPTER 1

INTRODUCTION AND OVERVIEW

1.1 Origin of the periodical sequence theory

About ten years ago, Professor Ke Wu had an idea for the establishment of a new theory of computational electromagnetism. Neither in time domain nor in frequency domain, it is a discrete numeric method that can be applied to any system with a periodic response when it is excited by a periodic input. The basic work of this theory has been done by Professor Wu.

This new theory is not only suitable to field theory, but also suitable to circuit theory.

1.2 Theory of periodic sequence

As the excitation is periodic, in a linear system, the response is periodic too. This idea is applied to second order linear equations of electromagnetic fields. The periodicity can be expressed as a circulant matrix. Then by means of the transformations, the coupling equations are decoupled in the process of the diagonalization. Finally, we obtain the decoupled equations. We call these equations a standard form. This idea and method is applied to both the theory of fields and the theory of circuits in this thesis.

In Chapter 2, we present this new theory. Maxwell's equations are taken as a model for applications of this theory in solving the problems of electric and magnetic fields. The original idea of this theory contains the process of the discretization, the transformations and the diagonalization. It derives the standard forms of decoupled equations. These standards can be used in many boundary problems.

1.3 Development of the periodic sequence theory

Chapter 3 presents general TEM, TE and TM waves. It introduces the product operation of two vectors which is used in Matlab. We obtain the wave equations expressed in components as well as the solutions of general plane wave. The relationship

between the traditional wavenumber k and the eigenvalues are obtained. Hence we can calculate the wavenumber from the eigenvalues.

We apply these results to rectangular waveguide in Chapter 4. As a result, the solutions of electric and magnetic fields in TM and TE modes are obtained, as well as a formula to calculate the cutoff frequency from the eigenvalues.

In Chapters 5 and 6, we apply the theory to analyze circuit. In Chapter 5, we apply this theory to lossless transmission lines. The analytic solutions of standard telegraph equations are presented and the relationship of the coefficients is analyzed. The accuracy of this numerical method is verified by comparing the voltages of a lossless transmission line obtained from the theoretical analysis and from calculations using the new theory. In Chapter 6, we study lossy transmission lines. The discussions of solutions are presented. The minimum number (N) of partitions is presented for complete wave and convergence. Many examples are given to find the influences exerted by the resistance R, the conductance G, the position z, and N in the calculations when using this method. Dr Xu F. found that the matrix is circulant. I used his discovery in my research for diagonalisation.

Chapter 7 discusses the characteristic parameters of transmission lines. The calculations of characteristic impedance, deflexion coefficient and input impedance and VSWR are presented. We also show the solutions of voltage and current at the input port and the load port followed by a discussion of the load matching and generator matching.

The ground dielectric slab waveguide is studied in Chapter 8. We obtained the solutions for TE modes and TM modes. We also discuss the solution of the transcendental equation for the cut-off frequency of both TM and TE modes.

1.4 Overview of the computational methods

Numerical computation plays a very important role in engineering. It is applied in many fields of the industry. The following eight examples are some of the most contemporary and emerging applications of numerical computation.

- radar-guide missile.

The problem lies in the interactions between the missile seeker's horn antenna and randomly generated errors in the angular location of a target.

- high-speed computer circuit-board module,

The digital circuits can be upset at very high clock rates due to parasitic coupling between signal paths.

- high-speed computer multi-chip module

The problem is to find the inductance of a complex MCM power distribution system.

- Microwave amplifier

The problem is with the linear and non linear characters of a 6-GHz amplifier.

- Cellular telephone

The problem is to design a cellphone which meets the safety standards for microwave exposure.

- Optical microdisk resonator

The problem is to discern how photonic integrated circuits are best used by these elements for ultrafast all-optical switching of signals based upon their wavelength.

- Photonic bandgap microcavity laser

People want to design the world's smallest laser sources based on PBG structures.

- Colliding spatial solitons

The project is to build the world's fastest all-optical switches with ordinary glass.

The modeling of microwave structures has been growing rapidly in the past few decades. It ranges from increasing various operating frequencies to reducing the design cycle. The accomplishing growth was made in numeric theory and computation. People often use two analysis methods to solve the problems of fields and circuits. One is Time Domain Analysis (TDA), another is Frequency Domain Analysis (FDA). Now we shall review both of them.

Finite difference method (FDM)

The finite difference method was first developed by A. Thom [1] in the 1960s. The FDM [2] is an old and popular method in numerical computation. This method is known to be simple and basic and it is applied in many domains to solve different problems.

The idea is to calculate the new values from previous ones by means of the Taylor series.

$$\phi(x_n + h) - \phi(x_n) = \phi'(x_n)h + \frac{1}{2!}\phi''(x_n)h^2 + \frac{1}{3!}\phi'''(x_n)h^3 + O(h^4)$$

$$\phi(x_n - h) - \phi(x_n) = -\phi'(x_n)h + \frac{1}{2!}\phi''(x_n)h^2 - \frac{1}{3!}\phi'''(x_n)h^3 + O(h^4)$$

Adding two equations, we can obtain

$$\phi(x_n) = \frac{\phi(x_n + h) + \phi(x_n - h)}{2} + \phi''(x_n)h^2 + O(h^4)$$

Hence

$$\phi(x_n) = \frac{\phi(x_n + h) + \phi(x_n - h)}{2} + O(h^2)$$

This is a second order of h. If the length of step h is small, it has a small error. In fact, the error is $O(h^2)$.

In general, the FDM has three steps:

(1) dividing the region of problems into a grid of nodes

(2) approximating the given differential equation using finite difference

(3) solving the difference equations subject to the prescribed initial conditions or boundary conditions.

The FDM has three types of differences: *the forward-difference, the back-ward difference, the central-difference.* The errors of the forward-difference and the backward-difference are first order. The central-difference error is second order.

Finite element method (FEM)

The finite element method [3]-[5] is a method similar to the finite difference method. The FEM has its origin in the field of structural analysis, but it has some advantages. FEM has been employed in diverse areas such as waveguide problems, electric machines, semiconductor devices, microstrips, and absorption of EM radiation. It can help solve problems with flexible features. The functional and variation expressions are applied to the region under consideration. The small segments are polygons. Usually, they are triangles or rectangles depending on whether they are two-dimensional

problems or three-dimensional problems, respectively. This method is flexible to sub-region which may be more or less polygons depending on the problems.

This method is very popular in electrical and magnetic field computations and mechanics in which the electrical field and the force are not homogenate. Lately, the boundary element method has been proposed. It uses the boundary integral equation and the discrete technique.

To apply FEM involves four steps:

(1) discretizing the region into some subregions

(2) deriving governing equations for a typical element

(3) assembling all elements in whole region

(4) solving the equations

Although the finite difference method and the method of moments are conceptually easier to program than the finite element method, FEM is a more powerful and versatile numerical technique. It is more useful for handling problems involving complex geometries and inhomogeneous media. This method makes it possible to construct a general-purpose computer program for solving a wide range of problems.

TLM method

The TLM method [6][7] converts the field problem to a three dimensional equivalent network problem. In this method the region or space is discretized into a two or three-dimensional lattice. The field components are represented by a hybrid TLM cell. The boundaries correspond to the electric wall and magnetic wall by short-circuited shunt nodes and open-circuited shunt nodes. The magnetic and dielectric materials are introduced by adding short or open-circuited series to the stub of half length of step at the series or shunt nodes. It can represent the loss by resistively loading the shunt nodes. The frequency response can be obtained by the Fourier transform.

In general, the TLM method involves two basic steps:

(1) Replacing the field problem by an equivalent network and deriving analogies between the field and network quantities.

(2) Solving the equivalent network

The structures of TLM are quite varied. Due to the introduction of periodic structures, there is a typical passband-stopband phenomenon. This is one of several precautions.

Integral equation method

The integral equation method [8] uses the integral of unknown quantities on boundary. This is the form of an integral equation; it uses the Fourier transform to convert two-dimensional Helmholtz equation to one dimensional ordinary equation, and then to find the solution. The Green function can be found by two-dimensional inverse Fourier transform. The variation method is used in it, too.

Method of moments (MOM) and Galerkin's method

Many electromagnetic problems can be stated in terms of an inhomogeneous equation

$$L\phi = g$$

where L is a differential and integral operator and g is an excited source. The MOM is a general procedure for solving this kind of equation.

The MOM [9]-[11] is concerned with the integral equation method. The integral equation has the following form

$$\int_D G(r,r')f(r')dr' = \rho(r), r \in D$$

Where ρ is the excitation function and G is the Green function. The step functions are used as basis function to express f. It is also used in delta functions as testing functions. These very popular basis and testing functions were introduced by Galerkin. It is called Galerkin's method.

The general MOM procedure involves four steps:

(1) Derivation of the appropriate integral equation.

(2) Discretization of the integral equation into a matrix equation using basis functions.

(3) Evaluation of the matrix elements

(4) Solving the matrix equation

Mode-matching method (MMM)

The Mode-matching method [12][13] is used to solve the problem of discontinuity structures such as a waveguide. The mode-matching procedure first involves the expansion of unknown fields in the individual regions by using the known normal modes. The problems are turned to determine the modal coefficients. In general, it is impossible to find the exact solution. People use this approximate technique to find approximate solutions. This method is applied to solve for scattering problems and eigenvalue problems.

Method of lines (MOL)

The method of lines [14][15] is similar to the finite difference method. In this method, the physical structure of two or three-dimensions is discretized for numerical computations while the analytical expressions are determined in the other dimension. This method has the advantage of giving discrete analytical solutions. MOL[16]-[18] has many advantages such as computational efficiency, numerical stability, and reduced programming effort and time.

To apply MOL, in general, involves the following five steps:

(1) partition of the region into layers.

(2) discretization of the differential equation in one dimension.

(3) transformation to obtain decoupled ordinary differential equations

(4) using inverse transform and initial or boundary conditions

(5) solution of equations

Spectral domain method (SDM)

The spectral domain method [19]-[11] is known as the Fourier transform version. The hybrid fields can be found from two potentials which are associated with electrical and magnetic components. Using Fourier transform, the problem is converted to spectral domain with structure conditions to find solutions. Then use inverse Fourier transform to obtain the solutions.

Finite-Difference Time-Domain method (FDTD)

The Finite-Difference Time-Domain method [22]-[24]is used to solve Maxwell's equations for phenomena of electromagnetic waves. Yee [22] in 1966 first employed a

uniform mesh of space having rectangular unit cells to approximate the surface of the structural feature. There has been great progress since the 1970s; Taflove and Brodwin [23][24] obtained the correct numerical stability criterion for Yee's algorithm. This method is efficient for a large structure. It uses iteration for the computation of the field. FDTD does not use linear algebra. The error in FDTD can be bounded to permit accurate models for a large variety of electromagnetic wave iteration problems. The FDTD can treat nonlinear problems. But this method requires a large random access memory. So it usually demands a powerful computer.

The FDTD is very popular today and there are lot of people working on it. After Yee and Taflove's works, Holland, Kunz and Lee applied Yee's algorithm to EMP problems [25][26]. Then Taflove coined the FDTD acronym and published the first validated FDTD models of sinusoidal steady state electromagnetic wave penetration into a three-dimensional metal cavity [27][28][30] etc.

Conclusion

In general, all of the above methods have advantages and disadvantages. Some of them are simple, and cannot easily solve complicate problems, while others are complex. The methods of time domain analysis are not easy to realize because they involve a large amount of computations, they require a high CPU and substantial memory. The frequency domain techniques present difficulties and tradeoffs. They are not very accurate, and they must calculate each frequency point in a band for spectral analysis. It is impossible to do so for a large band of frequency.

CHAPTER 2

APPLICATIONS OF PERIODIC SEQUENCE THOERY TO FIELD THOERY

2.1 Introduction

In this chapter, Maxwell's equations without source are taken as a model for the theory of periodic sequence. We shall demonstrate this new theory through the process of discretization, transformation, diagonalization, and solutions.

The system hypothesis is that, in the linear system, the response is periodic if the excitation is periodic. This is the theoretical basis of periodic sequence theory.

2.2 Theory of periodic sequence

We shall show the theory of periodic sequence in three steps: discretization, transformation and diagonalization.

2.2.1 Discretization

Maxwell's equations in lossless, without current source, homogenate, and isotropic medium are expressed as

$$\nabla \times \vec{E} = -\mu \frac{\partial \vec{H}}{\partial t}, \tag{2.1a}$$

$$\nabla \times \vec{H} = \varepsilon \frac{\partial \vec{E}}{\partial t}. \tag{2.1b}$$

where $\vec{E}, \vec{H}, \mu$ and ε are the electric field intensity, the magnetic field intensity, the permeability and the permittivity, respectively. We use the method of lines and the differences divided by time, and denote the length of partition interval as d. Then, rewrite (2.1). The discrete forms of Maxwell's equations can be obtained:

$$\nabla \times \vec{E} = \frac{\mu}{d} D^t \vec{H} + O(d), \tag{2.2a}$$

$$\nabla \times \vec{H} = \frac{\varepsilon}{d} D\vec{E} + O(d), \tag{2.2b}$$

where N is the number of lines within a period, T is the period of excitation, the superscript t in the D^t is the transpose of D and D is defined by

$$D = \begin{bmatrix} -1 & 1 & & \\ & \ddots & \ddots & \\ & & \ddots & 1 \\ 1 & & & -1 \end{bmatrix}. \tag{2.3}$$

Omitting the terms of O(d) from (2.2), we can be obtain the nice approximate equations:

$$\nabla \times \vec{E} = \frac{\mu}{d} D^t \vec{H}, \tag{2.4a}$$

$$\nabla \times \vec{H} = \frac{\varepsilon}{d} D\vec{E}. \tag{2.4b}$$

2.2.2 Transformations

We use the transformations to electric and magnetic fields as

$$\vec{E} = T_e \vec{e}\,, \tag{2.5a}$$

$$\vec{H} = T_h \vec{h}\,. \tag{2.5b}$$

Let

$$P = \begin{bmatrix} 2 & -1 & 0 & \cdots & 0 & -1 \\ -1 & 2 & -1 & \cdots & 0 & 0 \\ 0 & -1 & 2 & \cdots & 0 & 0 \\ & & & \cdots & & \\ 0 & 0 & 0 & \cdots & 2 & -1 \\ -1 & 0 & 0 & \cdots & -1 & 2 \end{bmatrix}. \tag{2.6}$$

The rotations of $\vec{e}$ and $\vec{h}$ in the following demonstration can be obtained by using (2.2) and (2.5):

$$\nabla \times \vec{e} = \nabla \times (T_e^t \vec{E})$$

$$= T_e^t (\nabla \times \vec{E})$$

$$= \frac{\mu}{d} T_e^t D^t \vec{H} + O(d)$$

$$= \frac{\mu}{d} T_e^t D^t T_h \vec{h} + O(d)$$

$$= \frac{\mu}{d} \delta^t \vec{h} + O(d). \qquad (2.7)$$

Let I_N be the identity matrix. By using $T_h T_h^t = I_N$, we obtain

$$\nabla \times \vec{h} = \nabla \times (T_h^t \vec{H})$$

$$= T_h^t (\nabla \times \vec{H})$$

$$= \frac{\varepsilon}{d} T_h^t D \vec{E} + O(d)$$

$$= \frac{\varepsilon}{d} T_h^t D T_e \vec{e} + O(d)$$

$$= \frac{\varepsilon}{d} \delta \ \vec{e} + O(d), \qquad (2.8)$$

where $\delta = T_h^t D T_e$. Neglecting O(d), the formulas (2.7) and (2.8) can be simplified as follows

$$\nabla \times \vec{e} = \frac{\mu}{d} \delta^t \vec{h}, \qquad (2.9a)$$

$$\nabla \times \vec{h} = \frac{\varepsilon}{d} \delta \vec{e} . \tag{2.9b}$$

2.2.3 Diagonalization

Using formulas (2.5) and (2.9) and omitting the term $O(d)$, we can obtain:

$$\nabla \times \nabla \times \vec{e} = \nabla \times \frac{\mu}{d} \delta^t \vec{h}$$

$$= \frac{\mu}{d} \delta^t \nabla \times \vec{h}$$

$$= \frac{\mu\varepsilon}{d^2} \delta^t \delta \vec{e} , \tag{2.10a}$$

and

$$\nabla \times \nabla \times \vec{h} = \nabla \times \frac{\varepsilon}{d} \delta \vec{e}$$

$$= \frac{\varepsilon}{d} \delta \nabla \times \vec{e}$$

$$= \frac{\mu\varepsilon}{d^2} \delta\delta^t \vec{h}. \tag{2.10b}$$

Simply, it can be written as such

$$\nabla \times \nabla \times \vec{e} = \frac{\mu\varepsilon}{d^2} \delta^t \delta \vec{e} , \tag{2.11a}$$

$$\nabla \times \nabla \times \vec{h} = \frac{\mu\varepsilon}{d^2} \delta\delta^t \vec{h} . \tag{2.11b}$$

Since $\delta\delta^t = \delta^t\delta$, we only need to calculate $\delta^t\delta$:

$$\delta^t \delta = T_e^t P T_e = \lambda^2, \tag{2.12a}$$

$$\delta^t \delta = T_h^t P T_h = \lambda^2. \tag{2.12b}$$

We choose T_e as

$$T_e = (T_{epk}), T_{epk} = \sqrt{\frac{2}{N}} \sin \frac{(N+8pk)\pi}{4N}, \text{ p, k=1,2, ... , N.} \tag{2.13}$$

It is easy to show that T_e is an orthogonal matrix. Similarly we choose the orthogonal matrix T_h such that (2.12b) holds. We can obtain the eigenvalues

$$\lambda^2 = diag(\lambda_k), \lambda_k = 4\sin^2\left(\frac{k\pi}{N}\right), \; k = 1,2, \ldots, N. \tag{2.14}$$

Therefore, λ is a diagonal matrix.

2.3 Standard forms

We obtain the following standard form of decoupled equations

$$\begin{cases} \nabla \times \nabla \times \vec{e} = \dfrac{\mu\varepsilon}{d^2} \lambda^2 \vec{e} \\ \nabla \times \nabla \times \vec{h} = \dfrac{\mu\varepsilon}{d^2} \lambda^2 \vec{h} \end{cases}. \tag{2.15}$$

CHAPTER 3

GENERAL TEM, TE AND TM WAVES

3.1 The Wave Equations

In the Cartesian coordinate system, the first order formulas in (2.9) are equivalent to the following system of scalar equations:

$$\frac{\partial \vec{e}_z}{\partial y} - \frac{\partial \vec{e}_y}{\partial z} = \frac{\mu}{d}\delta^t \vec{h}_x, \tag{3.1a}$$

$$\frac{\partial \vec{e}_x}{\partial z} - \frac{\partial \vec{e}_z}{\partial x} = \frac{\mu}{d}\delta^t \vec{h}_y, \tag{3.1b}$$

$$\frac{\partial \vec{e}_y}{\partial x} - \frac{\partial \vec{e}_x}{\partial y} = \frac{\mu}{d}\delta^t \vec{h}_z, \tag{3.1c}$$

$$\frac{\partial \vec{h}_z}{\partial y} - \frac{\partial \vec{h}_y}{\partial z} = \frac{\varepsilon}{d}\delta \vec{e}_x, \tag{3.1d}$$

$$\frac{\partial \vec{h}_x}{\partial z} - \frac{\partial \vec{h}_z}{\partial x} = \frac{\varepsilon}{d}\delta \vec{e}_y, \tag{3.1e}$$

$$\frac{\partial \vec{h}_y}{\partial x} - \frac{\partial \vec{h}_x}{\partial y} = \frac{\varepsilon}{d}\delta \vec{e}_z, \tag{3.1f}$$

The equations in field components in (2.15) become the equations of Helmholtz:

$$\frac{\partial^2 \vec{e}_x}{\partial x^2} + \frac{\partial^2 \vec{e}_x}{\partial y^2} + \frac{\partial^2 \vec{e}_x}{\partial z^2} + \frac{\mu\varepsilon}{\mathrm{d}^2}\lambda^2 \vec{e}_x = 0, \tag{3.2a}$$

$$\frac{\partial^2 \vec{e}_y}{\partial x^2} + \frac{\partial^2 \vec{e}_y}{\partial y^2} + \frac{\partial^2 \vec{e}_y}{\partial z^2} + \frac{\mu\varepsilon}{\mathrm{d}^2}\lambda^2 \vec{e}_y = 0, \tag{3.2b}$$

$$\frac{\partial^2 \vec{e}_z}{\partial x^2}+\frac{\partial^2 \vec{e}_z}{\partial y^2}+\frac{\partial^2 \vec{e}_z}{\partial z^2}+\frac{\mu\varepsilon}{\mathrm{d}^2}\lambda^2 \vec{e}_z = 0, \tag{3.2c}$$

$$\frac{\partial^2 \vec{h}_x}{\partial x^2}+\frac{\partial^2 \vec{h}_x}{\partial y^2}+\frac{\partial^2 \vec{h}_x}{\partial z^2}+\frac{\mu\varepsilon}{\mathrm{d}^2}\lambda^2 \vec{h}_x = 0, \tag{3.2d}$$

$$\frac{\partial^2 \vec{h}_y}{\partial x^2}+\frac{\partial^2 \vec{h}_y}{\partial y^2}+\frac{\partial^2 \vec{h}_y}{\partial z^2}+\frac{\mu\varepsilon}{\mathrm{d}^2}\lambda^2 \vec{h}_y = 0, \tag{3.2e}$$

$$\frac{\partial^2 \vec{h}_z}{\partial x^2}+\frac{\partial^2 \vec{h}_z}{\partial y^2}+\frac{\partial^2 \vec{h}_z}{\partial z^2}+\frac{\mu\varepsilon}{\mathrm{d}^2}\lambda^2 \vec{h}_x = 0, \tag{3.2f}$$

3.2 TEM Waves

Transverse electromagnetic (TEM) waves are characterized by setting $\vec{\mathrm{e}}_z = \vec{\mathrm{h}}_z = 0$. We then obtain the following equations

$$\frac{\partial^2 \vec{e}_x}{\partial z^2}+\frac{\mu\varepsilon}{d^2}\lambda^2 \vec{e}_x = 0, \tag{3.3a}$$

$$\frac{\partial^2 \vec{e}_y}{\partial z^2}+\frac{\mu\varepsilon}{d^2}\lambda^2 \vec{e}_y = 0, \tag{3.3b}$$

$$\frac{\partial^2 \vec{h}_x}{\partial z^2}+\frac{\mu\varepsilon}{d^2}\lambda^2 \vec{h}_x = 0, \tag{3.3c}$$

$$\frac{\partial^2 \vec{h}_y}{\partial z^2}+\frac{\mu\varepsilon}{d^2}\lambda^2 \vec{h}_y = 0. \tag{3.3d}$$

The formulas in (3.3) are the equations of plane waves in a lossless medium (cf. David M. Pozar [29] p16). Comparing (3.3) to (3.2), we have

$$\frac{\partial^2 \vec{e}_x}{\partial x^2}+\frac{\partial^2 \vec{e}_x}{\partial y^2} = 0, \tag{3.4a}$$

$$\frac{\partial^2 \vec{e}_y}{\partial x^2} + \frac{\partial^2 \vec{e}_y}{\partial y^2} = 0, \tag{3.4b}$$

$$\frac{\partial^2 \vec{h}_x}{\partial x^2} + \frac{\partial^2 \vec{h}_x}{\partial y^2} = 0, \tag{3.4d}$$

$$\frac{\partial^2 \vec{h}_y}{\partial x^2} + \frac{\partial^2 \vec{h}_y}{\partial y^2} = 0. \tag{3.4e}$$

Using the Laplacian operator $\nabla_t^2 = \partial^2/\partial x^2 + \partial^2/\partial y^2$ in the two transverse dimensions and $\overline{e}(x, y) = \hat{x}\vec{e}_x + \hat{y}\vec{e}_y$, we obtain

$$\nabla_t^2 \overline{e}(x, y) = 0, \tag{3.5a}$$

$$\nabla_t^2 \overline{h}(x, y) = 0. \tag{3.5b}$$

The results (3.5) are well known as the Laplace equations in two transverse dimensions. It shows that the transverse electric and magnetic fields, $\overline{e}$ (x, y) and $\overline{h}$ (x, y), of TEM waves satisfy Laplace's equations (cf. David M. Pozar [29] p107).

For the wave impedance of the TEM mode, the ratio of k-th components of the transverse electric and magnetic fields is the following:

$$\frac{e_x^{(k)}}{h_y^{(k)}} = -\frac{\mu}{\varepsilon} \frac{\dfrac{\partial h_y^{(k)}}{\partial z}}{\dfrac{\partial e_x^{(k)}}{\partial z}}. \tag{3.6}$$

Integrating both sides of (3.6), we obtain the wave impedance of TEM:

$$Z_{TEM} = \left| \frac{e_x^{(k)}}{h_y^{(k)}} \right| = \left| -\frac{e_y^{(k)}}{h_x^{(k)}} \right| = \sqrt{\frac{\mu}{\varepsilon}}. \tag{3.7}$$

3.3 TE Waves

Transverse electric TE waves are characterized by $\vec{e}_z = 0$ and $\vec{h}_z \neq 0$.

$$-\frac{\partial \vec{e}_y}{\partial z} = \frac{\mu\delta^t}{d}\vec{h}_x, \tag{3.8a}$$

$$\frac{\partial \vec{e}_x}{\partial z} = \frac{\mu\delta^t}{d}\vec{h}_y, \tag{3.8b}$$

$$\frac{\partial \vec{e}_y}{\partial x} - \frac{\partial \vec{e}_x}{\partial y} = \frac{\mu\delta^t}{d}\vec{h}_z, \tag{3.8c}$$

$$\frac{\partial \vec{h}_z}{\partial y} - \frac{\partial \vec{h}_y}{\partial z} = \frac{\varepsilon\delta}{d}\vec{e}_x, \tag{3.8d}$$

$$\frac{\partial \vec{h}_x}{\partial z} - \frac{\partial \vec{h}_z}{\partial x} = \frac{\varepsilon\delta}{d}\vec{e}_y, \tag{3.8e}$$

$$\frac{\partial \vec{h}_y}{\partial x} = \frac{\partial \vec{h}_x}{\partial y}. \tag{3.8f}$$

The formula (3.3f) can be obtained from (3.8)

$$\frac{\partial^2 \vec{h}_z}{\partial x^2} + \frac{\partial^2 \vec{h}_z}{\partial y^2} + \frac{\partial^2 \vec{h}_z}{\partial z^2} + \frac{\mu\varepsilon}{\mathrm{d}^2}\lambda^2 \vec{h}_z = 0.$$

3.4 TM Waves

Transverse electric TM waves are characterized by $\vec{h}_z = 0$ and $\vec{e}_z \neq 0$. From (3.1),

$$\frac{\partial \vec{e}_z}{\partial y} - \frac{\partial \vec{e}_y}{\partial z} = \frac{\mu\delta^t}{d}\vec{h}_x, \tag{3.9a}$$

$$\frac{\partial \vec{e}_x}{\partial z} - \frac{\partial \vec{e}_z}{\partial x} = \frac{\mu\delta^t}{d}\vec{h}_y, \tag{3.9b}$$

$$\frac{\partial \vec{e}_y}{\partial x} = \frac{\partial \vec{e}_x}{\partial y}, \tag{3.9c}$$

$$-\frac{\partial \vec{h}_y}{\partial z} = \frac{\varepsilon\delta}{d}\vec{e}_x, \tag{3.9d}$$

$$\frac{\partial \vec{h}_x}{\partial z} = \frac{\varepsilon\delta}{d}\vec{e}_y, \tag{3.9e}$$

$$\frac{\partial \vec{h}_y}{\partial x} - \frac{\partial \vec{h}_x}{\partial y} = \frac{\varepsilon\delta}{d}\vec{e}_z. \tag{3.9f}$$

The formula (3.3c) can be obtained from (3.9)

$$\frac{\partial^2 \vec{e}_z}{\partial x^2} + \frac{\partial^2 \vec{e}_z}{\partial y^2} + \frac{\partial^2 \vec{e}_z}{\partial z^2} + \frac{\mu\varepsilon}{\mathrm{d}^2}\lambda^2 \vec{e}_z = 0.$$

3.5 Solutions of General Plane Waves

Vector operations

For the expression of solutions and simple computation, we introduce the vector operations used in Matlab.

Let

$$\vec{a} = (a_k) = \begin{bmatrix} a_1 \\ \vdots \\ a_n \end{bmatrix}, \tag{3.10a}$$

and

$$\vec{b} = (b_k) = \begin{bmatrix} b_1 \\ \vdots \\ b_n \end{bmatrix}. \tag{3.10b}$$

The vector operations are defined as

$$\vec{a}.*\vec{b} = (a_1 b_1, a_2 b_2, \cdots, a_n b_n)^t, \tag{3.11a}$$

$$\vec{a}./\vec{b} = (a_1 / b_1, a_2 / b_2, \cdots, a_n / b_n)^t, \tag{3.11b}$$

$$\vec{a}^{\,p} = (a_1^p, a_2^p, \cdots, a_n^p)^t, \tag{3.11c}$$

$$\int \vec{a} = \left(\int a_1, \int a_2, \cdots, \int a_n \right)^t, \tag{3.11d}$$

$$\frac{d}{dx}\vec{a} = \left(\frac{d}{dx}a_1, \frac{d}{dx}a_2, \cdots, \frac{d}{dx}a_n \right)^t, \tag{3.11e}$$

$$\exp(\vec{a}) = (\exp(a_1), \exp(a_2), \cdots, \exp(a_n))^t, \tag{3.11f}$$

$$c\vec{a} = (ca_1, ca_2, \cdots, ca_n)^t, \tag{3.11g}$$

$$\vec{a} \pm \vec{b} = (a_1 \pm b_1, a_2 \pm b_2, \cdots, a_n \pm b_n)^t, \tag{3.11h}$$

where A^t is the transpose of A, c is a scalar constant, p is a nonnegative rational number and $b_i \neq 0$ in (3.11b). When p in (3.11) is not an integer, it takes the principle value of multi-values.

Solution of wave equations

Now, we can solve the equations in (3.2). Let n=N. Let u represent the N-dimension column vectors $\vec{e}_x, \vec{e}_y, \vec{e}_z, \vec{h}_x, \vec{h}_y$ and $\vec{h}_z$, respectively. The formula (3.2) can be written as

$$\frac{\partial^2 \vec{u}}{\partial x^2} + \frac{\partial^2 \vec{u}}{\partial y^2} + \frac{\partial^2 \vec{u}}{\partial z^2} + \vec{\Lambda}^2 \vec{u} = 0, \tag{3.12}$$

where

$$\vec{\Lambda}^2 .* \vec{u} = \frac{\mu\varepsilon}{d^2}\lambda^2 \vec{u}. \tag{3.13}$$

Let

$$\vec{F}(x) = (f_i(x)),\ \vec{G}(y) = (g_i(y)),\ \vec{H}(z) = (h_i(z)). \tag{3.14}$$

Then we assume that the solution of (3.12) can be written as

$$\vec{u}(x, y, z) = \vec{F}(x) .* \vec{G}(y) .* \vec{H}(z), \tag{3.15}$$

Substituting this form into (3.12) and using the commutative properties of vectors, we have

$$\vec{F}''(x) ./ \vec{F}(x) + \vec{G}''(y) ./ \vec{G}(y) + \vec{H}''(z) ./ \vec{H}(z) + \vec{\Lambda}^2 = 0, \tag{3.16}$$

where 0 is the zero vector. We notice that each term of $\vec{F}''./\vec{F}, \vec{G}''./\vec{G}$ and $\vec{H}''./\vec{H}$ must be equal to a constant vector, since they are independent of each other. Hence we define three column vectors $\vec{\Lambda}_x$, $\vec{\Lambda}_y$, and $\vec{\Lambda}_z$ such that

$$\vec{F}'' + \vec{\Lambda}_x^2 .* \vec{F} = 0;\ \vec{G}'' + \vec{\Lambda}_y^2 .* \vec{G} = 0;\ \vec{H}'' + \vec{\Lambda}_z^2 .* \vec{H} = 0, \tag{3.17}$$

and

$$\vec{\Lambda}_x^2 + \vec{\Lambda}_y^2 + \vec{\Lambda}_z^2 = \vec{\Lambda}^2. \tag{3.18}$$

Now we can give the solutions of equation (3.12)

$$\begin{aligned}\vec{u} = (&\exp(-j\vec{\Lambda}_x x).* \vec{A}^{(1)} + \exp(j\vec{\Lambda}_x x).* \vec{A}^{(2)}).* (\exp(-j\vec{\Lambda}_y y).* \vec{B}^{(1)} \\ &+ \exp(j\vec{\Lambda}_y y).\vec{B}^{(2)}).* (\exp(-j\vec{\Lambda}_z z).* \vec{C}^{(1)} + \exp(-j\vec{\Lambda}_z z).* \vec{C}^{(2)}),\end{aligned} \tag{3.19}$$

and $\vec{A}^{(i)}$, $\vec{B}^{(i)}$, and $\vec{C}^{(i)}$ (i=1,2) are arbitrary complex constant column vectors. Hence the electric field density is given by

$$\vec{E} = T_e(\vec{e}_x \hat{x} + \vec{e}_y \hat{y} + \vec{e}_z \hat{z}). \tag{3.20}$$

Denoting the coordinate vector by

$$\vec{\Lambda} \equiv \vec{\Lambda}_x \hat{x} + \vec{\Lambda}_y \hat{y} + \vec{\Lambda}_z \hat{z} = \begin{bmatrix} x_1\hat{x} + y_1\hat{y} + z_1\hat{z} \\ x_2\hat{x} + y_2\hat{y} + z_2\hat{z} \\ \vdots \\ x_N\hat{x} + y_N\hat{y} + z_N\hat{z} \end{bmatrix}. \tag{3.21}$$

Defining a position vector as

$$\vec{r} = x\hat{x} + y\hat{y} + z\hat{z}. \tag{3.22}$$

The dot product of $\vec{\Lambda}$ and $\vec{r}$ is

$$\vec{\Lambda} \cdot \vec{r} = \vec{\Lambda}_x x + \vec{\Lambda}_y y + \vec{\Lambda}_z z = \begin{bmatrix} x_1 x + y_1 y + z_1 z \\ \vdots \\ x_N x + y_N y + z_N z \end{bmatrix}. \tag{3.23}$$

The coordinate vectors are treated as a particular case of vectors. The dot product of two coordinates vectors $\vec{\Lambda}_1$ and $\vec{\Lambda}_2$ is

$$\vec{\Lambda}_1 \cdot \vec{\Lambda}_2 = \vec{\Lambda}_{1x} .* \vec{\Lambda}_{2x} + \vec{\Lambda}_{1y} .* \vec{\Lambda}_{2y} + \vec{\Lambda}_{1z} .* \vec{\Lambda}_{2z}, \tag{3.24}$$

where $\vec{\Lambda}_i$ has the form of (3.21). We have also

$$\vec{\Lambda}\cdot\vec{a}=\vec{a}\cdot\vec{\Lambda}=\begin{bmatrix}(x_1\hat{x}+y_1\hat{z}+z_1\hat{z})a_1\\ \vdots\\ (x_N\hat{x}+y_N\hat{z}+z_N\hat{z})a_N\end{bmatrix}, \tag{3.25}$$

where vectors $\vec{a}$ and $\vec{\Lambda}$ are defined in (3.10a) and (3.21). Then the electric field can be expressed by

$$\vec{e}=\exp(-j\vec{\Lambda}\cdot\vec{r}).*\vec{e}_0. \tag{3.26}$$

where $\vec{e}_0=\vec{a}\hat{x}+\vec{b}\hat{y}+\vec{c}\hat{z}$ is the electric field amplitude vector, and $\vec{a}$, $\vec{b}$, $\vec{c}$ are the arbitrary complex constant column vectors. Now we discuss the relation between $\vec{\Lambda}$ and $\vec{e}_0$. We define

$$\nabla\cdot(a_1,\cdots,a_N)^t\equiv(\nabla\cdot a_1,\cdots,\nabla\cdot a_N)^t, \tag{3.27}$$

The formula

$$\nabla\cdot\left(f\vec{V}\right)=\vec{V}\cdot\nabla f+f\nabla\cdot\vec{V}, \tag{3.28}$$

holds for a complex scalar mapping *f*. For simplicity of expression, we consider only the "incident wave"; the "reflection wave" is similar.

$$\nabla\cdot\vec{E}=T_e\nabla\exp(-j\vec{\Lambda}\cdot\vec{r}).*\vec{e}_0=-jT_e\exp(-j\vec{\Lambda}\cdot\vec{r}).*(\vec{\Lambda}\cdot\vec{e}_0). \tag{3.29}$$

From the divergence condition, we have

$$\vec{\Lambda}\cdot\vec{e}_0=0, \tag{3.30}$$

which means that the electric field amplitude vector $\vec{e}_0$ are "perpendicular" to $\vec{\Lambda}$ in the transformed fields

Now we turn to the relation among $\vec{E}$, $\vec{H}$ and $\vec{\Lambda}$. Simply calculating,

$$\nabla\times\vec{E}=\left(\nabla T_e\exp\left(-j\vec{\Lambda}\cdot\vec{r}\right)\right)\times\vec{e}_0=-j\vec{\Lambda}\times\vec{E}. \tag{3.31}$$

Hence

$$\vec{\Lambda}\times\vec{E}=j\frac{\mu}{d}D^t\vec{H}. \tag{3.32}$$

3.6 Wavenumber and Eigenvalues

In this section we discuss the relation between the traditional wavenumber and eigenvalues. The vector $\vec{\Lambda}$ of eigenvalues is given as (3.13). The elements of $\vec{\Lambda}$ are the eigenvalues (λ_k). The elements of $\vec{\Lambda}_x, \vec{\Lambda}_y, \vec{\Lambda}_z$ are $(\Lambda_{xk}), (\Lambda_{yk})$ and (Λ_{zk}), respectively. From (3.18), we have

$$\Lambda_{xk}^2 + \Lambda_{yk}^2 + \Lambda_{zk}^2 = \lambda_k^2 . \tag{3.33}$$

The traditional wavenumber is given by

$$k = \frac{2\pi}{T}\sqrt{\mu\varepsilon} . \tag{3.34}$$

The following proposition gives the formula which determines the relation between engenvalues and the traditional wavenumber.

Proposition 3.1 *For the given N, μ and ε, the mapping*

$$F\left(\vec{\Lambda}\right) = \frac{\sqrt{2}\pi}{N^{3/2}}\left[(\lambda_i)\right]_2 , \tag{3.35}$$

is from N-dimension complex Hilbert space to complex Hilbert space, where $[]_2$ is l_2 norm. We choose the principle branch of multi-values. Then there is the relation between wavenumber and eigenvalues

$$k = F(\vec{\Lambda}) . \tag{3.36}$$

We can verify this result through the following example 3.1.

Example 3.1 For $\varepsilon = \varepsilon_0, \mu = \mu_0, f = 1GH_z$, c is the speed of light in free space. In [29], the usual wavenumber is expressed in (3.34). We have the table 3.1.

From Table 3.1, we see that k and $F(\vec{\Lambda})$ are almost identical despite a small error of calculus or computer: the relative error of $F(\vec{\Lambda})$ is:

$$\frac{\left|k - F(\vec{\Lambda})\right|}{k} \le 4.973\times 10^{-14},$$

for $N \le 10^5$.

N	*Theory values of k*	$F(\vec{\Lambda})$
10	20.94395102393196	20.94395102393196
10^2	20.94395102393196	20.94395102393195
10^3	20.94395102393196	20.94395102393196
10^4	20.94395102393196	20.94395102393201
10^5	20.94395102393196	20.94395102393199

Table 3.1 Calculation of k and $F(\vec{\Lambda})$

3.7 Variance of electric field in t

We are interested in the variance of electric field on time t. Now we can also obtain the ratio of difference. Let us denote $\vec{E}_0 = (a_1, \cdots, a_N)^t$ as the constant column vector of the electric field. Then the variance of the electric field on time t will be

$$\begin{aligned} \frac{\Delta E_i}{\Delta t} &= \frac{E_i - E_{i-1}}{\Delta t} \\ &= \frac{1}{T}\sqrt{N}\sum_{k=1}^{N} \lambda_k \operatorname{Re}\left((1+j)\omega^k\right) e^{-j\Lambda_k \cdot \vec{r}} a_k, \end{aligned} \tag{3.37}$$

where $\omega = e^{(2i-1)j\pi/N}$. Similarly, we can obtain the magnetic variance in t.

CHAPTER 4

RECTANGULAR WAVEGUIDE

4.1 Introduction

Rectangular waveguides are one of the earliest types of transmission lines and are still used today in many applications. A lot of components such as couplers, detectors, isolators, attenuators, and slotted lines etc are commercially available for various standard waveguides. Because of a recent trend toward MMIC, the microwave circuits are using planar transmission lines. There is, however, still a need for waveguides in many applications such as high-power systems, millimeter wave systems, and in some precision test applications.

Waveguides, often consisting of a single conductor, support transverse electric TE waves and/or transverse magnetic TM waves. The hollow rectangular waveguide can propagate TM and TE modes, but not TEM waves, since only one conductor is present. We shall show the solutions of the transverse magnetic TM waves and the transverse electric TE waves. We obtain a formula which reveals the relation between the traditional cutoff frequency and eigenvalues. The elliptical conditions are presented.

In this chapter, the geometry of a rectangular waveguide is shown in Figure 4.1,

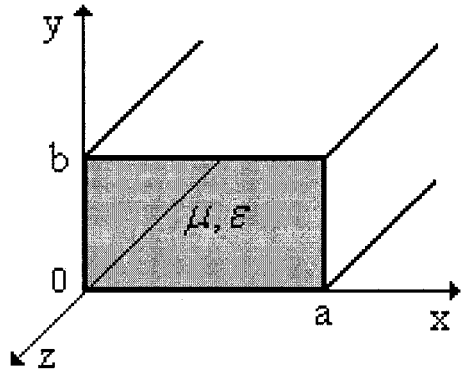

Figure 4.1 Geometry of a rectangular waveguide

where it is assumed that the guide is filled with material of permittivity ε and permeability μ.

4.2 TM Modes

Transverse magnetic TM waves are characterized by $\vec{H}_z$=0 and $\vec{E}_z$ ≠0. The wave equation and the boundary conditions are applied to $\vec{E}_z$:

$$\frac{\partial^2 \vec{E}_z}{\partial x^2}+\frac{\partial^2 \vec{E}_z}{\partial y^2}+\frac{\partial^2 \vec{E}_z}{\partial z^2}+\frac{\mu\varepsilon}{\mathrm{d}^2}P\vec{E}_z=0, \tag{4.1a}$$

$$\vec{E}_z\Big|_{x=0,a}=0, \tag{4.1b}$$

$$\vec{E}_z\Big|_{y=0,b}=0. \tag{4.1c}$$

By using (3.9) and (3.19), the solutions of (4.1) and other traverse field components for the TM mode can be computed as

$$\vec{E}_x = jT_eQ(\vec{\Theta}_m).*\vec{\Lambda}_z.*\cos(\vec{\Theta}_m x).*\sin(\vec{\Theta}_n y).*\left(\exp(j\vec{\Lambda}_z z).*\vec{a}_{mn}-\exp(-j\vec{\Lambda}_z z).*\vec{b}_{mn}\right), \tag{4.2a}$$

$$\vec{E}_y = jT_eQ(\vec{\Theta}_n).*\vec{\Lambda}_z.*\sin(\vec{\Theta}_m x).*\cos(\vec{\Theta}_n y).*\left(\exp(j\vec{\Lambda}_z z).*\vec{a}_{mn}-\exp(-j\vec{\Lambda}_z z).*\vec{b}_{mn}\right), \tag{4.2b}$$

$$\vec{E}_z = T_e\sin(\vec{\Theta}_m x).*\sin(\vec{\Theta}_n y)\left(\exp(j\vec{\Lambda}_z z).*\vec{a}_{mn}+\exp(-j\vec{\Lambda}_z z).*\vec{b}_{mn}\right), \tag{4.2c}$$

$$\vec{H}_x = \frac{\varepsilon}{d}T_h\delta Q(\vec{\Theta}_n).*\sin(\vec{\Theta}_m x).*\cos(\vec{\Theta}_n y).*\left(\exp(j\vec{\Lambda}_z z).*\vec{a}_{mn}+\exp(-j\vec{\Lambda}_z z).*\vec{b}_{mn}\right), \tag{4.2d}$$

$$\vec{H}_y = -\frac{\varepsilon}{d}T_h\delta Q(\vec{\Theta}_m).*\cos(\vec{\Theta}_m x).*\sin(\vec{\Theta}_n y).*\left(\exp(j\vec{\Lambda}_z z).*\vec{a}_{mn}+\exp(-j\vec{\Lambda}_z z).*\vec{b}_{mn}\right), \tag{4.2e}$$

where, in non TM_0 mode, and for any vector $\vec{A}$

$$Q(\vec{A}) = \vec{A}./\left(\vec{\Theta}_m^2+\vec{\Theta}_n^2\right), \tag{4.3}$$

and $\vec{\Theta}_m$ and $\vec{\Theta}_n$ are the vectors whose elements are $m_i\pi/a$ and $n_i\pi/b$, respectively, for some integers m_i and n_i.

Usually, the wave propagation along the +z-axis in the TM modes of a rectangular waveguide is studied.

4.3 TE Modes

Transverse electric TE waves are characterized by $\vec{E}_z$=0, while $\vec{H}_z$ must satisfy the wave equation:

$$\frac{\partial^2 \vec{H}_z}{\partial x^2}+\frac{\partial^2 \vec{H}_z}{\partial y^2}+\frac{\partial^2 \vec{H}_z}{\partial z^2}+\frac{\mu\varepsilon}{\mathrm{d}^2}P\vec{H}_z=0, \tag{4.4a}$$

The boundary conditions on the electric field components tangential to the waveguide walls are expressed as

$$\vec{E}_x|_{\mathrm{y=\,0,\,b}}=0, \tag{4.4b}$$

$$\vec{E}_y|_{\mathrm{x=\,0,\,a}}=0. \tag{4.4c}$$

Similarly, by using the equation (3.8), the solutions of (4.4) and other transverse field components for the TE mode can be computed as

$$\vec{E}_x=-\frac{\mu}{d}T_e\delta' Q(\vec{\Theta}_n).*\cos\left(\vec{\Theta}_m x\right).*\sin\left(\vec{\Theta}_n y\right).*(\exp(j\vec{\Lambda}_z z).*\vec{a}_{mn}+\exp(-j\vec{\Lambda}_z z).*\vec{b}_{mn}), \tag{4.5a}$$

$$\vec{E}_y=\frac{\mu}{d}T_e\delta' Q(\vec{\Theta}_m).*\sin\left(\vec{\Theta}_m x\right).*\cos\left(\vec{\Theta}_n y\right).*(\exp(j\vec{\Lambda}_z z).*\vec{a}_{mn}+\exp(-j\vec{\Lambda}_z z).*\vec{b}_{mn}), \tag{4.5b}$$

$$\vec{H}_x=-jT_h Q(\vec{\Theta}_m).*\vec{\Lambda}_z\sin\left(\vec{\Theta}_m x\right).*\cos\left(\vec{\Theta}_n y\right).*(\exp(j\vec{\Lambda}_z z).*\vec{a}_{mn}-\exp(-j\vec{\Lambda}_z z).*\vec{b}_{mn}), \tag{4.5c}$$

$$\vec{H}_y=jT_h Q(\vec{\Theta}_n).*\vec{\Lambda}_z.*\cos\left(\vec{\Theta}_m x\right).*\sin\left(\vec{\Theta}_n y\right).*(\exp(j\vec{\Lambda}_z z).*\vec{a}_{mn}-\exp(-j\vec{\Lambda}_z z).*\vec{b}_{mn}), \tag{4.5d}$$

$$\vec{H}_z=T_h\cos\left(\vec{\Theta}_m x\right).*\cos\left(\vec{\Theta}_n y\right).*(\exp(j\vec{\Lambda}_z z).*\vec{a}_{mn}+\exp(-j\vec{\Lambda}_z z).*\vec{b}_{mn}), \tag{4.5e}$$

where $\vec{\Theta}_m$ and $\vec{\Theta}_n$ are the vectors whose elements are $m_i\pi/a$ and $n_i\pi/b$, respectively, for some integers m_i and n_i.

4.4 Cutoff Frequency

4.4.1 Elliptical Conditions

Elliptical Conditions

We define the elliptical conditions of m_p, n_p and λ_p which are shown in Figure 4.2

$$\frac{m_p^2}{a^2}+\frac{n_p^2}{b^2}\le\left(\frac{\sqrt{\mu\varepsilon}N\lambda_p}{\pi T}\right)^2. \tag{4.6}$$

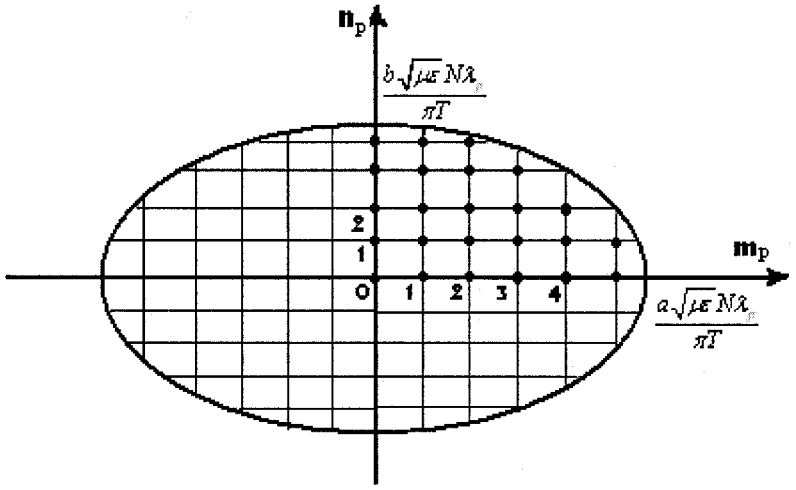

Figure 4.2 Elliptical conditions of m_p, n_p and λ_p

Cutoff frequencies in transformed fields

The ***eigenvalue vector*** is

$$\vec{\Lambda}^2=\vec{\Theta}_m^2+\vec{\Theta}_n^2+\vec{\Lambda}_z^2. \tag{4.7}$$

In the case of TM modes and TE modes, the ***vector*** $\vec{\Lambda}_z$ in transformed fields can be defined as

$$\vec{\Lambda}_z^2 = \vec{\Lambda}^2 - \vec{\Theta}_m^2 - \vec{\Theta}_n^2 . \tag{4.8}$$

which is seen to be real if it satisfies elliptical conditions shown in Figure 4.2. We define the cutoff frequency f_c^{ps} of TM and TE modes for a rectangular waveguide by

$$f_c^{ps} = \inf\left\{ f : \vec{\Lambda}_z(f)\Big|_i \text{ is real and } m_i = m, n_i = n \text{ for all } i = 1,2,\cdots,N-1 \right\}. \tag{4.9}$$

Set

$$\tilde{f}(p,m,n) = \frac{1}{2\pi\sqrt{\mu\varepsilon}} \sqrt{\left(\frac{\sqrt{\mu\varepsilon}}{d}\lambda_p\right)^2 - \left(\frac{m_p\pi}{a}\right)^2 - \left(\frac{n_p\pi}{b}\right)^2} . \tag{4.10}$$

4.4.2 Relation of cutoff frequencies between original fields and transformed fields

We consider original electric and magnetic fields $\vec{E}$ and $\vec{H}$. The following quantities are identical:

(a) The cutoff frequency f_c^{ps} of TE_{mn}, TM_{mn} is given by the definition in (4.10).

(b) $$f_c^{ps} = \frac{1}{\sqrt{N}} \left| \sum_{p=1}^{N} \sum_{i=1}^{N} \mathrm{Im}\left(T_{epk} \tilde{f}(i,\cdot,\cdot) \right) \right|. \tag{4.11}$$

(c) The traditional cutoff frequency f_{cmn}

$$f_c = \frac{1}{2\pi\sqrt{\mu\varepsilon}} \sqrt{\left(\frac{m\pi}{a}\right)^2 + \left(\frac{n\pi}{b}\right)^2} . \tag{4.12}$$

We omit the proof of the result; the accuracy of the statements can be verified by the numerical method in Example 4.1.

Mode	m	n	f_c (GHz)	f_c^{ps} (GHz)	$f_c - f_c^{ps}$ (Hz)
TE	1	0	6.561679790026246	6.561679790024629	0.001617
TE	2	0	13.12335958005249	13.12335958004993	0.002567
TE	3	0	19.68503937007874	19.68503937007514	0.003593
TE	0	1	14.76377952755905	14.76377952755623	0.002820
TE	0	2	29.52755905511811	29.52755905511379	0.004322
TE	0	3	44.29133858267716	44.29133858267220	0.004966
TE, TM	1	1	16.15626279822195	16.15626279821892	0.003032
TE, TM	1	2	30.24784926933362	30.24784926932926	0.004356
TE, TM	1	3	44.77475086599797	44.77475086599298	0.004989
TE, TM	2	1	19.75327194683775	19.75327194683421	0.003536
TE, TM	2	2	32.31252559644391	32.31252559643957	0.004337
TE, TM	2	3	46.19464514543545	46.19464514543044	0.005004
TE, TM	3	1	24.60629921259842	24.60629921259459	0.003826
TE, TM	3	2	35.48770940417312	35.48770940416853	0.004592
TE, TM	3	3	48.46878839466587	48.46878839466071	0.005165

Table 4.1 Comparison of fc between two methods

Observe that the transverse field components of TEmn modes and TMmn modes in (4.12) are zero if both m=n=0; thus there is neither TE_{00} mode nor a TM_{00} mode.

4.4.3 An Example

Example 4.1. We choose the parameters as a=2.286 cm, b=1.016 cm, $\varepsilon_r = 1$, $\mu = \mu_0$, T=0.1 ns. We denote by f_c and f_c^{ps} the traditional cutoff frequencies in (4.12) and the cutoff frequencies in the method of periodic sequence in (4.11), respectively. We choose N=2000 in this example.

From Table 4.1, we know that the absolute error for the cutoff frequency between two methods is less than one centi-Hz when N=2000, m=1, n=0. The relative error is

$$\frac{0.001617}{6.561679790026246 \cdot 10^9} = 2.464308 \times 10^{-13}.$$

Although the error is dependent on the number N, N does not influence the error too

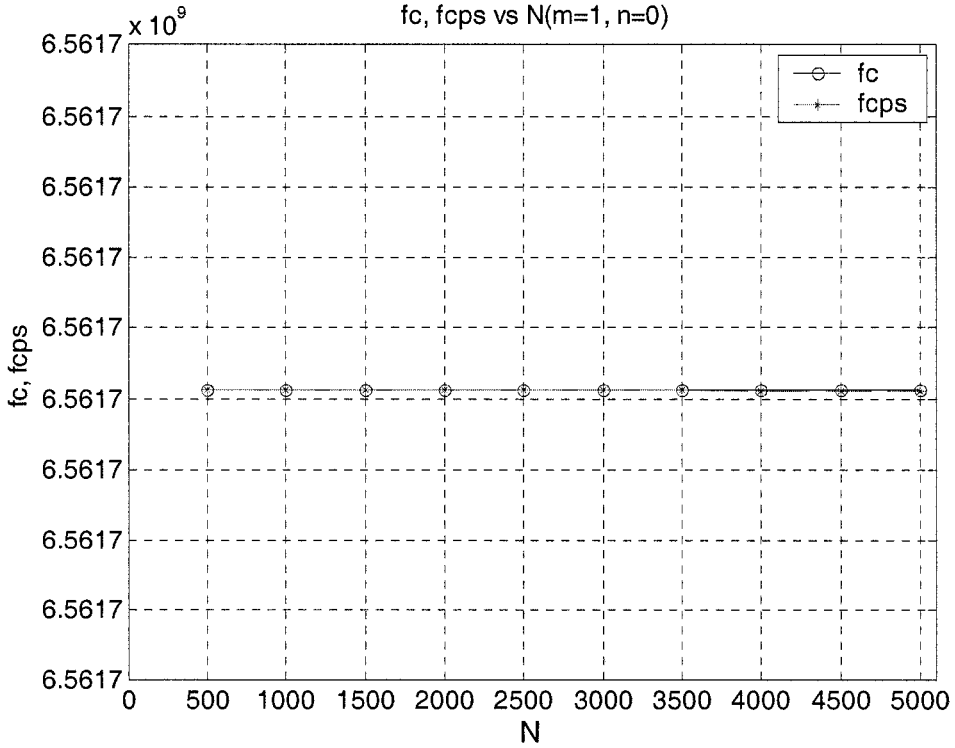

Figure 4.3 Cutoff frequencies vs N

much. We shall discuss this in the next section.

4.4.4 Convergence on N

We use the same parameters: a=2.286 cm, b=1.016 cm, $\varepsilon_r = 1$, $\mu = \mu_0$, T=0.1 ns, m=1, n=0. We choose a number N of lines from 500 to 5000.

The two curves in Fig.4.3 are the same in the case of m=1, n=0 because the difference between them is less than one Hz. The cutoff frequency of the periodic sequence method is convergent to 6.56167979002 GHz, which is equal to that of the traditional method. From Figure 4.3, we can see the two curves for the cutoff frequency coincide when N is verified from 500 to 5000. Hence, we can say that the two kinds of computation for cutoff frequencies in Figure 4.3 are convergent to the same value of N, and they coincide.

CHAPTER 5

APPLICATIONS OF PERIODIC SEQUENCE THEORY TO CIRCUIT THOERY: LOSSLESS TRANSMISSION LINES

5.1 Introduction

In this Chapter, we apply the theory of periodic sequence to lossless transmission lines. We assume that the medium of wave propagation is homogeneous, isotropic and linear.

In section 5.2, we shall demonstrate the method of this theory. We use this new theory and method for telegraph equations. The voltage and the current in the telegraph equations are discrete, transformed and decouple. In section 5.3, we shall give the analytic solutions of the wave equations and determine the coefficients using initial conditions. In section 5.4, we shall discuss the relation between the convergence and the number N of partition. In section 5.5, a numerical computation example will be given to show the theoretical curve and the new method curve for wave propagation of lossless transmission line.

Figure 5.1 shows the lossless transmission line modeling. The piece of transmission line of length Δz can be modeled as a lumped-element circuit of T-type equivalent modeling as in Figure 5.1, where the parameters L and C are inductance and capacitance per unit length of the line, respectively. In Figure 5.1, we assume that the wave propagates in the +z direction, from the generator to the load. The circuit model of transmission line in Figure 5.1 satisfies the telegraph equations

$$\frac{\partial V(z,t)}{\partial z} = -L\frac{\partial I(z,t)}{\partial t}, \tag{5.1a}$$

$$\frac{\partial I(z,t)}{\partial z} = -C\frac{\partial V(z,t)}{\partial t}. \tag{5.1b}$$

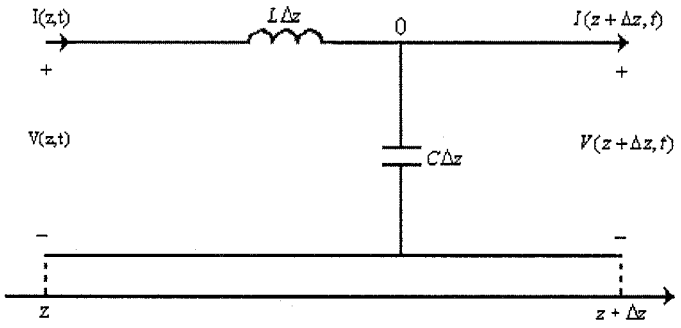

Figure 5.1. T-type equivalent circuit model of a lossless transmission line

5.2 Application of new theory to lossless transmission lines

We suppose that the system is linear. Hence the response is periodic if the excitation is periodic. Let us denote the period of excitation by T. We divide T into N intervals on t: $t_0 < t_1 < ... < t_N$. Let us denote by $\Delta t_n = t_n - t_{n-1} (n = 1,2,...,N)$ the length of n-th interval. Usually, we choose equal intervals. By means of difference in t, denote by $\vec{V} = (V_1, V_2, ...V_N)^t$ the column vector, where $V_n = V|_{t=t_n}$, by X^t the transpose of X and by N the number of intervals of partitions. We start with the equations in (5.1) and use the difference and method of line. The equations in (5.1) can be written as approximate forms of one order

$$\frac{\partial \vec{V}}{\partial z} = \frac{L}{h} D^t \vec{I}, \tag{5.2a}$$

$$\frac{\partial \vec{I}}{\partial z} = -\frac{C}{h} D\vec{V}, \tag{5.2b}$$

where

$$D = \begin{bmatrix} -1 & 1 & & \\ & \ddots & \ddots & \\ & & \ddots & 1 \\ 1 & & & -1 \end{bmatrix}_{N\times N}, \tag{5.3}$$

and

$$h = \|\Delta\| = \max_n \Delta t_n = \Delta t . \tag{5.4}$$

We use the transformations of this method

$$\vec{V} = T_1 \vec{v} , \tag{5.5a}$$

$$\vec{I} = T_2 \vec{i} . \tag{5.5b}$$

In this paper, all lowercase vectors are in the transformed domain; all uppercase vectors are in the original domain. We have

$$\frac{\partial^2 \vec{v}}{\partial z^2} = -\frac{LC}{h^2} T_1^{-1} D^t D T_1 \vec{v} , \tag{5.6a}$$

$$\frac{\partial^2 \vec{i}}{\partial z^2} = -\frac{LC}{h^2} T_2^{-1} D D^t T_2 \vec{i} . \tag{5.6b}$$

Set

$$\Theta = DD^t = D^t D = \begin{bmatrix} 2 & -1 & & & & -1 \\ -1 & 2 & -1 & & & \\ & -1 & 2 & \ddots & & \\ & & \ddots & \ddots & \ddots & \\ & & & -1 & 2 & -1 \\ -1 & & & & -1 & 2 \end{bmatrix}. \tag{5.7}$$

The matrix Θ is real and symmetric. According to the theory of real symmetric matrices, there exits an orthogonal matrix T such that

$$T^{-1} \Theta T = \Lambda_0^2 . \tag{5.8}$$

We can choose

$$T = \left(T_{pk}\right), T_{pk} = \sqrt{\frac{2}{N}} \sin \frac{(N + 8pk)\pi}{4N}, \text{ p, k=1,2, … , N.} \tag{5.9}$$

It is easy to show that T is an orthogonal matrix. The eigenvalues of Θ can be found as:

$$\Lambda_0^2 = 4 diag\left(\sin^2\left(\frac{\pi}{N}\right), \sin^2\left(\frac{2\pi}{N}\right), ..., \sin^2\left(\frac{(N-1)\pi}{N}\right), 0 \right). \tag{5.10}$$

Then, we have the standard forms

$$\frac{\partial^2 \vec{v}}{\partial z^2} = -\vec{\Lambda}^2 .* \vec{v} \ , \tag{5.11a}$$

$$\frac{\partial^2 \vec{i}}{\partial z^2} = -\vec{\Lambda}^2 .* \vec{i} \ , \tag{5.11b}$$

where $\vec{\Lambda} .* \vec{v} = \Lambda_0 \vec{v} / (v_p h)$ and $v_p = 1/\sqrt{LC}$ is the phase velocity. The operation ".*" is defined in section 3.5.

5.3 Solutions of telegraph equations

5.3.1 The form of solutions

The traveling wave solutions to (5.11) can be found as

$$\vec{v}(z) = e^{-j\vec{\Lambda} z} .* \vec{a}_1 + e^{j\vec{\Lambda} z} .* \vec{a}_2 , \tag{5.12a}$$

$$\vec{i}(z) = e^{-j\vec{\Lambda} z} .* \vec{b}_1 + e^{j\vec{\Lambda} z} .* \vec{b}_2 , \tag{5.12b}$$

where $\vec{a}_k$ and $\vec{b}_k$ are arbitrary constants.

5.3.2 The relation between $\vec{a}_k$ and $\vec{b}_k$

Now we discuss the relation between $\vec{a}_k$ and $\vec{b}_k$. Between $\vec{a}_k$ and $\vec{b}_k$, only one is independent. For example, we can determine $\vec{b}_k$ if $\vec{a}_k$ is given. In fact, from (5.5), (5.2) can be written as

$$\frac{\partial \vec{v}}{\partial z} = \frac{L}{h} T^{-1} D^t T \vec{i} \ , \tag{5.13a}$$

$$\frac{\partial \vec{i}}{\partial z} = -\frac{C}{h} T^{-1} D T \vec{v} \ . \tag{5.13b}$$

By (5.12) and (5.13), we can obtain

$$\vec{\Lambda} .* \vec{b}_1 = -j \frac{C}{h} T^{-1} D T \vec{a}_1 , \tag{5.14a}$$

$$\vec{\Lambda} .* \vec{b}_2 = j \frac{C}{h} T^{-1} D T \vec{a}_2 . \tag{5.14b}$$

We note that $\vec{\Lambda}$ and D are vector and singular matrix, respectively.

5.3.3 Determining $\vec{a}_k$

We suppose that $\vec{v} = \vec{v}_0$ at point $z = 0$. We can find the initial current $\vec{i}_0$ if we only know the initial voltage $\vec{v}_0$. We assume that

$$\vec{v}_0 = \vec{v}_0^+ \tag{5.15a}$$

Then

$$\vec{a}_1 + \vec{a}_2 = \vec{v}_0. \tag{5.15b}$$

We can find out $\vec{i}_0$ by

$$\vec{i}_0^+ = \Im^{-1}\left(\frac{\Im(\vec{v}_0^+)}{Z_0}\right) = \frac{\vec{v}_0}{Z_0}, \tag{5.16}$$

where $\Im$ is the discrete Fourier transform, $\Im^{-1}$ is the inverse Fourier transform and $Z_0 = \sqrt{L/C}$ is the characteristic impedance of the lossless transmission line.

We can find $\vec{a}_k$ if we know $\vec{v}_0$ and $\vec{i}_0$ from (5.14)

$$\vec{\Lambda}.*\left(-\vec{a}_1 + \vec{a}_2\right) = -j\frac{L}{h}T^{-1}D^tT\vec{i}_0, \tag{5.17}$$

From (5.15) and (5.17), we can obtain $\vec{a}_1$ and $\vec{a}_2$ as

$$\vec{\Lambda}.*\vec{a}_1 = \frac{1}{2}\left(\vec{\Lambda}.*\vec{v}_0 + j\frac{L}{h}T^{-1}D^tT\vec{i}_0\right), \tag{5.18a}$$

$$\vec{\Lambda}.*\vec{a}_2 = \frac{1}{2}\left(\vec{\Lambda}.*\vec{v}_0 - j\frac{L}{h}T^{-1}D^tT\vec{i}_0\right). \tag{5.18b}$$

5.4 Convergence on the number N of partitions

Let g(t) be the continuous-time signal by sample g(n Δt) and $\Delta f = 1/\Delta t$ be the sample rate . According to the uniform-sampling theorem of Nyquist, if g(t) is band limited with no components at frequencies greater than f_h Hz, then it is completely

specified by samples taken at the uniform rate $f_s > 2f_h$ Hz. Usually, f_h is a frequency which we are interested in the spectral space. In our case, the relation between the number N of partitions and f_h is as follows

$$N \geq N_0 = 2Tf_h ceil\left(\frac{z}{Tv_0}\right). \tag{5.19}$$

where T is the period of excitation, v_0 is the speed of light in a medium and ceil(x) returns the closest integer above x.

For example, if we consider that the frequency is within 100GHz, we take $f_h = 100GHz$. Then, we have

$$N > 200$$

if the period is $T = 1ns$ and z=70mm.

5.5 Wave propagation of the lossless transmission lines

We choose the periodic impulse as the periodic Gauss impulse:

$$g(t) = \begin{cases} e^{-c_0 t^2}, 0 \leq t \leq T/2. \\ e^{-c_0 (t-T)^2}, T/2 \leq t \leq T. \end{cases}$$

where $c_0 = (20/T)^2$. The parameters are as follows: T = 0.3333ns, L= 100nH, C= 111.11pF, z =6 cm, N=500. In Figure 5.2, one of the two curves is obtained using traditional theory. Another is obtained using the new method in this thesis. We can see two curves coincide well.

We have already demonstrated the application of this new theory to the lossless transmission lines. It involves less computation in the numerical computation than traditional methods. With this advantage, it will have many applications in electrical engineering, such as electric and magnetic field computing, filter design, etc.

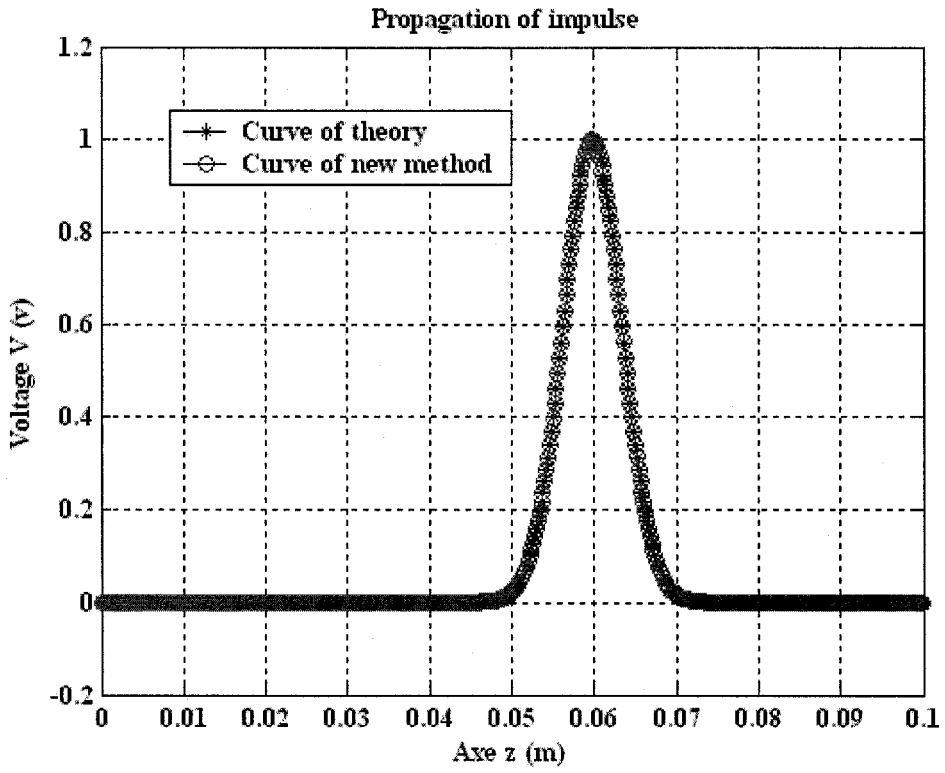

Figure 5.2 Curve comparisons between theory and new method for periodic impulse.

CHAPTER 6
APPLICATIONS OF KE WU'S THEORY TO LOSSY TRANSMISSION LINES

6.1 Introduction

In this chapter, we apply the periodic sequence theory to lossy transmission lines. From the previous chapter, we see that this new theory is neither time domain analysis nor frequency domain analysis. This theory can avoid the disadvantages of the frequency domain method and the time domain method.

In section 6.2, we demonstrate the theory of periodic sequence by using transformations and algebra theory. We apply the period sequence theory and method to telegraph equations. The voltage and the current in the telegraph equations are decoupled under the transforms and changed into the standard equations. In section 6.3, we give the analytic solutions of wave equations and determine the coefficients. In section 6.4, the relation between the complete signal and the number N of partitions is given. Section 6.5 gives the discussion of parameter influences on convergence. The numerical computing examples are given to show the difference between the theory curve and the new method curve of wave propagation for lossy transmission lines.

We assume that the medium of wave propagation is homogeneous, isotropic and linear. Figure 6.1 illustrates the transmission line modeling. The piece of transmission line of length Δz can be modeled as a lumped-element circuit of T-type equivalent modeling as in Figure 6.1, where the parameters R, L, G and C are resistance, inductance, conductance and capacitance per unit length of the line, respectively. In Figure 6.1, we assume that the wave propagates in the +z direction, from the generator to the load. The circuit model of transmission lines in Figure 6.1 satisfies the telegraph equations

$$-\frac{\partial V(z,t)}{\partial z} = RI(z,t) + L\frac{\partial I(z,t)}{\partial t}, \tag{6.1a}$$

$$-\frac{\partial I(z,t)}{\partial z} = GV(z,t) + C\frac{\partial V(z,t)}{\partial t}. \tag{6.1b}$$

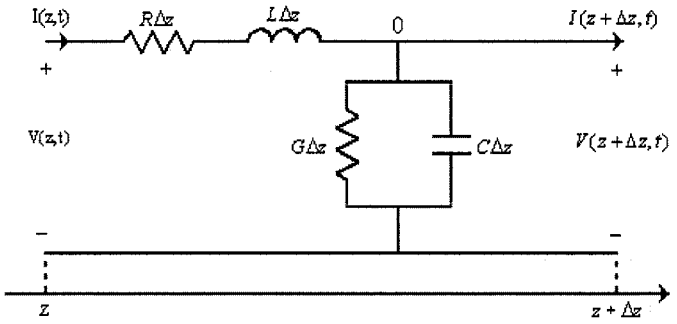

Figure 6.1. T-type equivalent circuit model of a transmission line

6.2 Application of New Theory to Telegraph Equations

The theoretic base of periodic sequence theory is, in a linear system, if the excitation is periodic then the response is too. We suppose that the voltage and current are functions of period T in time t. We do a partition Δ on t: $t_0 < t_1 < ... < t_N$ denoted by $\Delta t_n = t_n - t_{n-1} (n = 1, 2, ..., N)$ the length of the n-th interval. To simplify the calculation, we choose the equal interval partition in this chapter. By means of difference in t, denoted by $\vec{V} = (V_1, V_2, ...V_N)^t$ the column vector, where $V_n = V\big|_{t=t_n}$, by B^t the transpose of B and by N the number of intervals in partitions. Then, by means of the difference and method of lines, the equations in (6.1) can be written as approximate forms of one order

$$\frac{\partial \vec{V}}{\partial z} = \Theta_1 \vec{I}, \tag{6.2a}$$

$$\frac{\partial \vec{I}}{\partial z} = \Theta_2 \vec{V}, \tag{6.2b}$$

where

$$\Theta_1 = \begin{bmatrix} -\frac{R}{2}+\frac{L}{h} & -\frac{R}{2}-\frac{L}{h} & & \\ & \ddots & \ddots & \\ & & \ddots & -\frac{R}{2}-\frac{L}{h} \\ -\frac{R}{2}-\frac{L}{h} & & & -\frac{R}{2}+\frac{L}{h} \end{bmatrix}_{N\times N}, \tag{6.3}$$

$$\Theta_2 = \begin{bmatrix} -\frac{G}{2}-\frac{C}{h} & & & -\frac{G}{2}+\frac{C}{h} \\ -\frac{G}{2}+\frac{C}{h} & \ddots & & \\ & \ddots & \ddots & \\ & & -\frac{G}{2}+\frac{C}{h} & -\frac{G}{2}-\frac{C}{h} \end{bmatrix}_{N\times N}, \tag{6.4}$$

and

$$h = \|\Delta\| = \max_n \Delta t_n = \Delta t. \tag{6.5}$$

We use the following transformations

$$\vec{V} = T_1 \vec{v}, \tag{6.6a}$$

$$\vec{I} = T_2 \vec{i}. \tag{6.6b}$$

In this chapter, all lowercase vectors are in the transformed domain; all uppercase vectors are in the original domain. We have

$$\frac{\partial^2 \vec{v}}{\partial z^2} = T_1^{-1} \Theta T_1 \vec{v}, \tag{6.7a}$$

$$\frac{\partial^2 \vec{i}}{\partial z^2} = T_2^{-1} \Theta T_2 \vec{i}, \tag{6.7b}$$

where

$$c_1 = \left(-\frac{R}{2}+\frac{L}{h}\right)\left(-\frac{G}{2}-\frac{C}{h}\right)+\left(-\frac{R}{2}-\frac{L}{h}\right)\left(-\frac{G}{2}+\frac{C}{h}\right) = \frac{RG}{2}-\frac{2LC}{h^2}, \tag{6.8}$$

$$c_2 = \left(\frac{R}{2}+\frac{L}{h}\right)\left(\frac{G}{2}+\frac{C}{h}\right), \tag{6.9}$$

$$c_3 = \left(-\frac{R}{2} + \frac{L}{h}\right)\left(-\frac{G}{2} + \frac{C}{h}\right), \tag{6.10}$$

and

$$\Theta = \Theta_1\Theta_2 = \Theta_2\Theta_1 = \begin{bmatrix} c_1 & c_2 & & & & c_3 \\ c_3 & c_1 & c_2 & & & \\ & c_3 & c_1 & \ddots & & \\ & & \ddots & \ddots & \ddots & \\ & & & c_3 & c_1 & c_2 \\ c_2 & & & & c_3 & c_1 \end{bmatrix}, \tag{6.11}$$

Then Θ is a special Toepliz matrix, i.e., a circulant matrix. Set the polynomial

$$p(\lambda) = c_1 + c_2\lambda + c_3\lambda^{N-1}. \tag{6.12}$$

Then Θ can be written as

$$\Theta = p(C_0) = c_1 I_N + c_2 C_0 + c_3 C_0^{\,N-1}. \tag{6.13}$$

where

$$C_0 = \begin{bmatrix} 0 & 1 & & & \\ & 0 & 1 & & \\ & & \ddots & \ddots & \\ & & & \ddots & 1 \\ 1 & & & \cdots & 0 \end{bmatrix}. \tag{6.14}$$

Set

$$T = \frac{1}{\sqrt{N}} \begin{bmatrix} 1 & 1 & 1 & \cdots & 1 \\ 1 & \omega & \omega^2 & \cdots & \omega^{N-1} \\ 1 & \omega^2 & \omega^4 & \cdots & \omega^{2(N-1)} \\ & & & \cdots & \\ 1 & \omega^{N-1} & \omega^{2(N-1)} & \cdots & \omega^{(N-1)(N-1)} \end{bmatrix}. \tag{6.15}$$

where ω is an Nth root of unity. It is easy to show that T is a unitary matrix.

According to matrix theory,

$$T^*\Theta T = \Lambda_0^2, \tag{6.16}$$

where * is the conjugate transpose and

$$\Lambda_0^2 = diag\left(p(1), p(\omega), \cdots, p\left(\omega^{N-1}\right)\right). \tag{6.17}$$

Then, we have the standard forms

$$\frac{\partial^2 \vec{v}}{\partial z^2} = \Lambda_0^2 \vec{v}, \tag{6.18a}$$

$$\frac{\partial^2 \vec{i}}{\partial z^2} = \Lambda_0^2 \vec{i}, \tag{6.18b}$$

where Λ_0 is given in (6.17).

6.3 Solutions of telegraph equations

The traveling wave solutions to (6.18) are of the form

$$\vec{v}(z) = e^{-\vec{\Lambda} z} .* \vec{a}_1 + e^{\vec{\Lambda} z} .* \vec{a}_2, \tag{6.19a}$$

$$\vec{i}(z) = e^{-\vec{\Lambda} z} .* \vec{b}_1 + e^{\vec{\Lambda} z} .* \vec{b}_2, \tag{6.19b}$$

where $\vec{\Lambda} .* \vec{v} = \Lambda_0 \vec{v}$, $\vec{a}_k$ and $\vec{b}_k$ are arbitrary constants.

We shall discuss the properties of $\vec{\Lambda} = (\Lambda_n)$. Set

$$\Lambda_n = r_n + j s_n, n = 1, 2, \cdots, N. \tag{6.20}$$

There are multi-values in (6.20), we choose the principle values. From the properties of Λ, the equality

$$\Lambda_n = \overline{\Lambda}_{N-n}, \tag{6.21}$$

holds for $N/2 \le n \le N$ if N is even (6.or (6. $(N+1)/2 \le n \le N$ if N is odd).

Now, we want to prove that

$$r_n > 0 \text{ for n=1, 2,..., N in loss case.} \tag{6.22}$$

In fact, for all $n \le N$, we can obtain the following equality from (6.20)

$$p\left(\omega^{n-1}\right) = c_1 + (c_2 + c_3)\cos\left(\frac{2n\pi}{N}\right) + i(c_2 - c_3)\sin\left(\frac{2n\pi}{N}\right), \tag{6.23}$$

where

$$c_2 + c_3 = \frac{RG}{2} + \frac{2LC}{h^2}, \tag{6.24}$$

$$c_2 - c_3 = \frac{1}{h}(LG + RC), \tag{6.25}$$

From (6.21), we only need to prove that (6.22) holds for $n \le N/2$ if N is even (6.for $n \le (N-1)/2$ if N is odd). In a hypothetical case, we have $c_2 \neq c_3$. Then

$$\mathrm{Im}\left[p\left(\omega^{n-1}\right)\right] > 0, \tag{6.26}$$

Therefore, $r_n > 0$ for $n \le N/2$ if N is even (6.for $n \le (N-1)/2$ if N is odd). Therefore, (6.20) holds.

Now we'll determine the constants $\vec{a}_k$ and $\vec{b}_k$ in (6.19). For the symmetry $\vec{a}_k$ and $\vec{b}_k$, we need only to discuss $\vec{a}_k$.

In the lossy case, first of all, for n=N, we have

$$\Lambda_N = (c_1 + c_2 + c_3)^{1/2} = \sqrt{RG}. \tag{6.28}$$

Since the voltage and current must be zero when z tends to infinity, we have $\vec{a}_2|_{n=N} = 0$. For $n \le N/2 - 1$ if N is even (6.for $n \le (N-1)/2$ if N is odd), for the voltage and current must be zero when z tends to infinity, we can obtain that $\vec{a}_2|_{n \le N/2-1} = 0$ from (6.22a). For n=N/2 if N is even, we have

$$\Lambda_{N/2} = (c_1 - c_2 - c_3)^{1/2} = j\frac{2}{hv_p}, \tag{6.29}$$

where v_p is the speed of wave propagation in free space:

$$v_p = \frac{1}{\sqrt{LC}}. \tag{6.30}$$

For $N/2 \le n \le N$ if N is even (6.or $(N+1)/2 \le n \le N$ if N is odd), we can prove that $\vec{a}_2|_{n \ge N/2} = 0$. Therefore, $\vec{a}_2 = 0$. Hence

$$\vec{v}(z) = e^{-\vec{\Lambda}z} .* \vec{a}_1, \tag{6.31a}$$

$$\vec{i}(z) = e^{-\vec{\Lambda}z} .* \vec{b}_1, \tag{6.31b}$$

6.4 The Relation between Complete Signals and N

In this section we suppose that the transmission line has lower losses, that is, $R \ll \omega L$ and $G \ll \omega C$ so the influences of R and G are neglected. The convergence of numeric computation is dependent on the number N of partitions, z, and T. On one hand, the error is big if N is taken too small. On the other hand, the convergence is very good if we choose N "very big", but this may take a little longer. So choosing a suitable N is important for an engineer. We must know the inferior limit for N. Let the frequency which we are interested in be less than f_h. According to the sample theorem of Nyquist, the sampling frequency is $f_s \geq 2f_h$. In our lower loss case, N must satisfy

$$N \geq N_0 = 2Tf_h ceil\left(\frac{z}{Tv_0}\right), \tag{6.32}$$

where T is the period of excitation, v_0 is the speed of light in a medium and ceil(x) returns the closest integer above x. When we consider the Gauss impulse, the band is not limited. Equation (6.32) can be expressed in Δt:

$$\Delta t \leq \Delta t_0 = \left(2f_h ceil\left(\frac{z}{Tv_p}\right)\right)^{-1}, \tag{6.33}$$

The following function is used as Gauss's impulse

$$g(t) = \begin{cases} e^{-c_0 t^2}, 0 \leq t \leq T/2. \\ e^{-c_0 (t-T)^2}, T/2 \leq t \leq T. \end{cases} \tag{6.34}$$

where $c_0 = (20/T)^2$. We often use this pulse as an excitation. The theoretical values of traditional voltage and current are given by

$$V(z) = V_0^+ e^{-\gamma z} + V_0^- e^{\gamma z}, \tag{6.35a}$$

$$I(z) = I_0^+ e^{-\gamma z} + I_0^- e^{\gamma z}, \tag{6.35b}$$

where γ is given by

$$\gamma = \alpha + j\beta = \sqrt{(R + j\omega L)(G + j\omega C)}. \tag{6.36}$$

Example 6.1. We give a low loss example to see the effect of N in (6.32). We choose, throughout this chapter, $f_h = 200$ GHz. We'll discuss three cases N=20, 100, and 200.

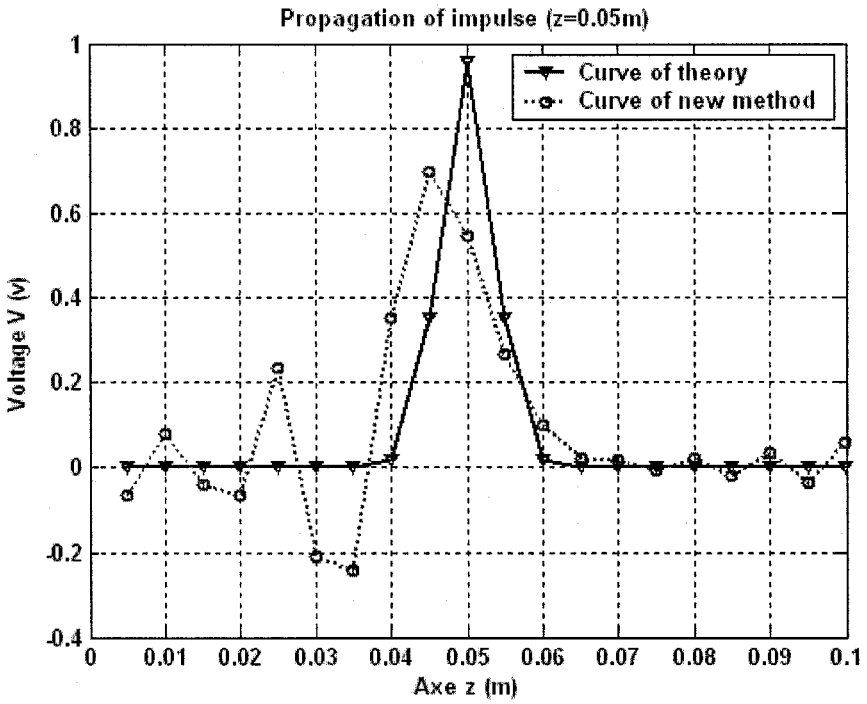

Figure 6.2 The case of N=20 < 134.

In Figure 6.2:

Parameters: L= 100nH, C= 111.11pF, $R = 10\Omega$, G=0.05S,
T = 0.3333ns, z = 50mm. N=20

Excitation: periodic Gaussian pulse in (6.34)

Curve models: Model of traditional theory in (6.35a).
Model of new method in (6.31a).

Condition (6.32): not satisfied

Analysis of Figure 6.2:

Figure 6.2 is the case where N=20< N_0 =134, condition (6.32) is not satisfied. The output signals are not complete. We can see that the two curves don't coincide because N is too small. When N is too small, there are not only incomplete signals at output, but also the two curves are not well fitting. That is to say, the error is too big in this case.

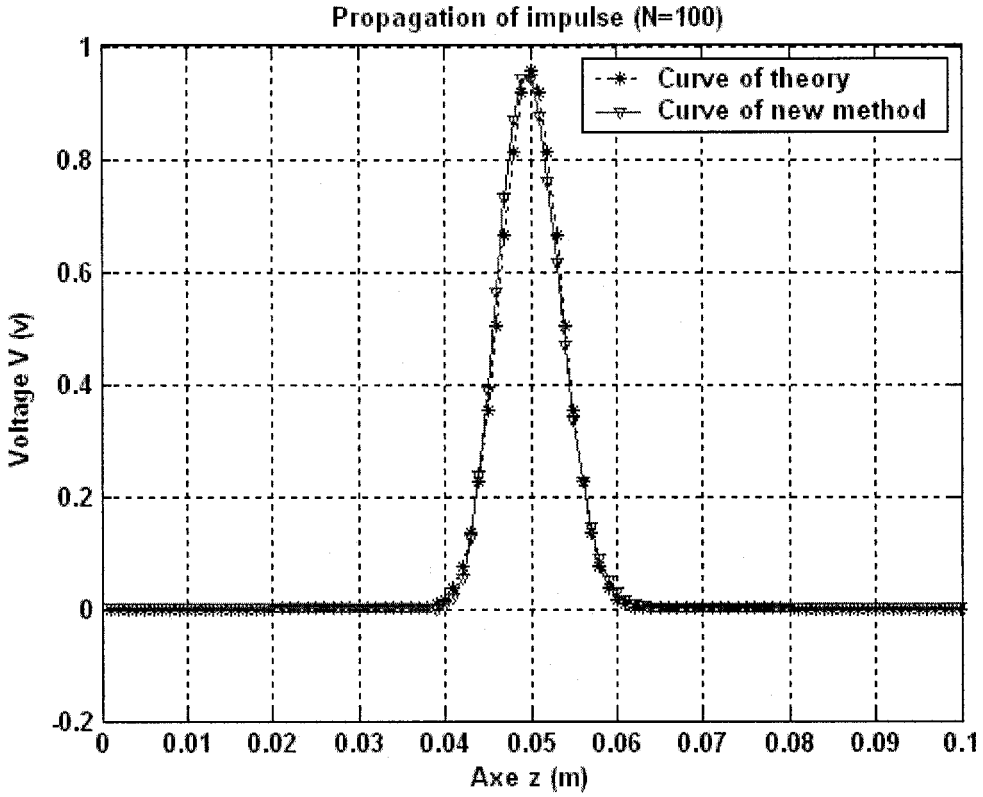

Figure 6.3 The case of z=50mm and N=100 < 134.

In Figure 6.3:

Parameters: L= 100nH, C= 111.11pF, $R = 10\Omega$, $G = 0.05S$,
T = 0.3333ns, z = 50mm. N=100

Excitation: periodic Gaussian pulse in (6.34)

Curve models: Model of traditional theory in (6.35a).
Model of new method in (6.31a).

Condition (6.32): not satisfied

Analysis of Figure 6.3:

Figure 6.3 is the case where $N = 100 < N_0 = 134$, condition (6.32) is not satisfied. But N is not too small and it approaches N_0. The output signals are nearly complete. We can see that the two curves almost coincide.

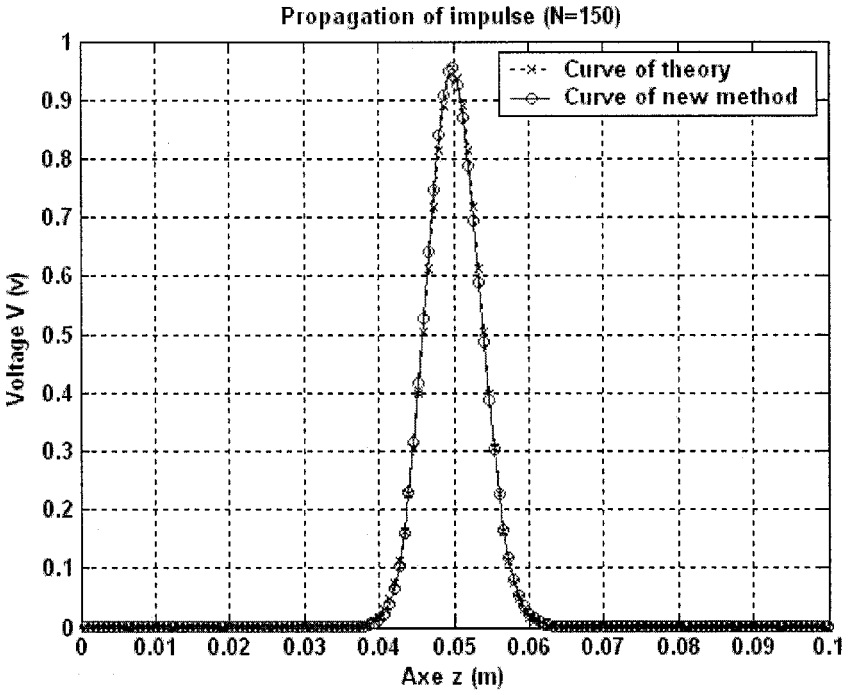

Figure 6.4 The case of z=50mm and N=150 > 134.

In Figure 6.4:

Parameters: L= 100nH, C= 111.11pF, $R = 10\Omega$, $G = 0.05S$,
T = 0.3333ns, z = 50mm. N=150

Excitation: periodic Gaussian pulse in (6.34)

Curve models: Model of traditional theory in (6.35a).
Model of new method in (6.31a).

Condition (6.32): satisfied

Analysis of Figure 6.4:

Figure 6.4 is the case of N=150 > $N_0 = 134$. Condition (6.32) is satisfied. The output signals are complete. We can see that the two curves coincide well.

Example 6.2 The parameters T, R, G, L, C, and the Gaussian impulse are the same as in Example 6.1. We consider that z is far from the origin, for example, z = 460mm. In this example $N_0 \approx 667$ .We take N=200, 400, 800 to see the effect of the two formulas.

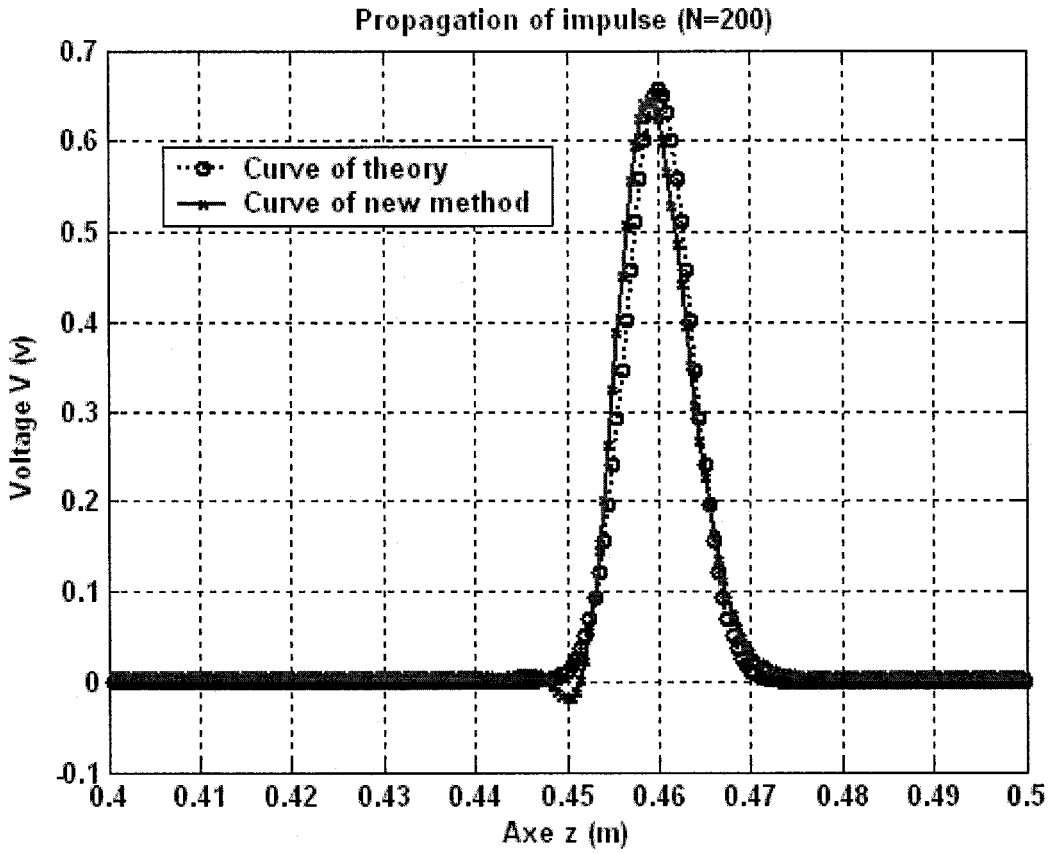

Figure 6.5 The case of z = 460mm and N=200 <667.

In Figure 6.5:

Parameters: L= 100nH, C= 111.11pF, $R = 10\Omega$, $G = 0.05S$,
T = 0.3333ns, z = 460mm. N=200

Excitation: periodic Gaussian pulse in (6.34)

Curve models: Model of traditional theory in (6.35a).
Model of new method in (6.31a).

Condition (6.32): not satisfied

Analysis of Figure 6.5:

Figure 6.5 is the case of N=200< N_0 =667. Condition (6.32) is not satisfied. The output signals of the new method are not complete. There is distortion and they are incomplete if N is much lower than N_0. The error is too big in this case.

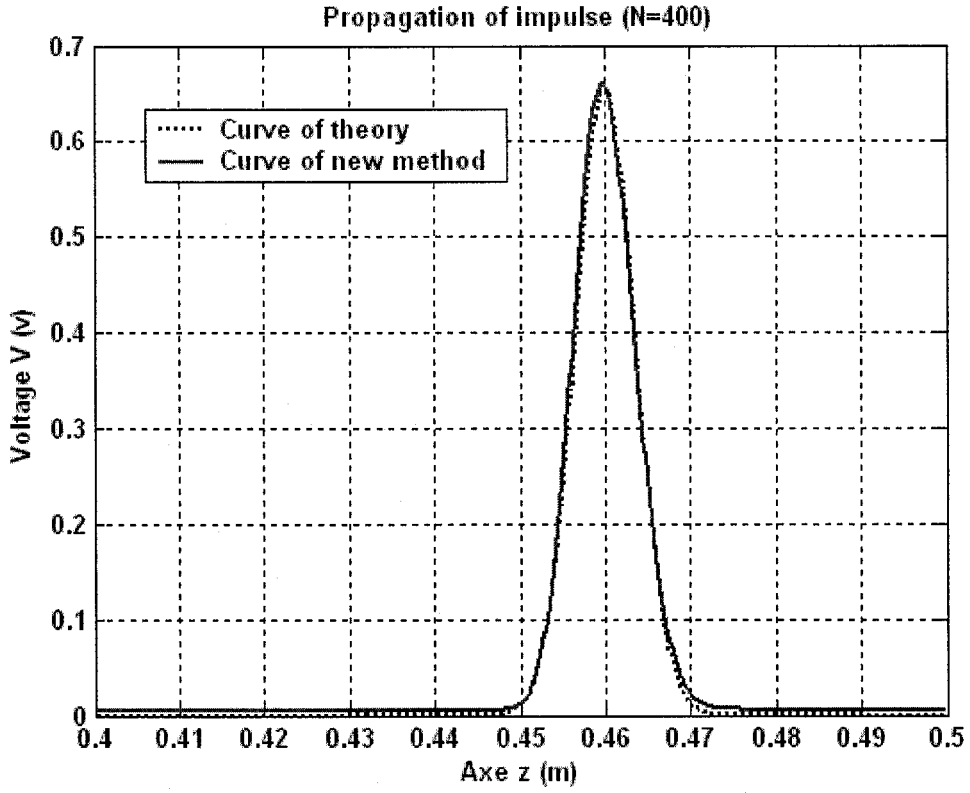

Figure 6.6 The case of z=460mm and N=400 <667.

In Figure 6.6:

Parameters: L= 100nH, C= 111.11pF, $R = 10\Omega$, $G = 0.05S$,
T = 0.3333ns, z = 460mm. N=400

Excitation: periodic Gaussian pulse in (6.34)

Curve models: Model of traditional theory in (6.35a).
Model of new method in (6.31a).

Condition (6.32): not satisfied

Analysis of Figure 6.6:

Figure 6.6 is the case where N=400< N_0 =667, condition (6.32) is not satisfied. But N is not too small, it nearly approaches N_0. The output signals are almost complete. We can see that the two curves almost coincide. The error is small in this case. From figure 6.6, we see that the voltage amplitude decays 1/3 at point z. The wave can be decayed a lot if z is far from the source even if in lower case (not lossless).

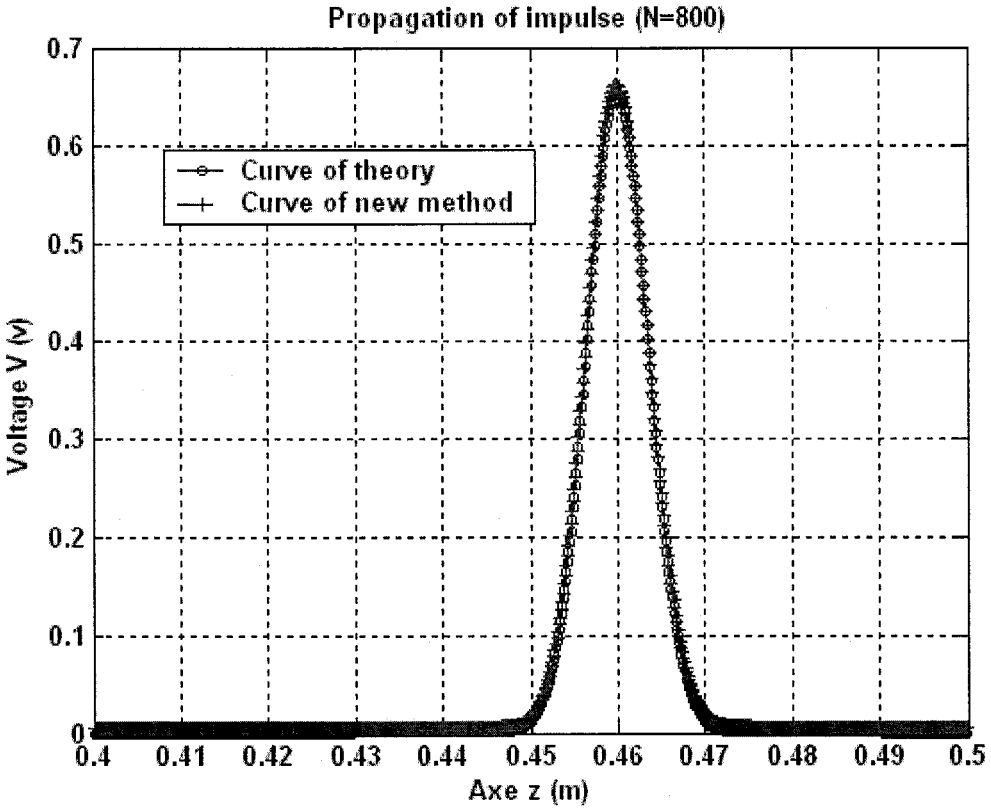

Figure 6.7 The case of z=460mm and N=800 >667.

In Figure 6.7:

Parameters: L= 100nH, C= 111.11pF, $R = 10\Omega$, $G = 0.05S$,
T = 0.3333ns, z = 460mm. N=800

Excitation: periodic Gaussian pulse in (6.34)

Curve models: Model of traditional theory in (6.35a).
Model of new method in (6.31a).

Condition (6.32): satisfied

Analysis of Figure 6.7:

Figure 6.7 is the case where N=800> N_0 =667, condition (6.32) is satisfied. The output signals are complete. We can see that the two curves coincide well. There is little error in this case.

6.5 Numeric computations and convergence

The parameters in this section are given as: T = 0.3333ns, L= 100nH, C= 111.11pF. The impulse is given in (6.34). We shall discuss the following cases:

(a). The lossless case.

(b). The effect of position z on wave propagation.

(c). The convergence on N.

(d). The effect of R and G.

We can discuss the influence of Δt instead of N. In fact, a tiny Δt is equal to a big N if the period of the pulse is fixed.

6.5.1 The lossless case

The lossless transmission lines were discussed in Chapter 5. The lossless case is not included in (6.31) as a particular case. Although most demonstrations in this Chapter can be suitable for lossless cases, the conditions at infinity are different. Hence the solution discussions and the constants that were determined are different. So the solutions in this chapter are not suitable for the lossless case, that is, we cannot obtain the voltage and current of lossless transmission lines in (6.31) by choosing R=G=0. That's why we discuss them separately. If one chooses that R=G=0 in (6.31), what will happen? It will yield the wrong results. We can see this from Example 6.3.

Example 6.3 In this example, at first, we'll show figure 6.8 which wrongly uses (6.31) by setting R = G =0. The R and G could not equal zero at the same time in (6.31), that is, the lossless case is not included in (6.31). Then we want to know whether the new theory is suitable or not if R and G approach zero in (6.31). Figures 6.9-6.11, in the second part of this example, will answer this question.

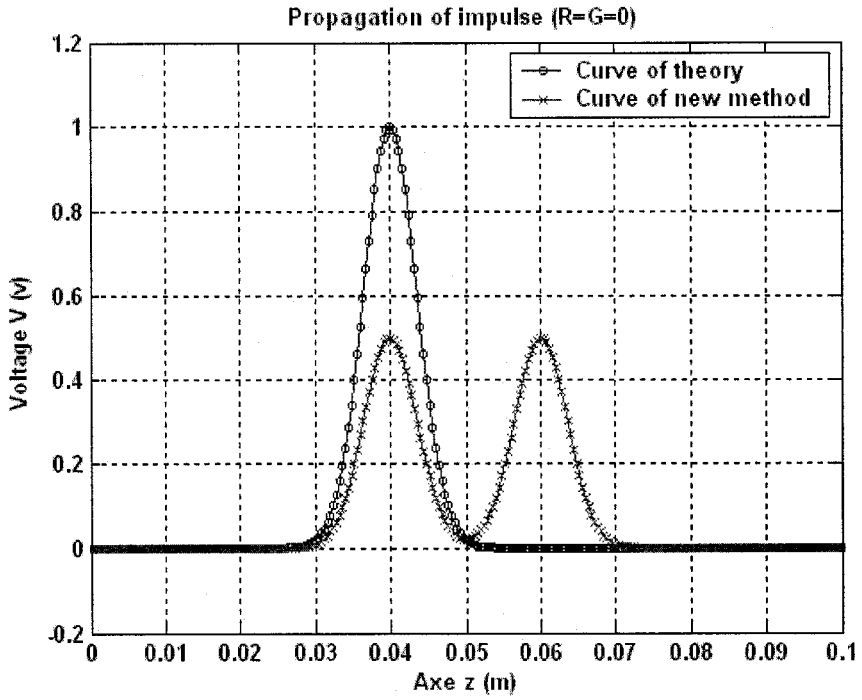

Figure 6.8 The wrong use of the solutions (6.31) by choosing R=G=0.

In Figure 6.8:

Parameters: T= 0.3333ns, L= 100nH, C= 111.11pF, R=0, G=0
z = 40mm. N=250

Excitation: periodic Gaussian pulse in (6.34)

Curve models: Model of traditional theory in (6.35a).
Model of new method in (6.31a).

Condition of lossy case: not satisfied

Analysis of Figure 6.8:

Figure 6.8 shows that the output is two pulses when the input is one pulse. The energy is divided into two equal parts at the output. The voltage amplitude is reduced to half of the input.

The theory curve is one pulse. Hence the result of the lossless case by choosing R=G=0 in (6.31) is wrong.

Therefore, formulas (6.31) of the lossy case are not inclusive for a lossless case in particular.

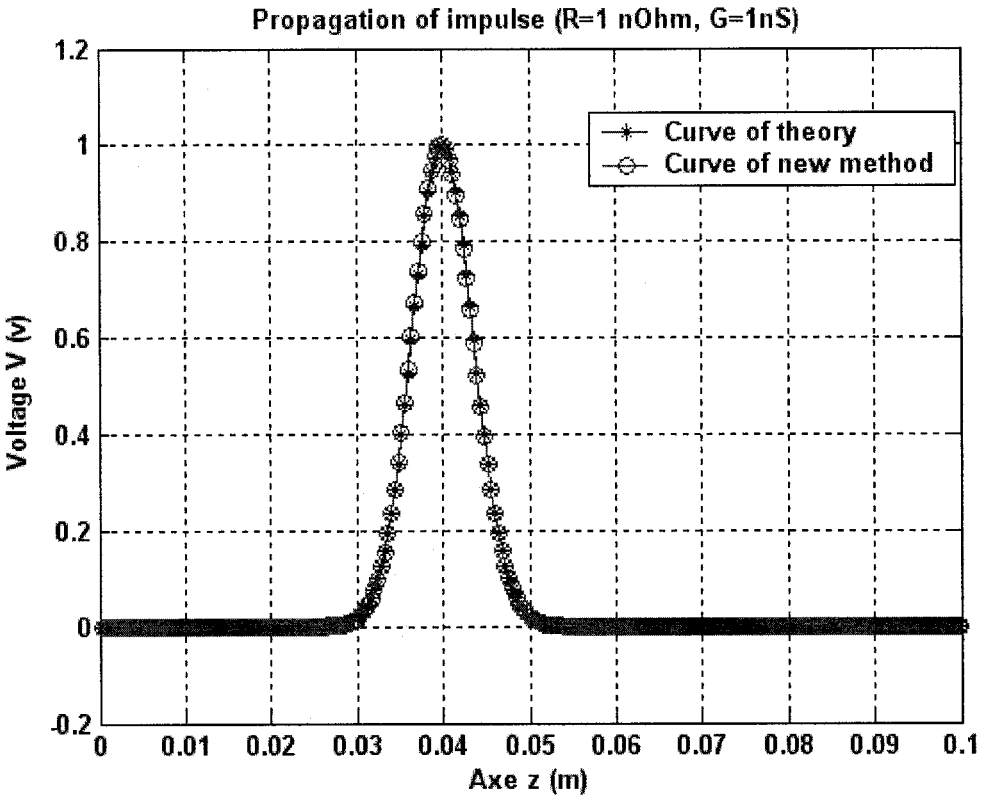

Figure 6.9 The case of R= 1 nΩ and G=1nS.

In Figure 6.9:

Parameters: T= 0.3333ns, L= 100nH, C= 111.11pF, R= 1nΩ, G=1nS
z = 40mm. N=250

Excitation: periodic Gaussian pulse in (6.34)

Curve models: Model of traditional theory in (6.35a).
Model of new method in (6.31a).

Condition of lossy case: satisfied

Condition (6.33): satisfied

Analysis of Figure 6.9:

We want to know whether the new theory is suitable when both R and G are tiny. In Figure 6.9, we set $G=10^{-9}$ S, R= $10^{-9}\Omega$ which approach zero. Figure 6.9 shows that there is no phenomenon of two pulses. The response signals are complete and the curve of the new method coincides well with that of traditional theory.

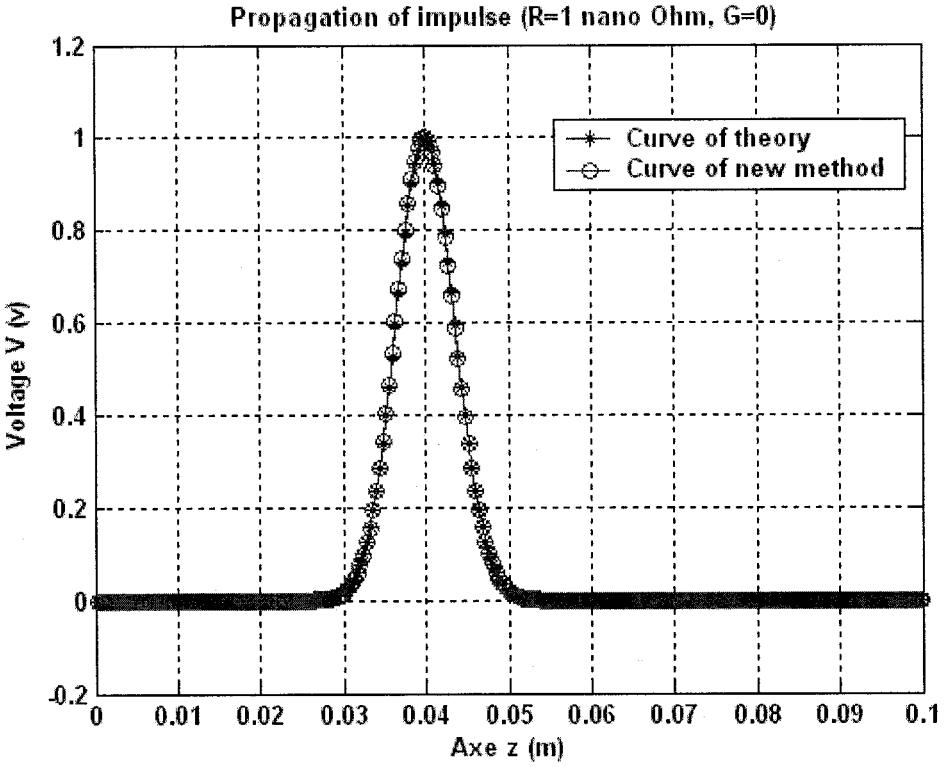

Figure 6.10 The case of R= 1nΩ and G=0.

In Figure 6.10:

Parameters: T= 0.3333ns, L= 100nH, C= 111.11pF, R= 1nΩ, G=0
z = 40mm. N=250

Excitation: periodic Gaussian pulse in (6.34)

Curve models: Model of traditional theory in (6.35a).
Model of new method in (6.31a).

Condition of lossy case: satisfied

Condition (6.33): satisfied

Analysis of Figure 6.10:

We want to know whether the new theory is suitable if R or G is zero, and the other is very small. In Figure 6.10, we choose G=0, R= $10^{-9}\Omega$. Figure 6.10 shows that there is no phenomenon of two pulses. Besides, the response signals are complete and the curve of the new method coincides well with that of traditional theory.

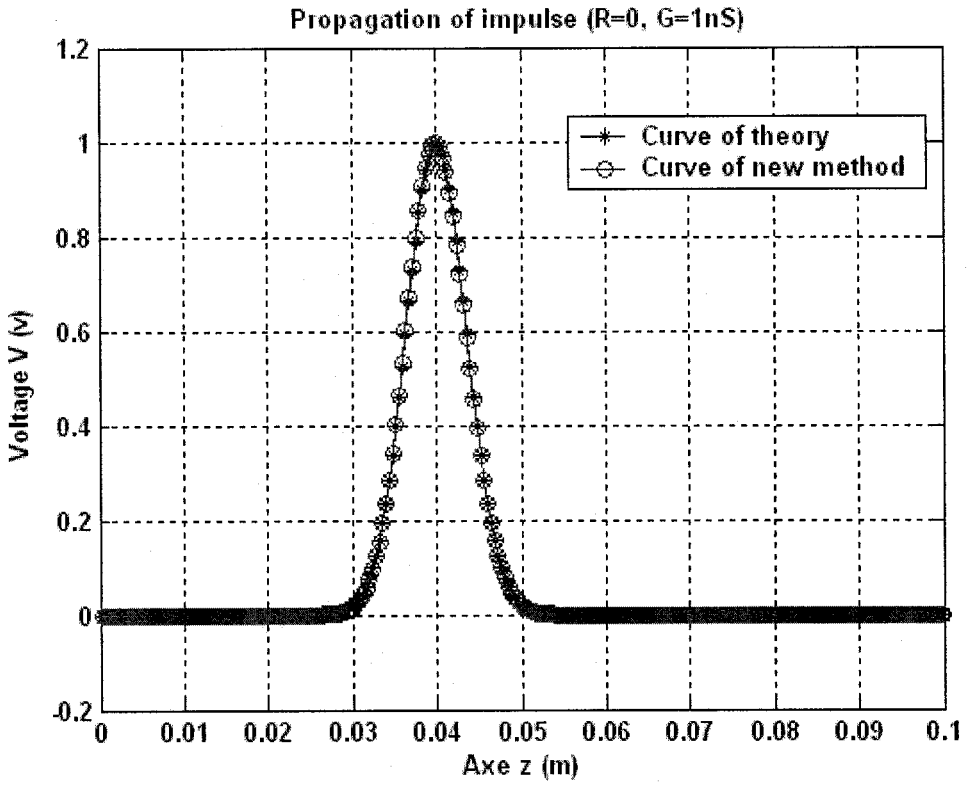

Figure 6.11 The case of R= 0 and G=1nS.

In Figure 6.11:

Parameters: T= 0.3333ns, L= 100nH, C= 111.11pF, R= 0, G=1nS
z = 40mm. N=250

Excitation: periodic Gaussian pulse in (6.34)

Curve models: Model of traditional theory in (6.35a).
Model of new method in (6.31a).

Condition of lossy case: satisfied

Condition (6.33): satisfied

Analysis of Figure 6.11:

This time we change to R=0 and G=10^{-9} S is very small to see whether the new theory is correct. Figure 6.11 shows that there is no phenomenon of two pulses, neither. The response signals are complete and the curve of the new method coincides well with that of traditional theory.

6.5.2 The effect of position z on wave propagation

Now we turn to study the effect of position z on wave propagation.

Example 6.4 We'll show the effects of position z=0, 70, 260, 540, 850 (mm), respectively.

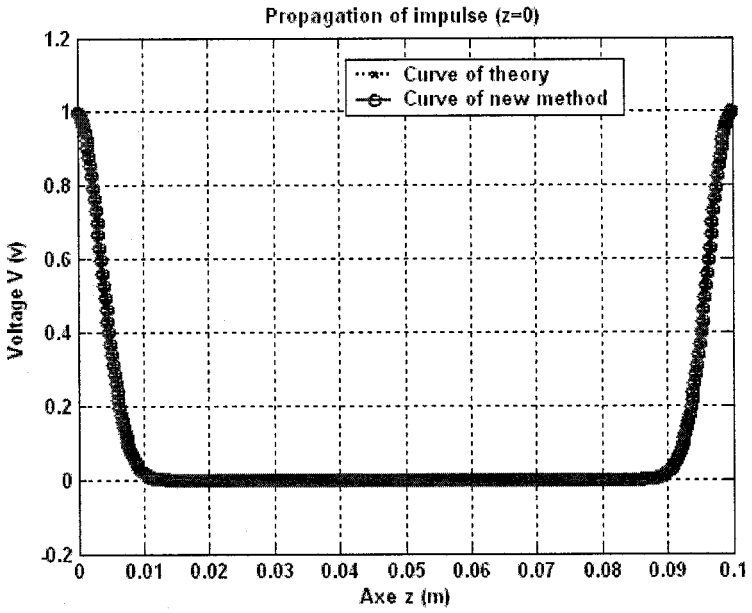

Figure 6.12 The case of z = 0 and N=500.

In Figure 6.12:

Parameters: T= 0.3333ns, L= 100nH, C= 111.11pF, R=10 Ω , G=0.05S
N=500, z =0

Excitation: periodic Gaussian pulse in (6.34)

Curve models: Model of traditional theory in (6.35a).
Model of new method in (6.31a).

Condition (6.32): satisfied

Analysis of Figure 6.12:

Figure 6.12 shows the result of the simulation of the wave propagating over one wave length. The wave does not yet propagate at the origin. The theoretical curve represents the excitation over one period. So we can say in this case that the curve of the new method coincides well with that of traditional theory.

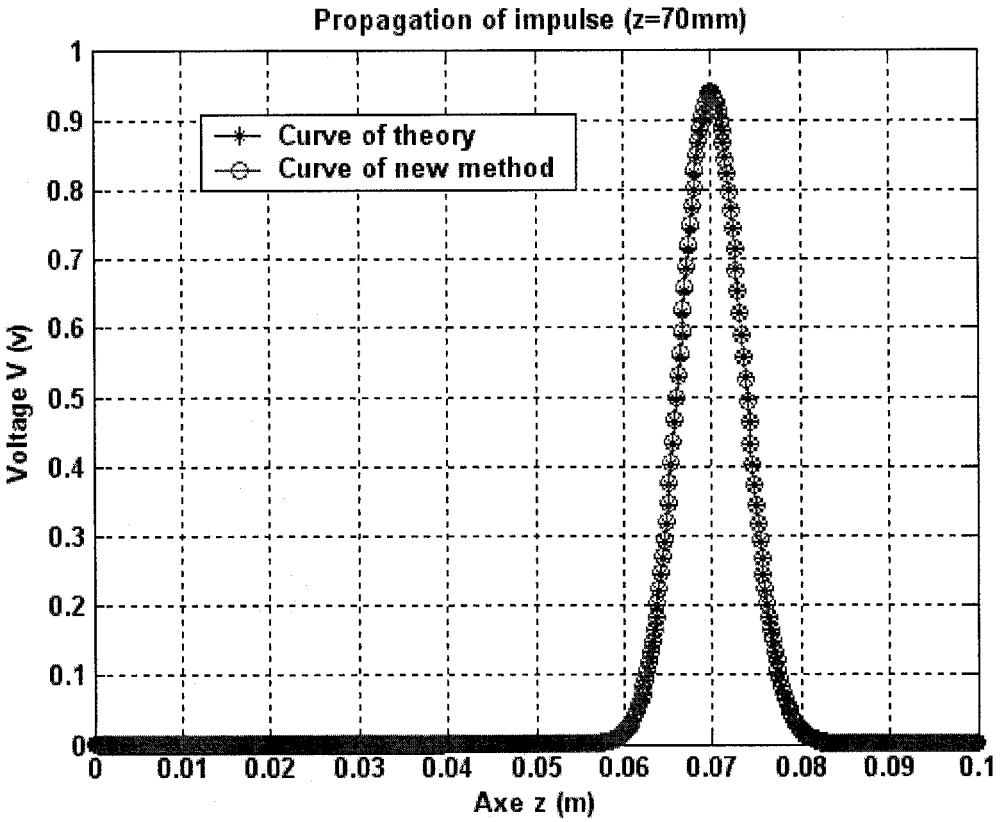

Figure 6.13 The case of z = 70mm and N=500.

In Figure 6.13:

Parameters: T= 0.3333ns, L= 100nH, C= 111.11pF, R=10 Ω , G=0.05S
N=500, z =70mm

Excitation: periodic Gaussian pulse in (6.34)

Curve models: Model of traditional theory in (6.35a).
Model of new method in (6.31a).

Condition (6.32): satisfied

Analysis of Figure 6.13:

Figure 6.13 shows that the simulation of a front wave arrives at z=70mm, conditions (6.32) and (6.33) are satisfied for N_0 =133. Hence the curve of the new method coincides well with that of traditional theory in this case. There is 0.05 V(0.5dB) loss in the voltage amplitude at point z which is within one wave length.

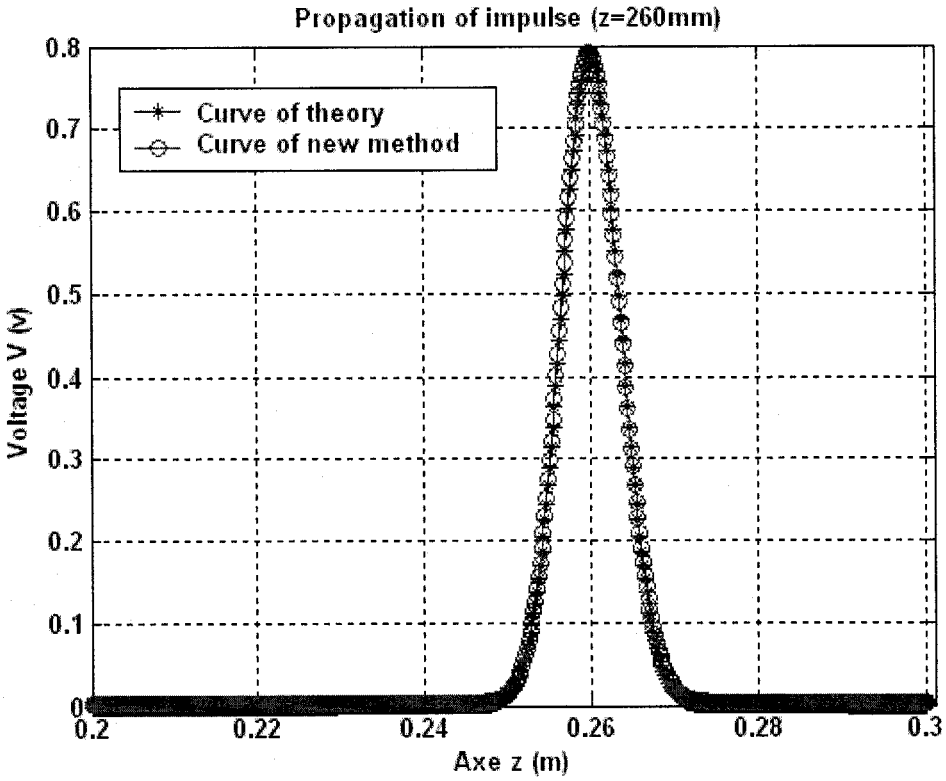

Figure 6.14 The case of z = 260mm and N=500.

In Figure 6.14:

Parameters: T= 0.3333ns, L= 100nH, C= 111.11pF, R=10 Ω , G=0.05S
N=500, z =260mm

Excitation: periodic Gaussian pulse in (6.34)

Curve models: Model of traditional theory in (6.35a).
Model of new method in (6.31a).

Condition (6.32): satisfied

Analysis of Figure 6.14:

Figure 6.14 shows that the simulation of the front wave arrives at z=260mm. We obtain N_0 =400 in (6.32) for this case. Conditions (6.32) and (6.33) are satisfied. Hence the curve of the new method coincides well with that of traditional theory in this case. There is a 0.2 V (2dB) loss in voltage amplitude at point z which is within three wave lengths.

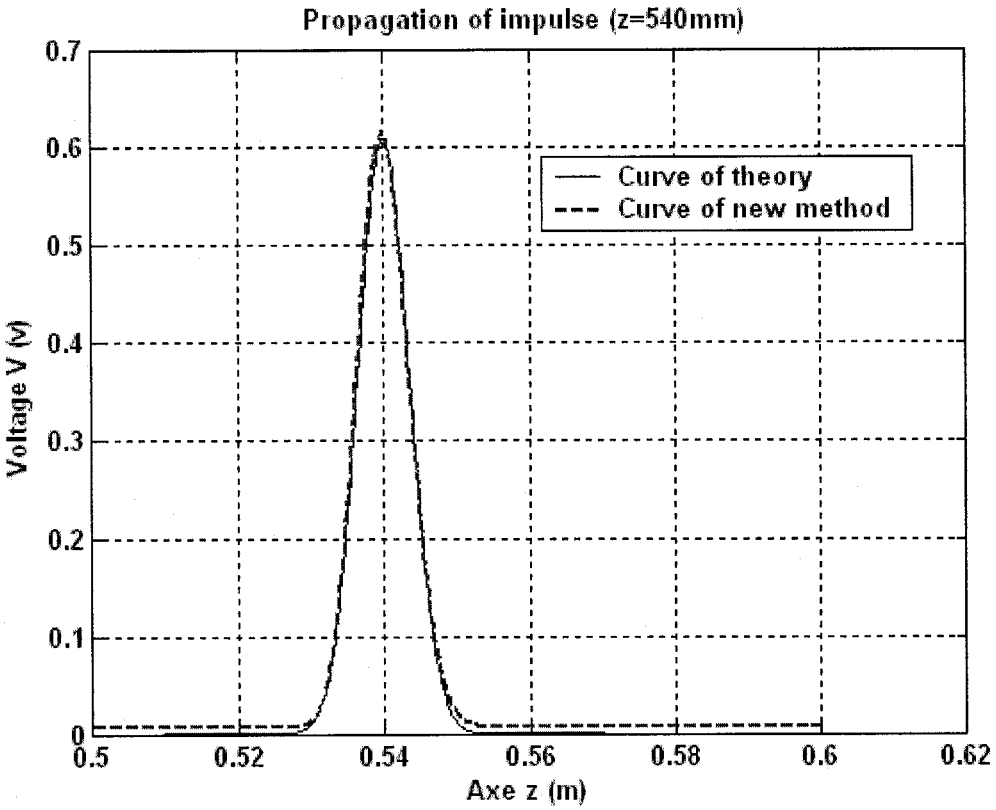

Figure 6.15 The case of z = 540mm and N=500.

In Figure 6.15:

Parameters: T= 0.3333ns, L= 100nH, C= 111.11pF, R=10 Ω , G=0.05S
N=500, z =540mm

Excitation: periodic Gaussian pulse in (6.34)

Curve models: Model of traditional theory in (6.35a).
Model of new method in (6.31a).

Condition (6.32): not satisfied

Analysis of Figure 6.15:

Figure 6.15 shows the simulation of the front wave arriving at z=540mm. We obtain N_0 =800 from (6.32) in this case. Conditions (6.32) and (6.33) are not satisfied. Hence the curve of the new method differs slightly with that of traditional theory. There is a 0.4 V (4.5dB) loss in voltage amplitude at point z which is within six wave lengths.

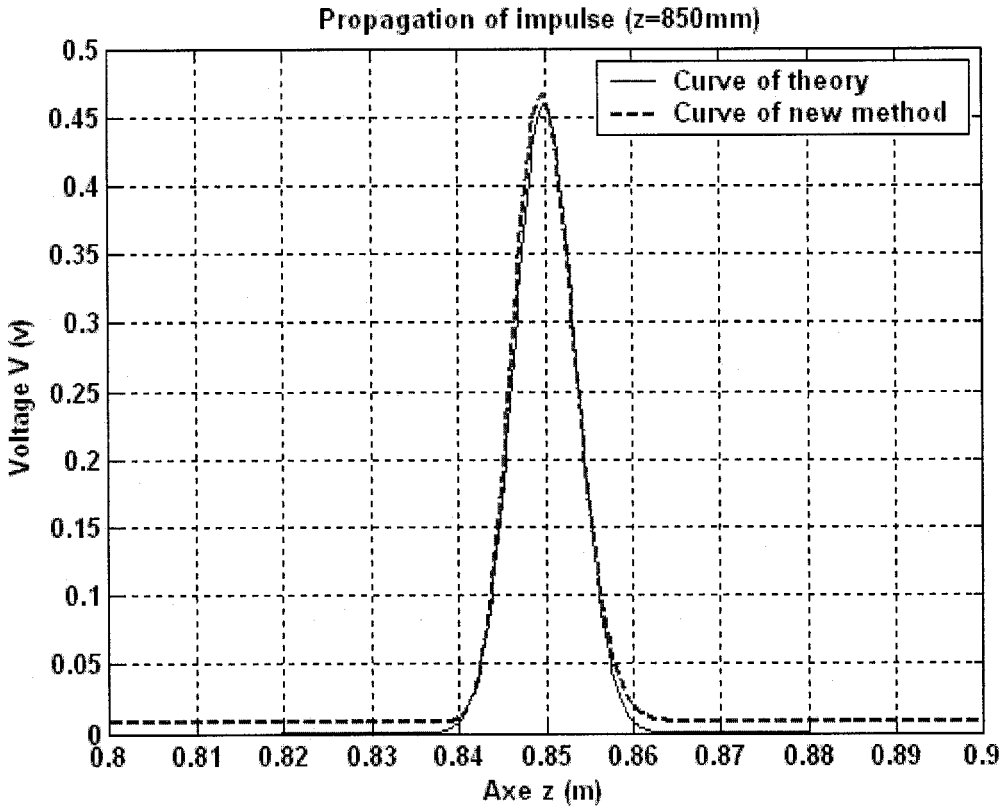

Figure 6.16 The case of z = 850mm and N=500.

In Figure 6.16:

Parameters: T= 0.3333ns, L= 100nH, C= 111.11pF, R=10 Ω , G=0.05S
N=500, z =850mm

Excitation: periodic Gaussian pulse in (6.34)

Curve models: Model of traditional theory in (6.35a).
Model of new method in (6.31a).

Condition (6.32): not satisfied

Analysis of Figure 6.16:

This time we choose z far from the origin at z=850mm. In this case, N_0 =1200. Conditions (6.32) and (6.33) are not satisfied. The curve of the new method is obviously different with that of traditional theory. There is a 0.57 V (6.5dB) loss in voltage amplitude at point z which is within nine wave lengths.

6.5.3 The convergence on N

We'll discuss the influence of the number N of partition on wave propagation.

Example 6.5 We'll choose N=100, 300, 500, respectively, to see the effect of N.

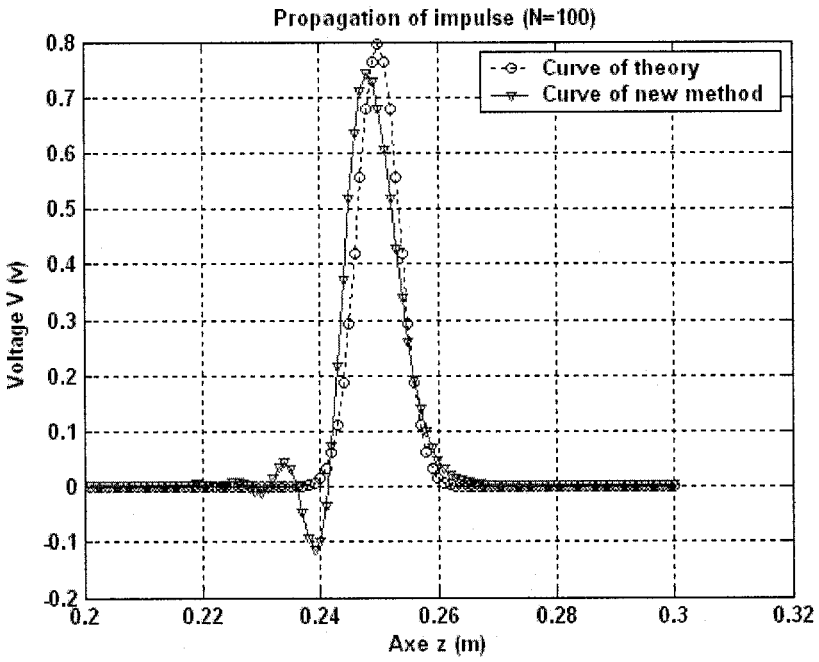

Figure 6.17 The case of N=100 and z=250mm.

In Figure 6.17:

Parameters: T= 0.3333ns, L= 100nH, C= 111.11pF, R=10 Ω , G=0.05S
z =250mm, N=100

Excitation: periodic Gaussian pulse in (6.34)

Curve models: Model of traditional theory in (6.35a).
Model of new method in (6.31a).

Condition (6.32): not satisfied

Analysis of Figure 6.17:

In this case N_0 =400. Conditions (6.32) and (6.33) are not satisfied. The curve of the new method is obviously different with that of traditional theory. There is distortion with the new method. There is a 0.2 V (2dB) loss in voltage amplitude at point z which is within three wave lengths.

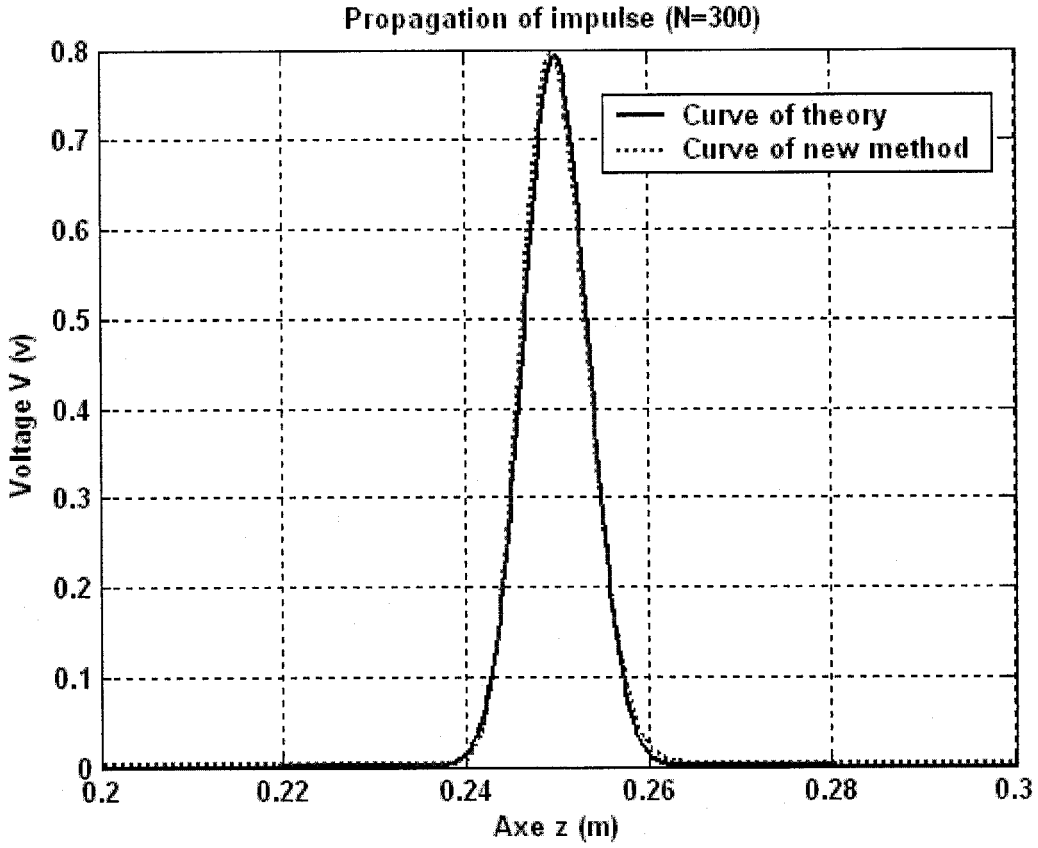

Figure 6.18 The case of N=300 and at point z=250mm.

In Figure 6.18:

Parameters: T= 0.3333ns, L= 100nH, C= 111.11pF, R=10 Ω , G=0.05S
z =250mm, N=300

Excitation: periodic Gaussian pulse in (6.34)

Curve models: Model of traditional theory in (6.35a).
Model of new method in (6.31a).

Condition (6.32): not satisfied

Analysis of Figure 6.18:

In this case N_0 =400. Conditions (6.32) and (6.33) are not satisfied. The curve of the new method is a little different with that of traditional theory. There is a 0.2 V (2dB) loss in voltage amplitude at point z which is within three wave lengths.

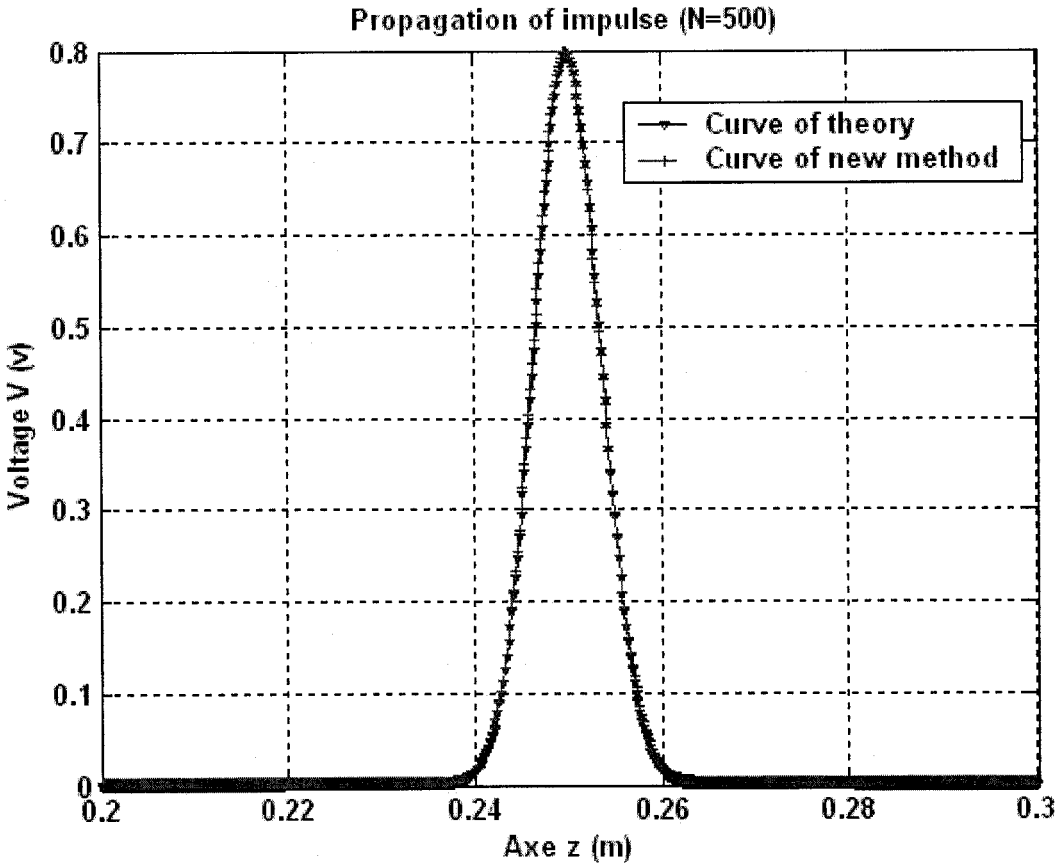

Figure 6.19 The case of N=500 at point z=250mm.

In Figure 6.19:

Parameters: T= 0.3333ns, L= 100nH, C= 111.11pF, R=10 Ω , G=0.05S
z =250mm, N=500

Excitation: periodic Gaussian pulse in (6.34)

Curve models: Model of traditional theory in (6.35a).
Model of new method in (6.31a).

Condition (6.32): satisfied

Analysis of Figure 6.19:

In this case N_0 =400. Conditions (6.32) and (6.33) are satisfied. The curve of the new method coincides with that of traditional theory. There is a 0.2 V (2dB) loss in voltage amplitude at point z which is within three wave lengths.

6.5.4 The effect of R and G

Now we want to know the effects of R and G when they are increasing.

Example 6.6 We fix R=10Ω, and choose G=0.08, 0.1, 0.15 and 0.2 S, respectively. We choose N and z such that (6.32) and (6.33) are satisfied.

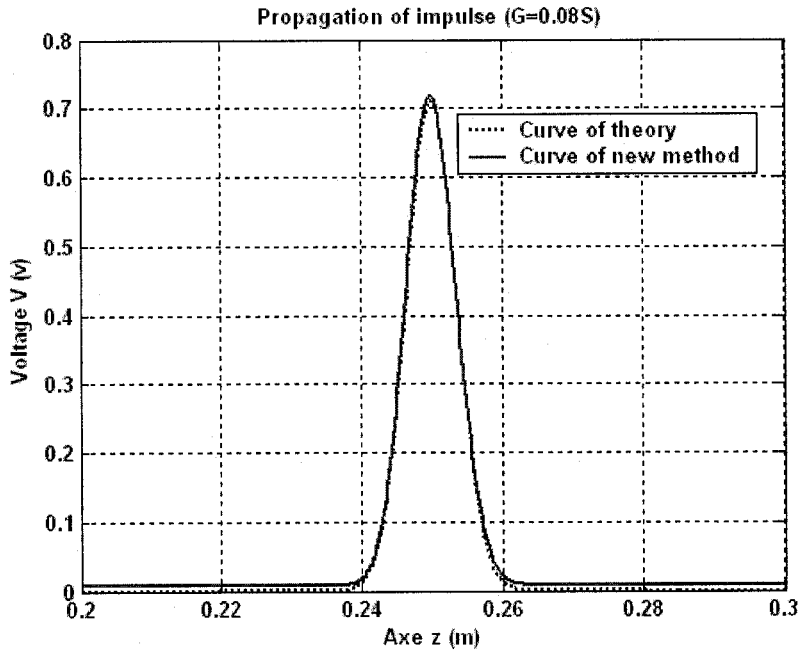

Figure 6.20 The case of G=0.08S and $R = 10\Omega$.

In Figure 6.20:

Parameters: T= 0.3333ns, L= 100nH, C= 111.11pF, z =250mm, N=500
R=10Ω, G=0.08S

Excitation: periodic Gaussian pulse in (6.34)

Curve models: Model of traditional theory in (6.35a).
Model of new method in (6.31a).

Condition $G << \omega C$ satisfied

Analysis of Figure 6.20:

The lower loss condition $G << \omega C$ shows that $G << 2S$ and $\omega C / G$=25. The curve of the new method coincides with that of traditional theory. There is a 0.3 V (3dB) loss in voltage amplitude at point z which is within three wave lengths.

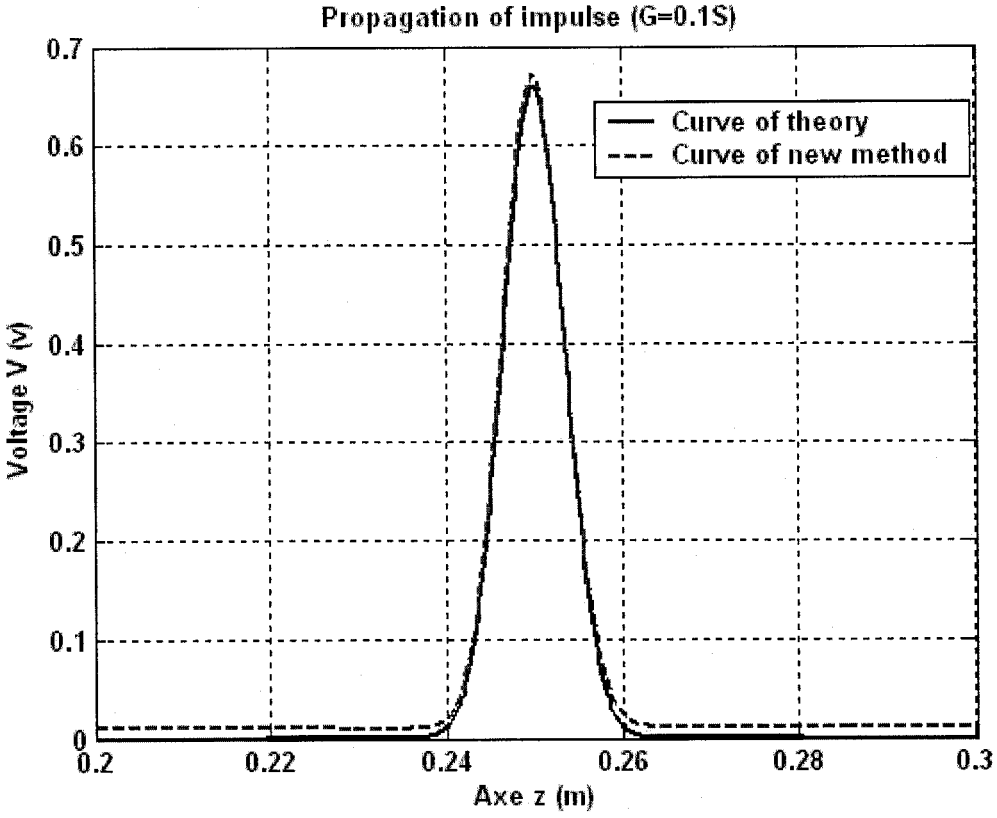

Figure 6.21 The case of G=0.1S and $R = 10\Omega$.

In Figure 6.21:

Parameters: T= 0.3333ns, L= 100nH, C= 111.11pF, z =250mm, N=500
R=10 Ω, G=0.1S

Excitation: periodic Gaussian pulse in (6.34)

Curve models: Model of traditional theory in (6.35a).
Model of new method in (6.31a).

Condition lower loss: almost satisfied

Analysis of Figure 6.21:

In this case $\omega C / G$ =20. We think that the conditions of lower loss are almost satisfied. The curve of the new method is a little different than that of traditional theory. There is a 0.35 V (3.7dB) loss in voltage amplitude at point z which is within three wave lengths. R and G influence the effects of wave propagation and simulation

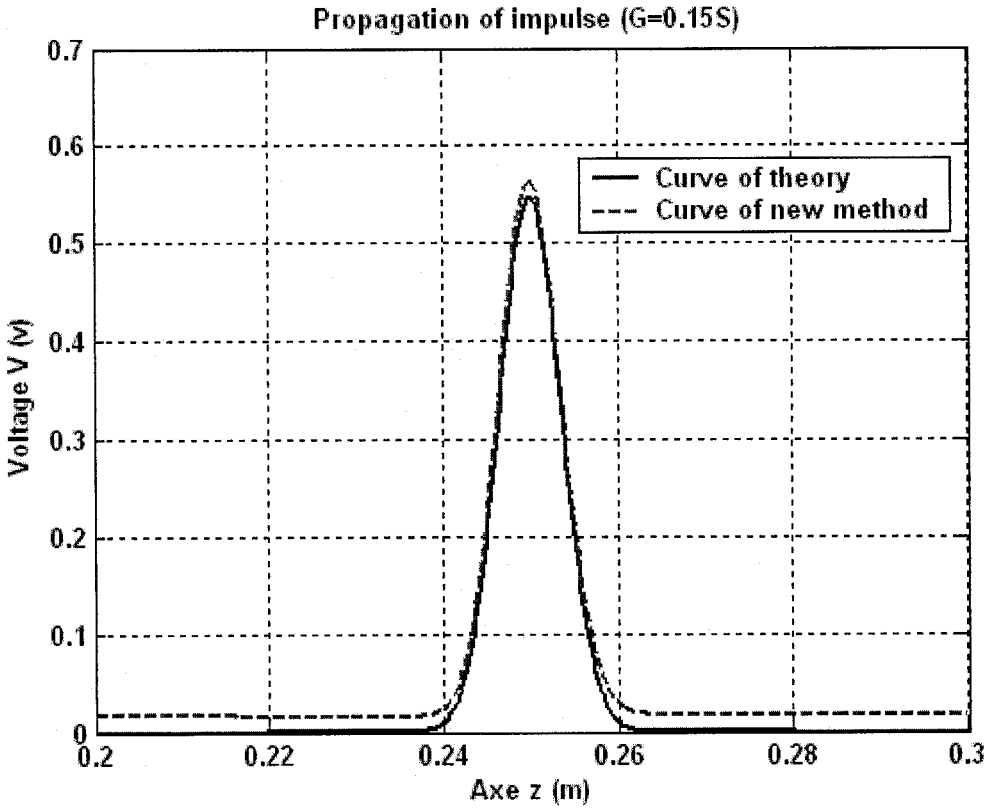

Figure 6.22 The case of G=0.15S and $R = 10\Omega$.

In Figure 6.22:

Parameters: T= 0.3333ns, L= 100nH, C= 111.11pF, z =250mm, N=500
R=10Ω, G=0.15S

Excitation: periodic Gaussian pulse in (6.34)

Curve models: Model of traditional theory in (6.35a).
Model of new method in (6.31a).

Condition lower loss: almost not satisfied

Analysis of Figure 6.22:

In this case $\omega C / G$=13. We think that the conditions of lower loss are almost not satisfied in this case. The curve of the new method differs from that of traditional theory. There is a 0.45 V (5dB) loss in voltage amplitude at point z which is within three wave lengths.

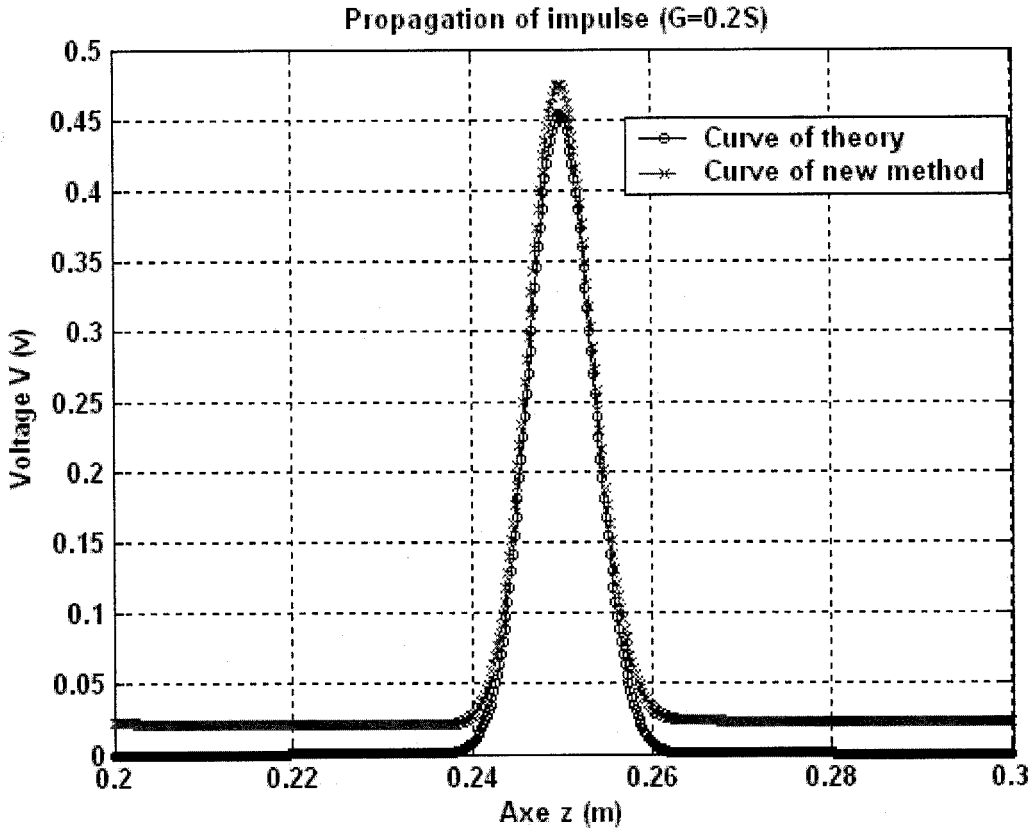

Figure 6.23 The case of G=0.2S and $R = 10\Omega$.

In Figure 6.23:

Parameters: T= 0.3333ns, L= 100nH, C= 111.11pF, z =250mm, N=500
R=10Ω, G=0.2S

Excitation: periodic Gaussian pulse in (6.34)

Curve models: Model of traditional theory in (6.35a).
Model of new method in (6.31a).

Condition lower loss: not satisfied

Analysis of Figure 6.23:

In this case $\omega C / G = 10$. We think that the conditions of lower loss are not satisfied in this case. The curve of the new method is much different with that of traditional theory. There is a 0.55 V (7dB) loss in voltage amplitude at point z which is within three wave lengths.

Example 6.7 Now we set G=0.05S and choose R=100 Ω ,200 Ω ,300 Ω , 400 Ω , respectively.

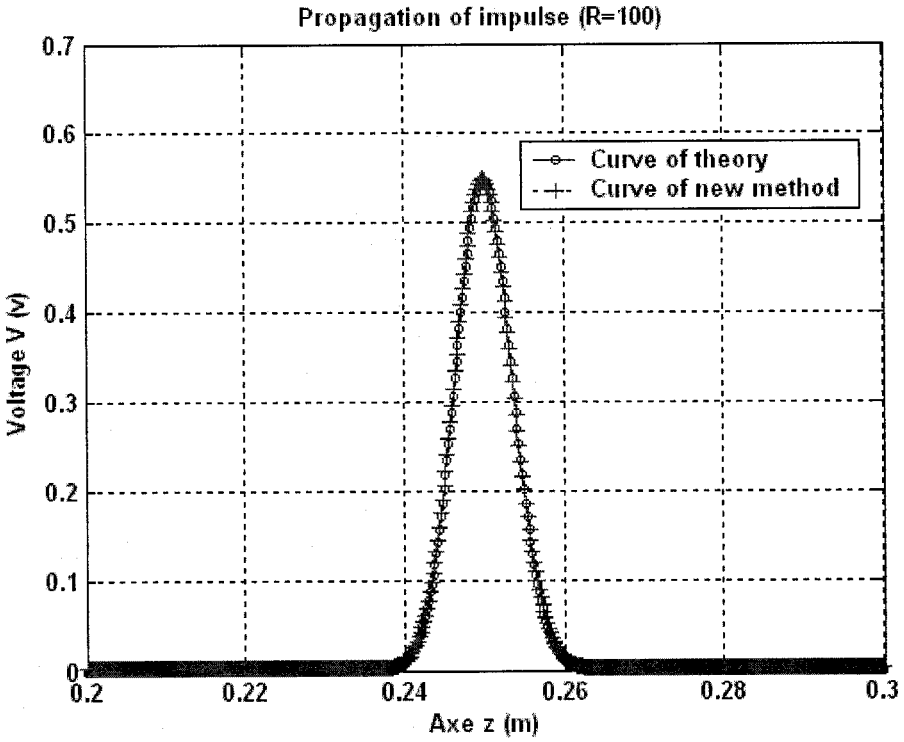

Figure 6.24 The case of $R = 100\Omega$ and G=0.05S.

In Figure 6.24:

Parameters: T= 0.3333ns, L= 100nH, C= 111.11pF, z =250mm, N=500
G=0.05S, R=100 Ω

Excitation: periodic Gaussian pulse in (6.34)

Curve models: Model of traditional theory in (6.35a).
Model of new method in (6.31a).

Condition lower loss: satisfied

Analysis of Figure 6.24:

The lower loss condition $R << \omega L$ shows that $R << 1900\Omega$. In this case $\omega L / R$=19. We think that the conditions of lower loss are satisfied in this case. The curve of the new method coincides with that of traditional theory. There is a 0.35 V (3.7dB) loss in voltage amplitude at point z which is within three wave lengths.

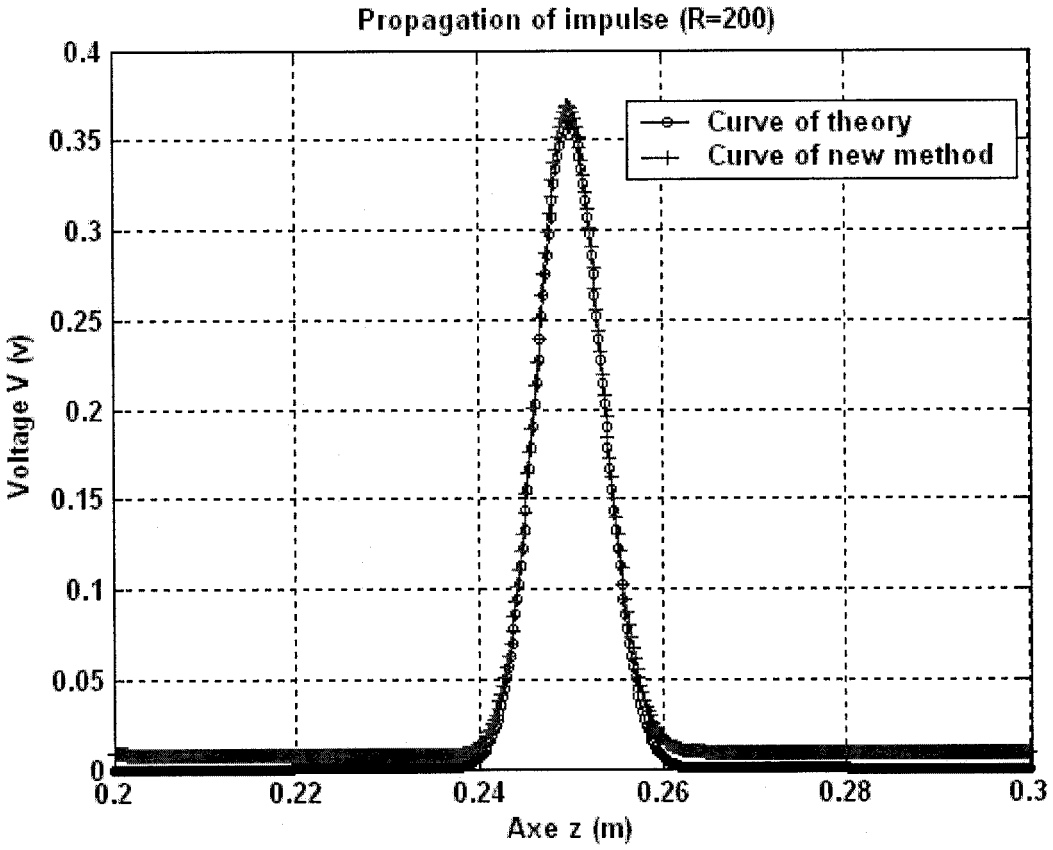

Figure 6.25 The case of $R = 200\Omega$ and G=0.05S

In Figure 6.25:

Parameters: T= 0.3333ns, L= 100nH, C= 111.11pF, z =250mm, N=500
G=0.05S, R=200 Ω

Excitation: periodic Gaussian pulse in (6.34)

Curve models: Model of traditional theory in (6.35a).
Model of new method in (6.31a).

Condition lower loss: almost satisfied

Analysis of Figure 6.25:

In this case $\omega L / R$ =9.5. We think that the conditions of lower loss are almost satisfied in this case. The curve of the new method is a little different from that of traditional theory. There is a 0.65 V (9dB) loss in voltage amplitude at point z which is within three wave lengths.

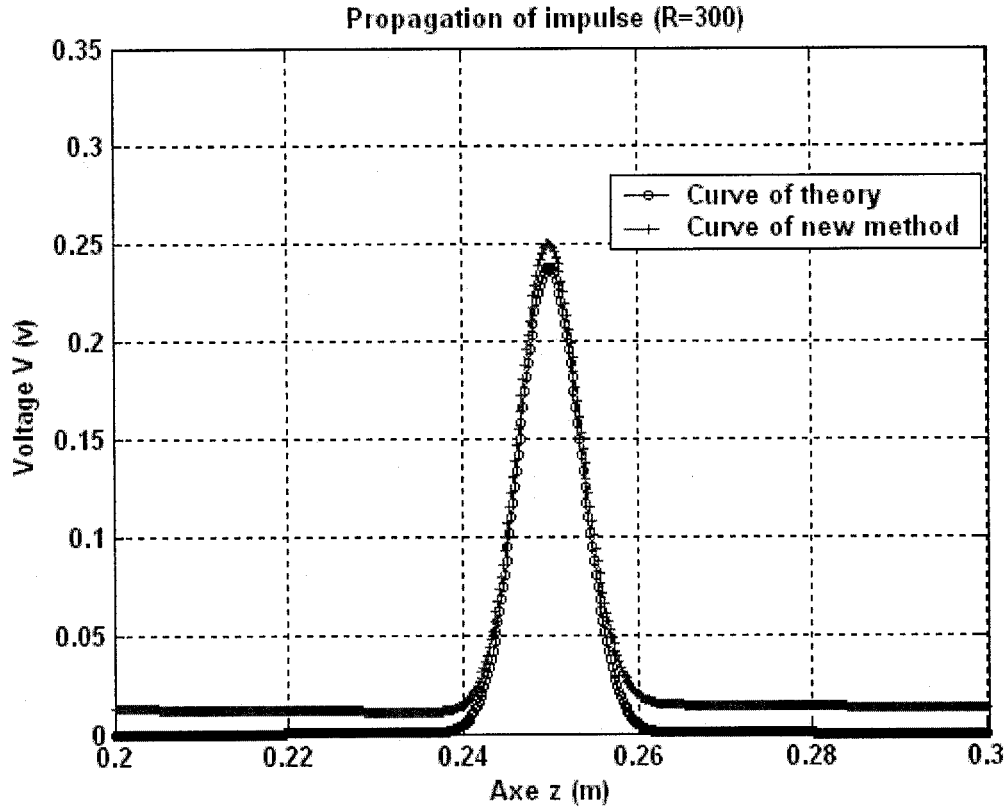

Figure 6.26 The case of R=300 Ω and G=0.05S

In Figure 6.26:

Parameters: T= 0.3333ns, L= 100nH, C= 111.11pF, z =250mm, N=500
G=0.05S, R=300 Ω

Excitation: periodic Gaussian pulse in (6.34)

Curve models: Model of traditional theory in (6.35a).
Model of new method in (6.31a).

Condition lower loss: not satisfied

Analysis of Figure 6.26:

In this case $\omega L / R$=6.3. We think that the conditions for lower loss are not satisfied in this case. The curve of the new method is obviously different from that of traditional theory. There is a 0.77 V (12.8dB) loss in voltage amplitude at point z which is within three wave lengths.

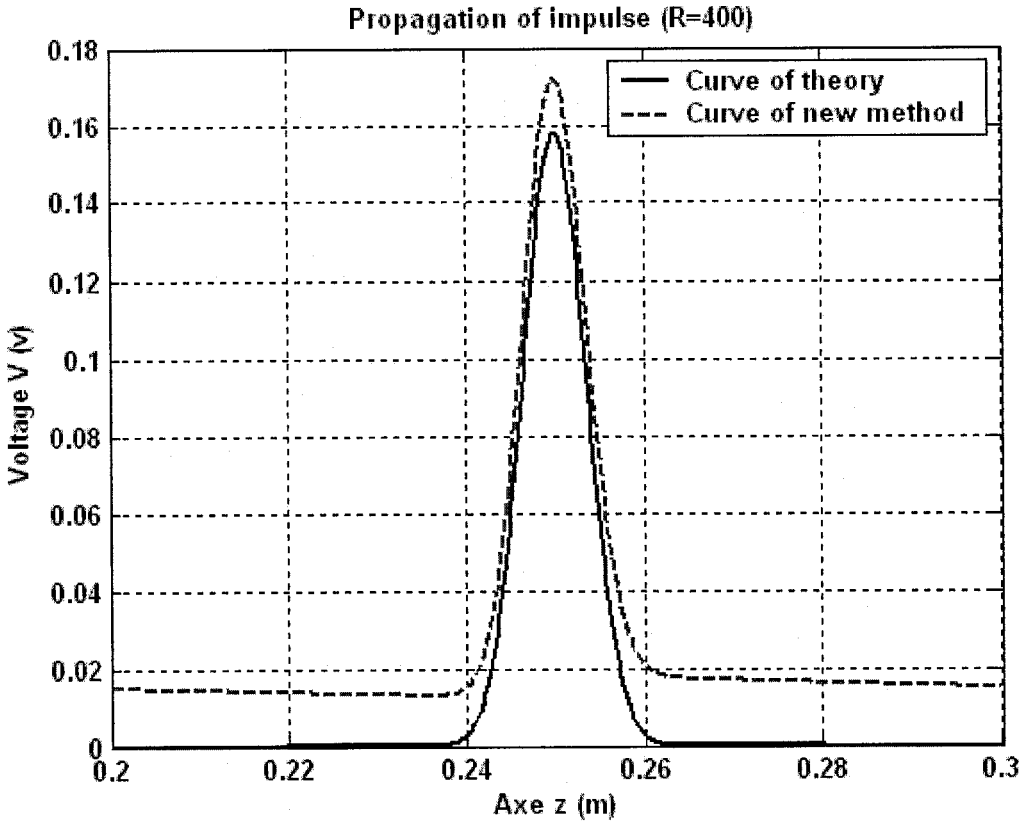

Figure 6.27 The case of R=400 Ω and G=0.05S

In Figure 6.27:

Parameters: T= 0.3333ns, L= 100nH, C= 111.11pF, z =250mm, N=500
G=0.05S, R=400 Ω

Excitation: periodic Gaussian pulse in (6.34)

Curve models: Model of traditional theory in (6.35a).
Model of new method in (6.31a).

Condition lower loss: not satisfied

Analysis of Figure 6.27:

In this case $\omega L / R$ =4.75. We think that the conditions for lower loss are obviously not satisfied in this case. The curve of the new method is greatly different from that of traditional theory. There is a 0.84 V (16dB) loss in voltage amplitude point z which is within three wave lengths.

CHAPTER 7

CHARACTERISTIC PARAMETERS OF TRANSMISSION LINES

In this chapter, we shall discuss the characteristic parameters of lossless transmission lines such as characteristic impedance, reflection coefficient, input impedance, voltage standing-wave ratio (VSWR) and generator and load matching etc.

7.1 Characteristic impedance

In this chapter, the uppercase letters represent the quantities in the original domain; the lowercase letters present the quantities in the transformed domain. We can rewrite the solutions (5.12) of telegraph equations in short form

$$\vec{v}(z)=\vec{v}^{+}(z)+\vec{v}^{-}(z), \tag{7.1a}$$

$$\vec{i}(z)=\vec{i}^{+}(z)+\vec{i}^{-}(z), \tag{7.1b}$$

where $\vec{v}^{+}=e^{-\vec{\Lambda}z}.*\vec{a}_1$ and $\vec{v}^{-}=e^{\vec{\Lambda}z}.*\vec{a}_2$, and $\vec{i}^{+}$ and $\vec{i}^{-}$ have similar forms.

In Chapters 5, 6, we have already demonstrated that the term $\vec{V}^{+}$ coincides with the traditional incident voltage. Hence $\vec{V}^{+}$ in that case is just the incident voltage. In the original domain, the characteristic impedance Z_0 can be defined by the current and voltage as

$$\vec{V}_0^{+}=Z_0\vec{I}_0^{+}. \tag{7.2}$$

Another relation of current and voltage can be obtained as

$$\vec{V}_0^{-}=-Z_0\vec{I}_0^{-}. \tag{7.3}$$

We come to the following conclusion:

The characteristic impedance Z_0 is invariant under the transformations of the new theory.

That is

$$\vec{v}_0^{+} = Z_0 \vec{i}_0^{+}. \tag{7.4}$$

7.2 Voltage and current expressed by input

Let $\vec{v}_0$ and $\vec{i}_0$ be the voltage and current at input port z=0 in the transformed domain. Then, the expressions of voltage and current by input port can be written as

$$\vec{v}(z) = \frac{\vec{v}_0 + Z_0 \vec{i}_0}{2} .* e^{-\vec{\Lambda} z} + \frac{\vec{v}_0 - Z_0 \vec{i}_0}{2} .* e^{\vec{\Lambda} z}, \tag{7.5a}$$

$$\vec{i}(z) = \frac{\vec{v}_0 + Z_0 \vec{i}_0}{2Z_0} .* e^{-\vec{\Lambda} z} - \frac{\vec{v}_0 - Z_0 \vec{i}_0}{2Z_0} .* e^{\vec{\Lambda} z}, \tag{7.5b}$$

Now, we assume that the voltage $\vec{V}_0$ and the current $\vec{I}_0$ at the input port are given as shown in Figure 7.1. The solutions of voltage and current at the input port in the original domain can be written as

$$\vec{V}(z) = T \frac{\vec{v}_0 + Z_0 \vec{i}_0}{2} .* e^{-\vec{\Lambda} z} + T \frac{\vec{v}_0 - Z_0 \vec{i}_0}{2} .* e^{\vec{\Lambda} z}, \tag{7.6a}$$

$$\vec{I}(z) = T \frac{\vec{v}_0 + Z_0 \vec{i}_0}{2Z_0} .* e^{-\vec{\Lambda} z} - T \frac{\vec{v}_0 - Z_0 \vec{i}_0}{2Z_0} .* e^{\vec{\Lambda} z}. \tag{7.6b}$$

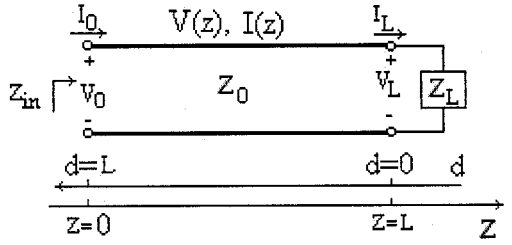

Figure 7.1 A transmission line terminated by load impedance Z_L

7.3 Voltage and current expressed by output

Now we assume that there is a load Z_L at the terminal port. We denote by $\vec{v}_L$ and $\vec{i}_L$ the terminated voltage and current in the transformed domain. Then

$$\vec{v}_L = \vec{v}_0^{+} .* e^{-\vec{\Lambda} L} + \vec{v}_0^{-} .* e^{\vec{\Lambda} L}, \tag{7.7a}$$

$$\vec{i}_L = \vec{i}_0^{+} .* e^{-\vec{\Lambda} L} + \vec{i}_0^{-} .* e^{\vec{\Lambda} L} . \tag{7.7b}$$

The solutions of voltage and current at the terminal port in the original domain can be written as

$$\vec{v}(z) = \frac{\vec{v}_L + Z_0 \vec{i}}{2} .* e^{\vec{\Lambda}(L-z)} + \frac{\vec{v}_L - Z_0 \vec{i}}{2} .* e^{-\vec{\Lambda}(L-z)}, \tag{7.8a}$$

$$\vec{i}(z) = \frac{\vec{v}_L + Z_0 \vec{i}_L}{2Z_0} .* e^{\vec{\Lambda}(L-z)} - \frac{\vec{v}_L - Z_0 \vec{i}_L}{2Z_0} .* e^{-\vec{\Lambda}(L-z)} . \tag{7.8b}$$

Let us set $d = L - z$. Formulas (7.8) can be rewritten as

$$\vec{v}(d) = \frac{\vec{v}_L + Z_0 \vec{i}}{2} .* e^{\vec{\Lambda} d} + \frac{\vec{v}_L - Z_0 \vec{i}}{2} .* e^{-\vec{\Lambda} d}, \tag{7.9a}$$

$$\vec{i}(d) = \frac{\vec{v}_L + Z_0 \vec{i}_L}{2Z_0} .* e^{\vec{\Lambda} d} - \frac{\vec{v}_L - Z_0 \vec{i}_L}{2Z_0} .* e^{-\vec{\Lambda} d} . \tag{7.9b}$$

The solutions of voltage and current at the input port in the original domain can be written as

$$\vec{V}(d) = T \frac{\vec{v}_L + Z_0 \vec{i}}{2} .* e^{\vec{\Lambda} d} + T \frac{\vec{v}_L - Z_0 \vec{i}}{2} .* e^{-\vec{\Lambda} d}, \tag{7.10a}$$

$$\vec{I}(d) = T \frac{\vec{v}_L + Z_0 \vec{i}_L}{2Z_0} .* e^{\vec{\Lambda} d} - T \frac{\vec{v}_L - Z_0 \vec{i}_L}{2Z_0} .* e^{-\vec{\Lambda} d} . \tag{7.10b}$$

7.4 Reflection coefficients

The traditional load impedance at d=0 in the original domain can be defined as

$$\vec{V}(0) = Z_L \vec{I}(0) . \tag{7.11}$$

The relation among voltage, current and traditional load impedance at d=0 in the transformed domain can be expressed as

$$\vec{v}(0) = Z_L \vec{i}(0) . \tag{7.12}$$

Let us denote by Γ_L the traditional load reflection coefficient in the original domain. Then, at d=0

$$\vec{V}_L^{-} = \Gamma_L \vec{V}_L^{+} . \tag{7.13}$$

We have the following property:

The load reflection coefficient Γ_L is invariant under the transformations of the new theory

In fact, from (7.13) we can derive

$$\vec{v}_L^- = \Gamma_L \vec{v}_L^+ . \tag{7.14}$$

Then, (7.12) gives

$$\Gamma_L = \frac{Z_L - Z_0}{Z_L + Z_0} . \tag{7.15}$$

The voltage and current on the lines can be written as

$$\vec{v}(d) = \vec{v}_L^+ .*\left(e^{\bar{\Lambda} d} + \Gamma_L e^{-\bar{\Lambda} d}\right), \tag{7.16a}$$

$$\vec{i}(d) = \frac{\vec{v}_L^+}{Z_0} .*\left(e^{\bar{\Lambda} d} - \Gamma_L e^{-\bar{\Lambda} d}\right). \tag{7.16b}$$

The reflection coefficient $\Gamma_{in}(d)$ at the position d is defined as:

$$\Im\left(\vec{V}^-(d)\right) = \Gamma_{in}(d)\Im\left(\vec{V}^+(d)\right), \tag{7.17}$$

where $\Im$ is the Fourier transform, and Γ_{in} is dependent on ω. The load reflection coefficient Γ_L is Γ_{in} at $d = 0$.

7.5 Input impedance

The input impedance $Z_{in}(d)$ can be defined as

$$\Im\left(\vec{V}(d)\right) = Z_{in}(d)\Im\left(\vec{I}(d)\right). \tag{7.18}$$

where Z_{in} is dependent on ω. From (7.17), we can obtain

$$Z_{in}(d) = Z_0 \frac{1+\Gamma_{in}(d)}{1-\Gamma_{in}(d)} . \tag{7.19}$$

Then, if we take d=0 in (7.19), there will be

$$Z_{in}(0) = Z_L = Z_0 \frac{1+\Gamma_L}{1-\Gamma_L}, \tag{7.20}$$

which is the same as in (7.15).

7.6 Voltage standing-wave ratio (VSWR)

The voltage standing-wave ratio is defined by

$$VSWR = \frac{1+|\Gamma_L|}{1-|\Gamma_L|}. \tag{7.21}$$

The Voltage standing-wave ratio is invariant under the transmission of the new theory since Γ_L is invariant.

7.7 Generator and load matches

Figure 7.2 shows a transmission line with an arbitrary generator and load impedances, Z_g and Z_L. We consider the lossless case.

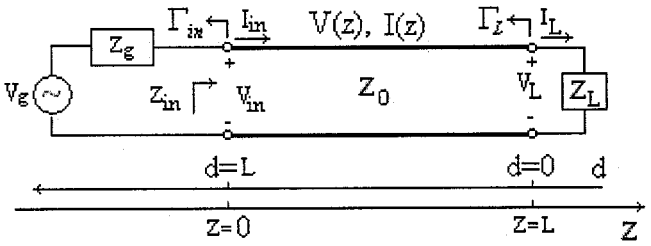

Figure 7.2 Transmission line circuit for mismatched load and generator

The input impedance looking into the terminated transmission line from the generator is given by (7.18). The reflection coefficient Γ_L of the load is given by (7.15). From (7.16), at d=L, the voltage on the line can be written as

$$\vec{V}_{in} = \vec{V}_L^{+}.*\left(e^{\bar{\Lambda}L} + \Gamma_L e^{-\bar{\Lambda}L}\right). \tag{7.22}$$

We can obtain $\vec{V}_L^{+}$ from the voltage at the generator end, where d=L.

$$\Im\left(\vec{V}_{in}\right) = \frac{Z_{in}}{Z_{in}+Z_0}\Im\left(\vec{V}_g\right). \tag{7.23}$$

Let us denote by Γ_g the reflection coefficient seen looking into the generator. Through a similar discussion, we can obtain:

$$\Gamma_g = \frac{Z_g - Z_0}{Z_g + Z_0}. \tag{7.24}$$

Then, $\vec{V}_L^+$ can be found from (7.22) and (7.23).

For a given value of Z_g, the maximum power delivered to Z_{in} can be found by setting $Z_{in} = Z_g^*$.

Load matched to line

The load is matched if $\Gamma_L = 0$. In this case VSWR=1 in (7.21). From (7.15), we conclude that the load matching condition is given as

$$Z_L = Z_0 . \tag{7.25}$$

Generator matched to loaded line

In this case Z_L and Z_0 are chosen to make the input impedance $Z_{in} = Z_g$, so that the generator is matched to the load presented by the terminated transmission line. The total overall reflection coefficient $\Gamma_{in} = 0$:

$$\Gamma_{in} = \frac{Z_{in} - Z_g}{Z_{in} + Z_g} = 0 . \tag{7.26}$$

In this case, the power delivered to Z_{in} is not maximal.

There are other parameters and a lot of problems in transmission lines. The researchers can continue to work on thses.

CHAPTER 8

GROUNDED DIELECTRIC SLAB WAVEGUIDE

8.1 Introduction

In this section, we will study the grounded dielectric slab waveguide. Figure 8.1 shows the geometry of a grounded dielectric slab with the thickness d and relative dielectric constant ε_r. The slab is assumed to be infinite in the yoz plane. We assume that propagation is in the +z direction and that there is no variation in the y direction ($\partial / \partial y = 0$).

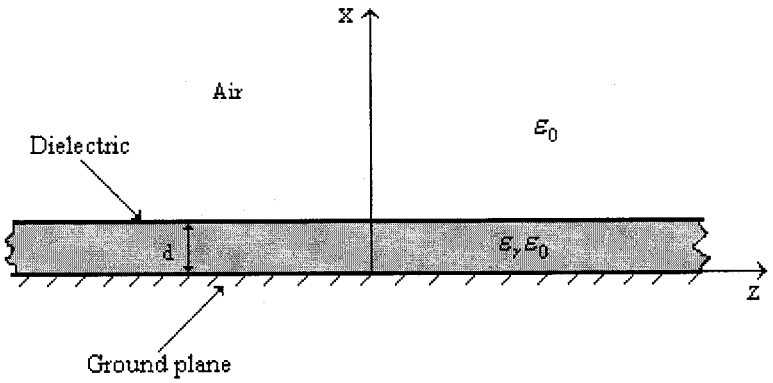

Figure 8.1 Geometry of a grounded dielectric slab

8.2 TM Modes

We transform the electric and magnetic fields $\vec{E}$ and $\vec{H}$ to the standard fields $\vec{e}$ and $\vec{h}$ using $\vec{E} = T_e \vec{e}$ and $\vec{H} = T_h \vec{h}$. The component $\vec{e}_z$ of $\vec{e}$ must satisfy Helmholtz's equation (3.2) and it can be assumed to equal $\exp(-j\vec{\Lambda}_z z).*\vec{M}(x, y)$ from the solution of (3.2), where $\vec{\Lambda}_z$ and $\vec{M}$ are column vectors. Equation (2.1) in this problem becomes

$$\left(\frac{\partial^2}{\partial x^2} + \varepsilon_r \vec{K}_0^2 - \vec{\Lambda}_z^2\right).*\vec{e}_z = 0, \quad for \quad 0 \le x \le d, \tag{8.1a}$$

$$\left(\frac{\partial^2}{\partial x^2}+\vec{\kappa}_0^2-\vec{\Lambda}_z^2\right).*\vec{e}_z=0,\quad for\quad d\le x<\infty, \tag{8.1b}$$

where $\vec{\kappa}_0^2=\vec{\Lambda}_0^2\varepsilon_0\mu/d_0^2$ is a column vector, $\vec{\Lambda}_0^2$ is an eigenvalue vector and d_0 is the length of the interval of partitions on t. We introduce two vectors

$$\vec{K}_c^2=\varepsilon_r\vec{\kappa}_0^2-\vec{\Lambda}_z^2, \tag{8.2a}$$

$$\vec{\Theta}^2=\vec{\Lambda}_z^2-\vec{\kappa}_0^2, \tag{8.2b}$$

and the "sign" of $\vec{\Theta}$ is selected as exponentially decaying for $x>d$ and the vector functions

$$\sin\vec{A}\equiv\frac{1}{2j}\left(e^{j\vec{A}}-e^{-j\vec{A}}\right),$$

$$\cos\vec{A}\equiv\frac{1}{2}\left(e^{j\vec{A}}+e^{-j\vec{A}}\right),$$

for a vector $\vec{A}$. The general solutions of (8.1) are then

$$\vec{M}(x,y)=\sin(\vec{K}_c x).*\vec{A}+\cos(\vec{K}_c x).*\vec{B},\quad for\quad 0\le x\le d, \tag{8.3a}$$

$$\vec{M}(x,y)=\exp(\vec{\Theta}x).*\vec{C}+\exp(-\vec{\Theta}x).*\vec{D},\quad for\quad d\le x<\infty, \tag{8.3b}$$

where $\vec{A}$, $\vec{B}$, $\vec{C}$ and $\vec{D}$ are constant column vectors. From the hypotheses and (3.9), $\vec{h}_x=\vec{e}_y=\vec{h}_z=0$. We use the following boundary conditions to set the constants:

$$\vec{e}_z(x,y,z)=0,\quad at\quad x=0, \tag{8.4a}$$

$$\vec{e}_z(x,y,z),\quad convergent,\quad as\quad x\to\infty, \tag{8.4b}$$

$$\vec{e}_z(x,y,z),\quad continuous\quad at\quad x=d, \tag{8.4c}$$

$$\vec{h}_y(x,y,z),\quad continuous\quad at\quad x=d. \tag{8.4d}$$

We obtain that $\vec{B}$=0 for (8.4a). We must choose $\vec{\Theta}$ such that $\vec{e}_z$ is exponentially decaying for x>d. Condition (8.4b) implies that $\vec{C}=0$ or $\vec{D}=0$. Without loss of generalization, we assume that $\vec{C}=0$. From the continuity of $\vec{e}_z$ at x=d, we have

$$\sin(\vec{K}_c d).*\vec{A}=\exp(-\vec{\Theta}d).*\vec{D}. \tag{8.5}$$

By integration, we obtain

$$\vec{h}_y = -\frac{\varepsilon_r \varepsilon_0}{d_0}\delta \exp(-j\vec{\Lambda}_z z).*\cos(\vec{K}_c x).*\vec{A}./\vec{K}_c, \quad 0 \le x \le d, \tag{8.6a}$$

$$\vec{h}_y = -\frac{\varepsilon_0}{d_0}\delta \exp(-j\vec{\Lambda}_z z)./\vec{\Theta}.*\exp(-\vec{\Theta}x).*\vec{D}, \quad d \le x < \infty, \tag{8.6b}$$

The condition (8.4d) leads to

$$\varepsilon_r \cos(\vec{K}_c d).*\vec{A}./\vec{K}_c = \exp(-\vec{\Theta}d).*\vec{D}./\vec{\Theta}. \tag{8.7}$$

For a nontrivial solution, the determinant of the equations in (8.5) and (8.7) must vanish, thus

$$d\vec{K}_c.*\tan(\vec{K}_c d) = \varepsilon_r d\vec{\Theta}. \tag{8.8}$$

From (8.2),

$$\left(d\vec{K}_c\right)^2 + \left(d\vec{\Theta}\right)^2 = (\varepsilon_r - 1)(d\vec{K}_0)^2. \tag{8.9}$$

Formula (8.9) means that each element in the vectors satisfies a circle equation. The curve of (8.9) is a group of circles. The radius of the ith circle is $\sqrt{\varepsilon_r - 1}d\kappa_{0i}$. We plot the curves in (8.8). The intersections of these curves are the solutions of (8.8) and (8.9). For a nonzero thickness grounded slab with $\varepsilon_r > 1$, there is at least a dominant mode TM_0 for the slab waveguide with zero cutoff frequency.

Once we have choosen $\vec{K}_c$ and $\vec{\Theta}$ for a particular surface wave mode, we can determine $\vec{\Lambda}_z$. From (8.6), we can derive that

$$\vec{e}_x = j\vec{\Lambda}_z.*\exp(-j\vec{\Lambda}_z z).*\cos(\vec{K}_c x).*\vec{A}./\vec{K}_c, \quad 0 \le x \le d, \tag{8.10a}$$

$$\vec{e}_x = j\vec{\Lambda}_z.*\exp(-j\vec{\Lambda}_z z).*\exp(-\vec{\Theta}(x-d)).*\sin(\vec{K}_c d).*\vec{A}./\vec{\Theta}, \quad d \le x < \infty. \tag{8.10b}$$

After obtaining the standard field expression, we can determin the original field $\vec{E}$ and $\vec{H}$. The expressions of original field can then be given by

$$\vec{E}_z = T_e \exp(-j\vec{\Lambda}_z z).*\sin(\vec{K}_c x).*\vec{A}, \quad for \quad 0 \le x \le d, \tag{8.11a}$$

$$\vec{E}_z = T_e \exp(-j\vec{\Lambda}_z z).*\exp(-\vec{\Theta}(x-d)).*\sin(\vec{K}_c d).*\vec{A}, \quad for \quad d \le x < \infty, \tag{8.11b}$$

$$\vec{E}_x = jT_e\vec{\Lambda}_z.*\exp(-j\vec{\Lambda}_z z).*\cos(\vec{K}_c x).*\vec{A}./\vec{K}_c, \quad for \quad 0 \le x \le d, \tag{8.11c}$$

$$\vec{E}_x = jT_e\vec{\Lambda}_z.*\exp(-j\vec{\Lambda}_z z).*\exp(-\vec{\Theta}(x-d)).*\sin(\vec{K}_c d).*\vec{A}./\vec{\Theta}, for \quad d \le x < \infty, \tag{8.11d}$$

$$\vec{H}_y = -\frac{\varepsilon_r\varepsilon_0}{d_0}T_h\delta\exp(-j\vec{\Lambda}_z z).*\cos(\vec{K}_c x).*\vec{A}./\vec{K}_c, \quad for \quad 0 \le x \le d, \tag{8.11e}$$

$$\vec{H}_y = -\frac{\varepsilon_0}{d_0}T_h\delta\exp(-j\vec{\Lambda}_z z).*\exp(-\vec{\Theta}(x-d)).*\sin(\vec{K}_c d).*\vec{A}./\vec{\Theta}, for \quad d \le x < \infty, \tag{8.11f}$$

Figures 8.2 and 8.3 show the graphical solution of the transcendental equation for the cutoff frequency of a TM surface wave mode with d=2mm, i=N/5 and d=5mm, i=N/2, where i correspondents to the ith component.

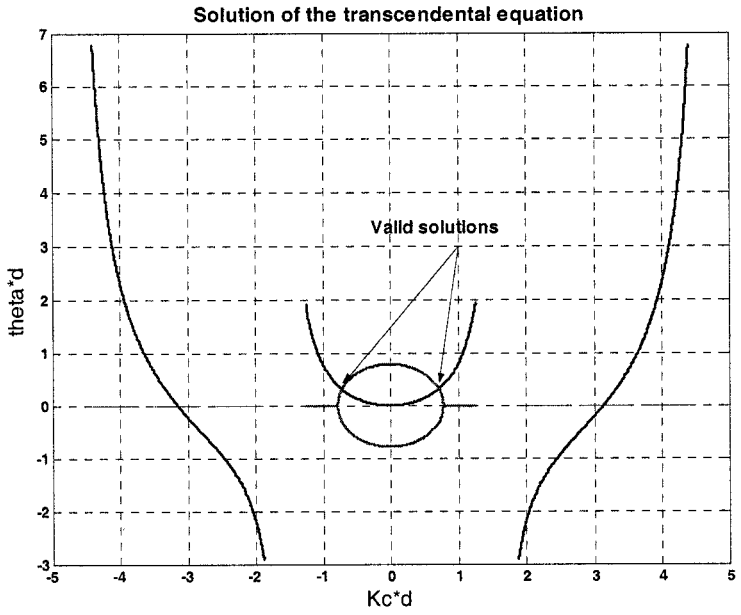

Figure 8.2 Graphical solution of the transcendental equation for the cutoff frequency of a TM mode with d=2mm, i=N/5

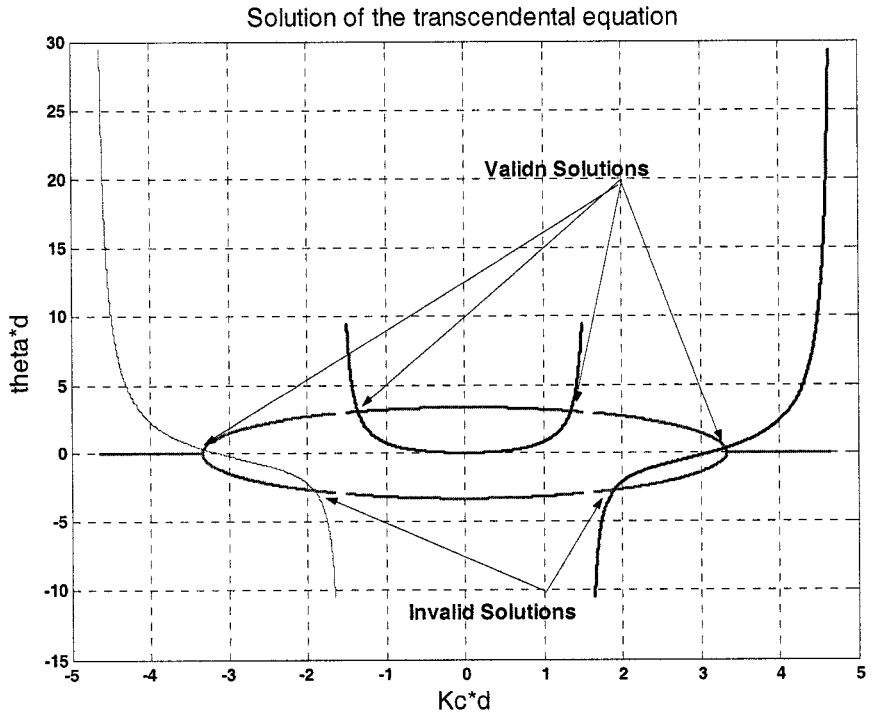

Figure 8.3 Graphical solution of the transcendental equation for the cutoff frequency of a TM mode with d=5 mm, i=N/2

8.3 TE Modes

The grounded dielectric slab waveguide can also support TE modes. As in the discussion above for TM modes, the equations of the standard fields $\vec{e}$ and $\vec{h}$ are

$$\left(\frac{\partial^2}{\partial x^2}\vec{I}+\vec{K}_z^2\right).*\vec{h}_z=0, \quad for \quad 0\le x\le d, \tag{8.12a}$$

$$\left(\frac{\partial^2}{\partial x^2}\vec{I}-\vec{\Theta}_z^2\right).*\vec{h}_z=0, \quad for \quad d\le x<\infty. \tag{8.12b}$$

The solutions of (8.12) are

$$\vec{h}_z=\exp(-j\vec{\Lambda}_z z).*\left(\sin(\vec{K}_c x).*\vec{A}+\cos(\vec{K}_c x).*\vec{B}\right), \quad for \quad 0\le x\le d, \tag{8.13a}$$

$$\vec{h}_z=\exp(-j\vec{\Lambda}_z z).*\left(\exp(\vec{\Theta}x).*\vec{C}+\exp(-\vec{\Theta}x).*\vec{D}\right), \quad for \quad d\le x<\infty. \tag{8.13b}$$

By using the boundary condition of radiation, we have $\vec{C}$=0. We can find $\vec{e}_y$ from $\vec{h}_z$. We can determine the constants for $\vec{A}$=0 by using $\vec{e}_y = 0$ for x=0. By the continuities of $\vec{e}_y$ and $\vec{h}_z$ at x=d, we have

$$\sin(\vec{K}_c d).*\vec{B}./\vec{K}_c = -\exp(-\vec{\Theta} d).*\vec{D}./\vec{\Theta}, \tag{8.14a}$$

$$\cos(\vec{K}_c d).*\vec{B} = \exp(-\vec{\Theta} d).*\vec{D}. \tag{8.14b}$$

The formula (8.14) leads to

$$-d\vec{K}_c.*\cot(\vec{K}_c d) = d\vec{\Theta}. \tag{8.15a}$$

Another equation deduced from (8.2) is

$$\left(d\vec{K}_c\right)^2 + \left(d\vec{\Theta}\right)^2 = (\varepsilon_r - 1)(d\vec{K}_0)^2. \tag{8.15b}$$

The two equations can be solved as for TM modes

After determining the constant matrix $\vec{K}_c$ and $\vec{\Theta}$, the field expressions can be derived as

$$\vec{H}_z = T_h \exp(-j\vec{\Lambda}_z z).*\cos(\vec{K}_c x).*\vec{B}, \quad for \quad 0 \le x \le d, \tag{8.16a}$$

$$\vec{H}_z = T_h \exp(-j\vec{\Lambda}_z z).*\exp(-\vec{\Theta}(x-d)).*\cos(\vec{K}_c d).*\vec{B}, \quad for \quad d \le x < \infty, \tag{8.16b}$$

$$\vec{H}_x = jT_h\vec{\Lambda}_z.*\exp(-j\vec{\Lambda}_z z).*\sin(\vec{K}_c x).*\vec{B}./\vec{K}_c, \quad for \quad 0 \le x \le d, \tag{8.16c}$$

$$\vec{H}_x = jT_h\vec{\Lambda}_z.*\exp(-j\vec{\Lambda}_z z).*\exp(-\vec{\Theta}(x-d)).*\cos(\vec{K}_c d).*\vec{B}./\vec{\Theta}, for \ d \le x < \infty, \tag{8.16d}$$

$$\vec{E}_y = \frac{\mu_0}{d_0} T_e \delta \exp(-j\vec{\Lambda}_z z).*\sin(\vec{K}_c x).*\vec{B}./\vec{K}_c, \quad for \quad 0 \le x \le d, \tag{8.16e}$$

$$\vec{E}_y = -\frac{\mu_0}{d_0} T_e \delta \exp(-j\vec{\Lambda}_z z).*\exp(-\vec{\Theta}(x-d)).*\cos(\vec{K}_c d).*\vec{B}./\vec{\Theta}, for \ d \le x < \infty, \tag{8.16f}$$

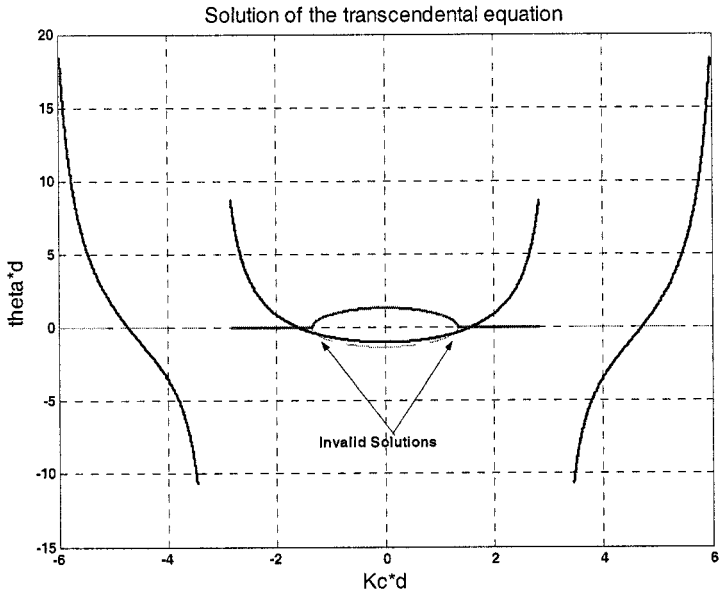

Figure 8.4 Graphical solution of the transcendental equation for the cutoff frequency of a TM mode with d=2 mm, i=N/2

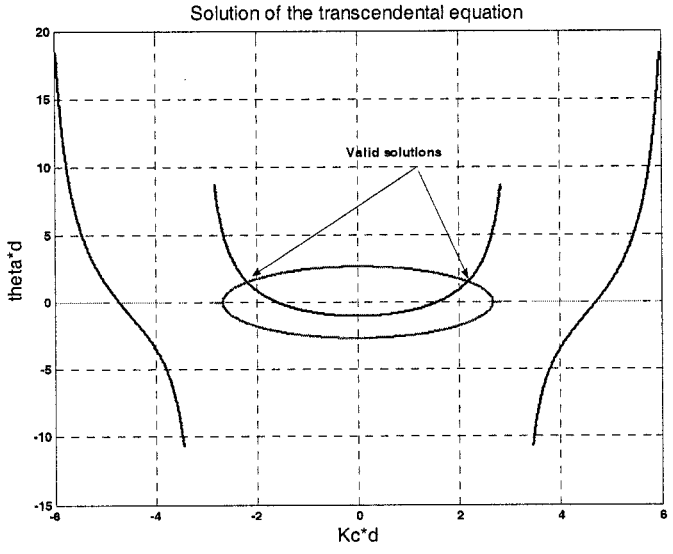

Figure 8.5 Graphical solution of the transcendental equation for the cutoff frequency of a TM mode with d=4 mm, i=N/2

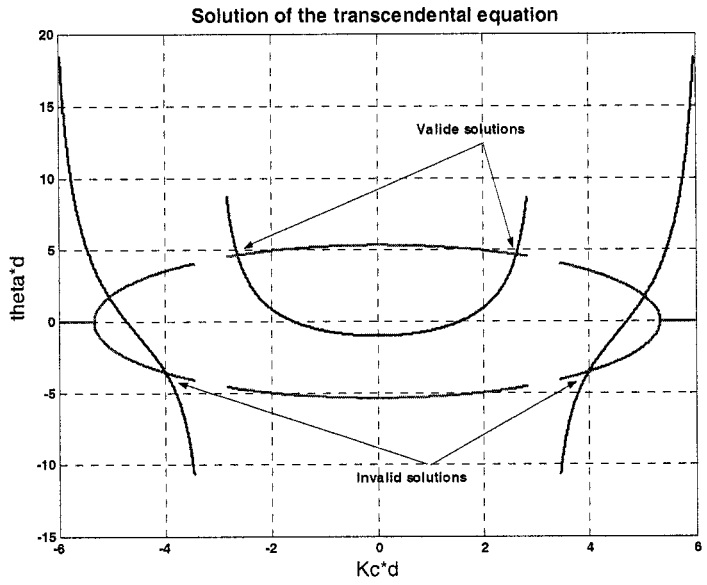

Figure 8.6 Graphical solution of the transcendental equation for the cutoff frequency of a TM mode with d=8 mm, i=N/2

Figures 8.4, 8.5 and 8.6 show the graphical solutions of the transcendental equation for the cutoff frequency of a TE surface wave mode with d=2mm, d=4mm and d=8mm at position i=N/2.

The curves show the surface wave propagation constants for the grounded dielectric slab with ε_r=2.55.

Conclusion

This thesis presents the theory of periodic sequence and its development. Through the applications of this theory to both field theory and circuit theory, the theory of periodic sequence presents the following advantages:

1. This theory can be applied to linear and nonlinear systems in electromagnetic engineering.
2. It can solve problems of both field theory and circuit theory.
3. The analytic solutions are given. We don't need iterations like in FDTD to calculate the solutions.
4. It yields less error. Because of analytic solutions, we need fewer steps to calculate. Hence the error is less and it can be controlled too.
5. This theory, as a method of numerical computation is effective, accurate and simple.
6. It can calculate very fast and is programmable.

BIBLIOGRAPHY

[1] A. Thom and C. J. Apelt, Field computations in engineering and physics, London: D.Van Nostrand, 1961.

[2] G. Mur, "Finite difference method for the solution of electromagnetic waveguide discontinuity problem," *IEEE Trans. Microwave Theory Tech.*,vol. MTT-22,pp. 54-57, Jan 1974.

[3] P. Silvester, "Finite element analysis of planar microwave networks," *IEEE Trans. Microwave Theory Tech.*, vol. MTT-21,pp. 104-108, Feb 1973.

[4] P. Dalay, "Hybrid-mode analysis of microstrip by finite element method," *IEEE Trans. Microwave Theory Tech.*, vol. MTT-19,pp. 19-25, Jan 1971.

[5] P. Silvester, *Finite elements for electrical Engineers*, Cambridge University Press, New York, 1983.

[6] S. Akhtarzad and P. B. Johns, "Three-dimensional transmission-line matrix computer analusis of microstrip resonators," *IEEE Trans. Microwave Theory Tech.*, vol. MTT-19,pp. 990-997, Dec 1975.

[7] W. J. R. Hoefer and A. Ros, "Fin line parameters calculated with the TLM-method," *IEEE MTT-S Ins. Microwave Symp. Dig.*,,pp. 341-343, Avr.-May 1979.

[8] W. C. Chew and J. A. Kong, "Resonance of axial-symmetric modes in microstrip disk resonators," *J. Math. Phys.*, vol. 21, pp. 582-591, mar. 1980.

[9] R. F. Harrington, *Field Computation by Moment Methods,* Macmillan, New York, 1968.

[10] D. S. Jones, *The theory of Electromagnetism,* Pergamon, New York, 1964.

[11] R. W. Jackson and D. M. Pozer, "Full-wave analysis of microstrip open-end and gap discontinuities," *IEEE Trans. Microwave Theory Tech.*, vol. MTT-33,pp. 1036-1042, Oct. 1985.

[12] Y. C. Shih and K. G. Gray, "Convergency of numerical solutions of step-type waveguide distontinuity problems by modal analysis," *IEEE MTT-S Ins. Microwave Symp. Dig.*,,pp. 233-235, May 1983.

[13] T. S. Chu, T. Itoh, and Y.-C. Shih, "Comparative study of mode-matching

formulations for microstrip discontinuity problems," *IEEE Trans. Microwave Theory Tech.,* vol. MTT-33,pp. 1018-1023, Oct. 1985.

[14] U. Schulz and R. Pregla, "A new technique for the analysis of the dispersion characteristics of planar waveguides and its application to microstrips with tuning septums," *Radi Sci.,* vol. 16, pp. 1173-1178, Nov.-Dec. 1981.

[15] S. B. Worm and R. Pregla, "Hybrid-mode analysis of arbitrarily shaped planar microwave structures by the method of lines," *IEEE Trans. Microwave Theory Tech.,* vol. MTT-33,pp. 1018-1023, Oct. 1985.

[16] O. A. Liskovets, "The method of line," *Review, Differ. Uravneniya,* vol. 1, pp. 1662- 1678, 1965.

[17] B. P. Demidowitsch et al., *numerical method of analysis* (in German), Chapter 5, VEB Wissenschaften, Berlin, 1969.

[18] S. G. Michlin and C. Smolizki, *Näherungsmethoden zur Lösung von differentialund integralgleichungen,* pp. 238-243, Teubner1980.

[19] T. Itoh, and R. Mittra, "Spectral-domain approach for calculating the dispersion characteristics of microstrip line," *IEEE Trans. Microwave Theory Tech.,*vol. MTT-21,pp. 496-499, July 1973.

[20] E. J. Denlinger, "A frequency dependent solution for microstrip transmission lines," *IEEE Trans. Microwave Theory Tech.,*vol. MTT-19,pp. 30-39, Jan. 1971.

[21] T. Itoh, "Spectral domain immittance approach for dispersion characteristics of generated printed transmission line," *IEEE Trans. Microwave Theory Tech.,*vol. MTT-28,pp. 733-736, July 1980.

[22] Yee, K. S., "Numerical solution of initial boundary value problems involving Maxwell's equations in isotropic media," *IEEE Trans. Antennas and propagations,* vol.14 ,pp. 302-307, 1973.

[23] Taflove, A., and M. E. Brodwin, "Numerical solution of steady-state electromagnetic scattering problems using the time-dependent Maxwell's equations," *IEEE Trans. Microwave Theory Tech.,*vol. MTT-23,pp. 623-630, July 1975.

[24] Taflove, A., and M. E. Brodwin, "Computation of thr electromagnetic fields and induced temperatures within a model of the microwave-irradiated human eyes," *IEEE Trans. Microwave Theory Tech.,*vol. MTT-23,pp. 888-896, July 191975.

[25] Holland, R., "Threde: a free-field EMP coupling and scattering code," *IEEE Trans. Nuclear Science*, vol. 24, 1977, pp. 2416-2421.

[26] Kunz, K. S., AND K. M. Yee, "A three-dimensional finite-difference solution of the external response of an aircraft to a complex transient EM environment I: The method and its implementation," *IEEE Trans. Electromagnetic Compatibility,* Vol. 20, 1978, pp. 328-333.

[27] Taflove, A., "Application of the finite-difference time-domain method to sinusoidal steady-state electromagnetic penetration problems," *IEEE Trans.* Electromagnetic Compatibility, Vol. 22, 1980, pp. 191-202.

[28] Itoh, T., *Numerical Techniques for Microwave and Millimeter-Wave Passive Structures*, New York: Wiley, 1989.

[29] Pozar, D. M., *Microwave Engineering, 2nd ed.*, New York: Wiley, 1998.

[30] Taflove, A., and Hagness, S. C., "*Computational Electrodynamics: The Finite-Difference Time-Domaine Method*', *2nd ed.,* Boston: Artech, 2000.

[31] Ortega, M. James, *Matrix Theory*, New York : Plenum, 1987.

APPENDIX A: POLARIZED WAVES

We will discuss polarized plane waves, as well as incident, reflection and propagation waves.

A.1 Linearly Polarized Waves

We call a field **a transformed field** if it is a field after an orthogonal transformation. Otherwise a field is called **an original field**. In a transformed electric field, an $\hat{x}$ linearly polarized wave with constant amplitude vector $\vec{e}_0$ traveling in the positive z-axis direction has the form

$$\vec{e} = \exp(-j\vec{\Lambda}_z z).*\vec{e}_0\hat{x}\,, \tag{A.1}$$

where $\vec{\Lambda}_z$ is a matrix. Going back to the original electric field, this linearly polarized wave in $\vec{E}$ field will have the form

$$\vec{E} = T_e \exp(-j\vec{\Lambda}_z z).*\vec{E}_0\hat{x}\,. \tag{A.2}$$

We shall discuss some of the properties of this linearly polarized wave.

A.2 Wave Shapes

Now we consider other excitation waves such as trianglular, square and impulse waves. If we choice $\vec{E}_0$ properly, we can obtain the following graphs. Although this corresponds to the choice of excitation, the components of $\vec{E}_0$ are only chosen from two values: 0 and 1. This is like a numeric signal input. We can obtain various forms of waves.

(a) Sinusoid

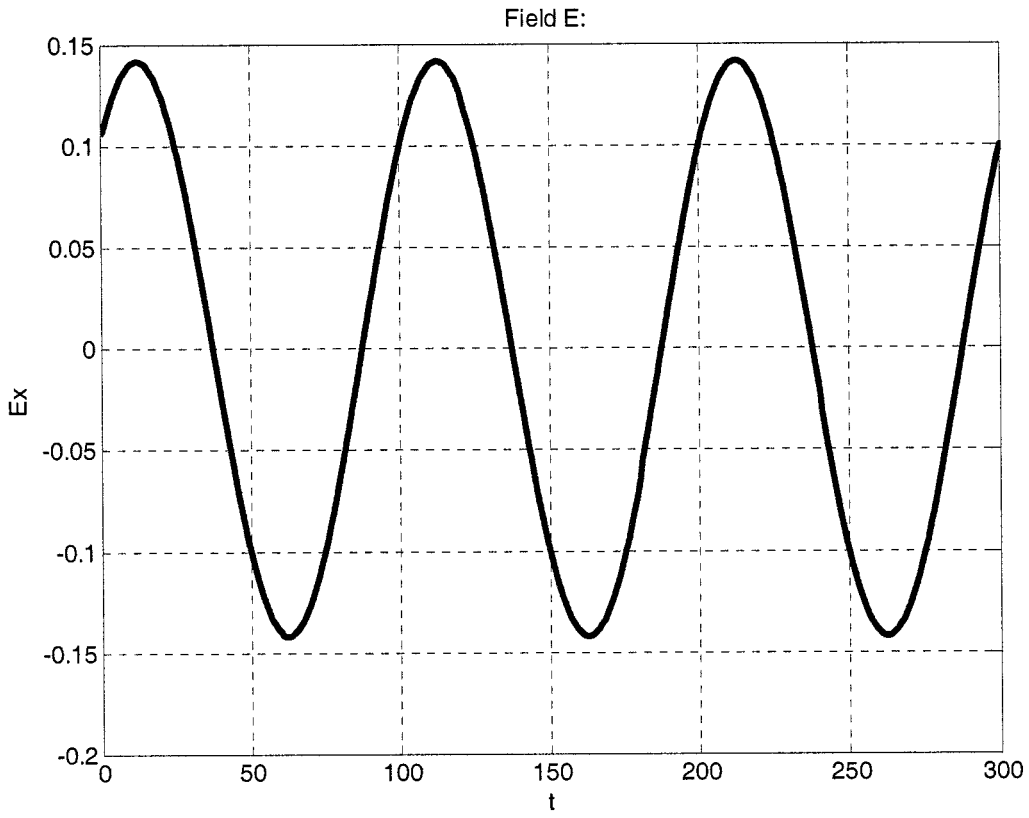

Figure A.1 Sinusoidal wave in E

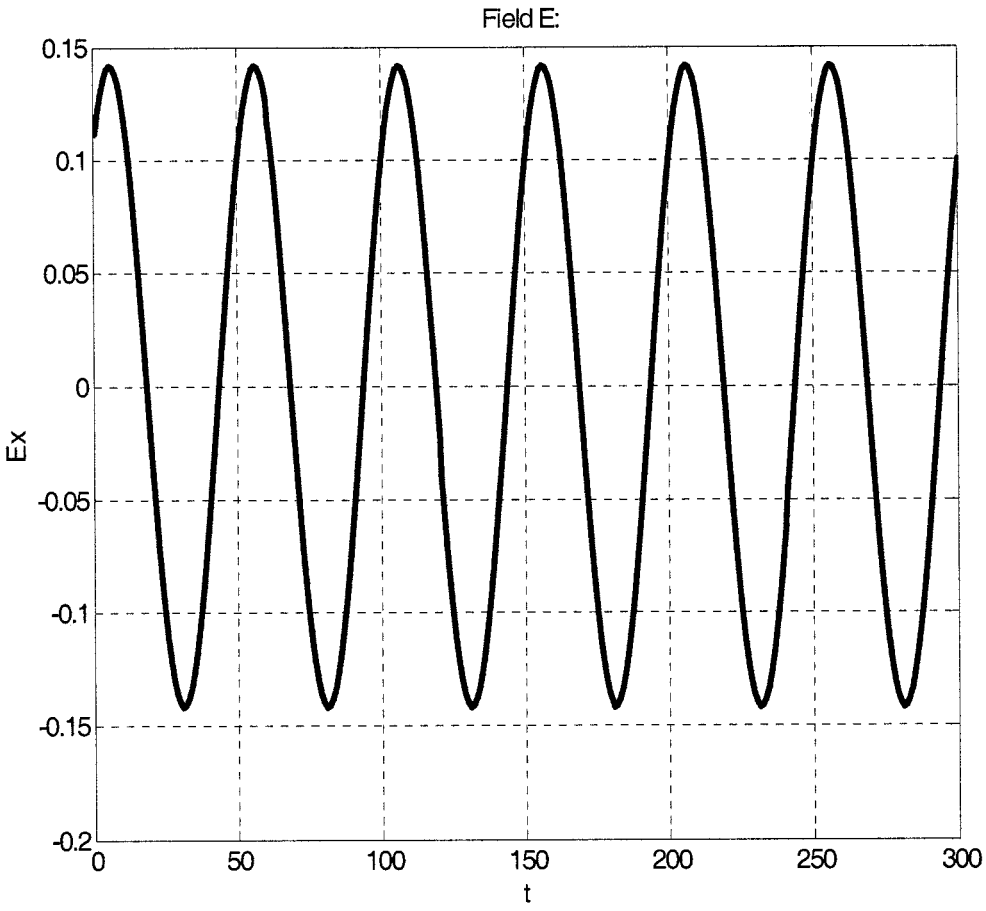

FigureA.2 Another sinusoidal wave in E

(b) Distorted sinusoid

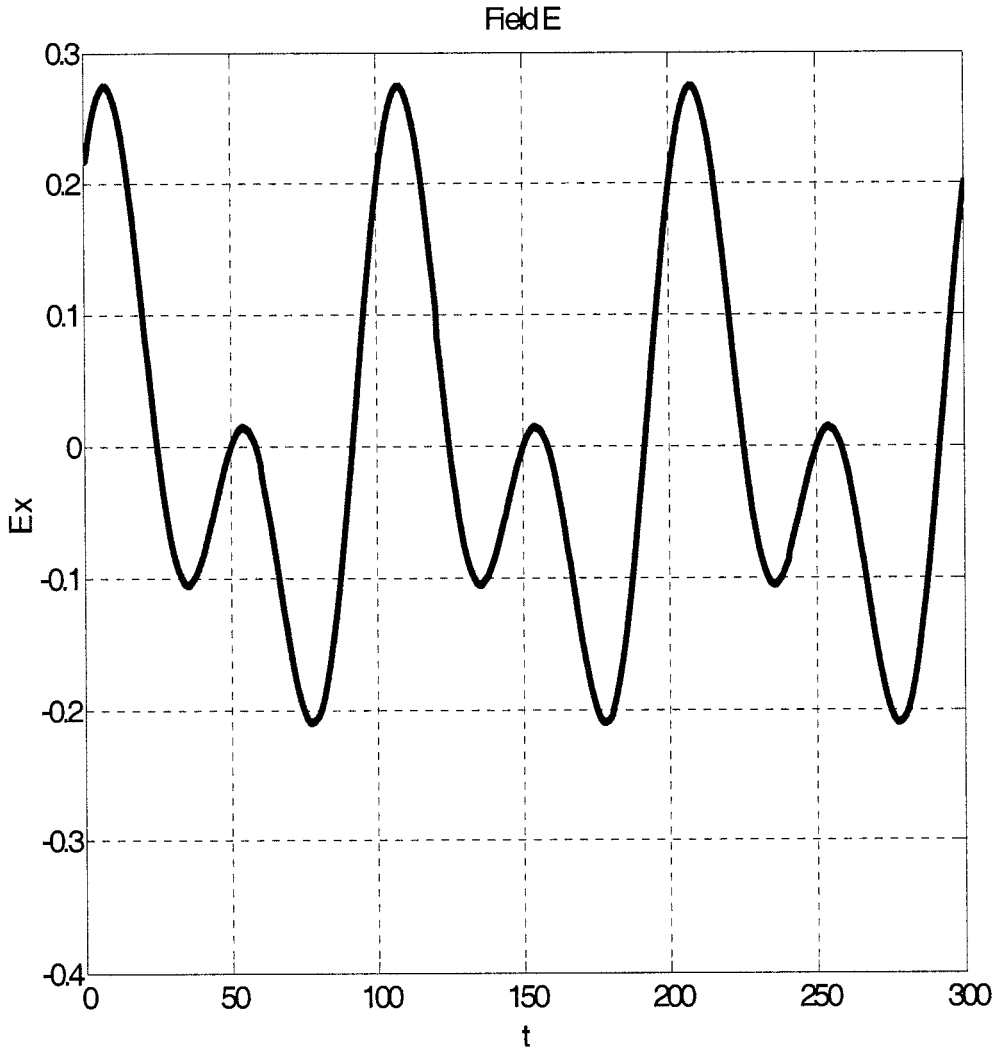

Figure A.3 Distorted sinusoid I in E

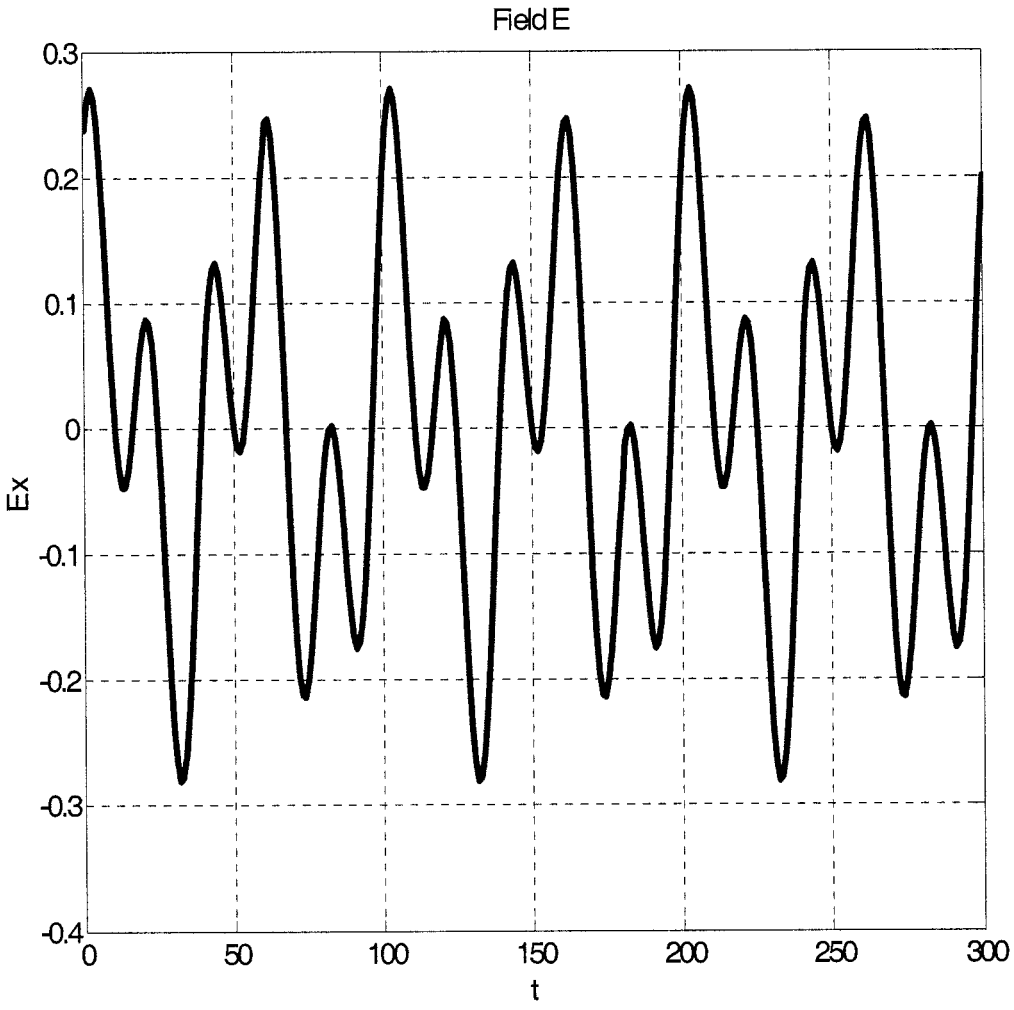

Figure A.4 Distorted sinusoid II in E

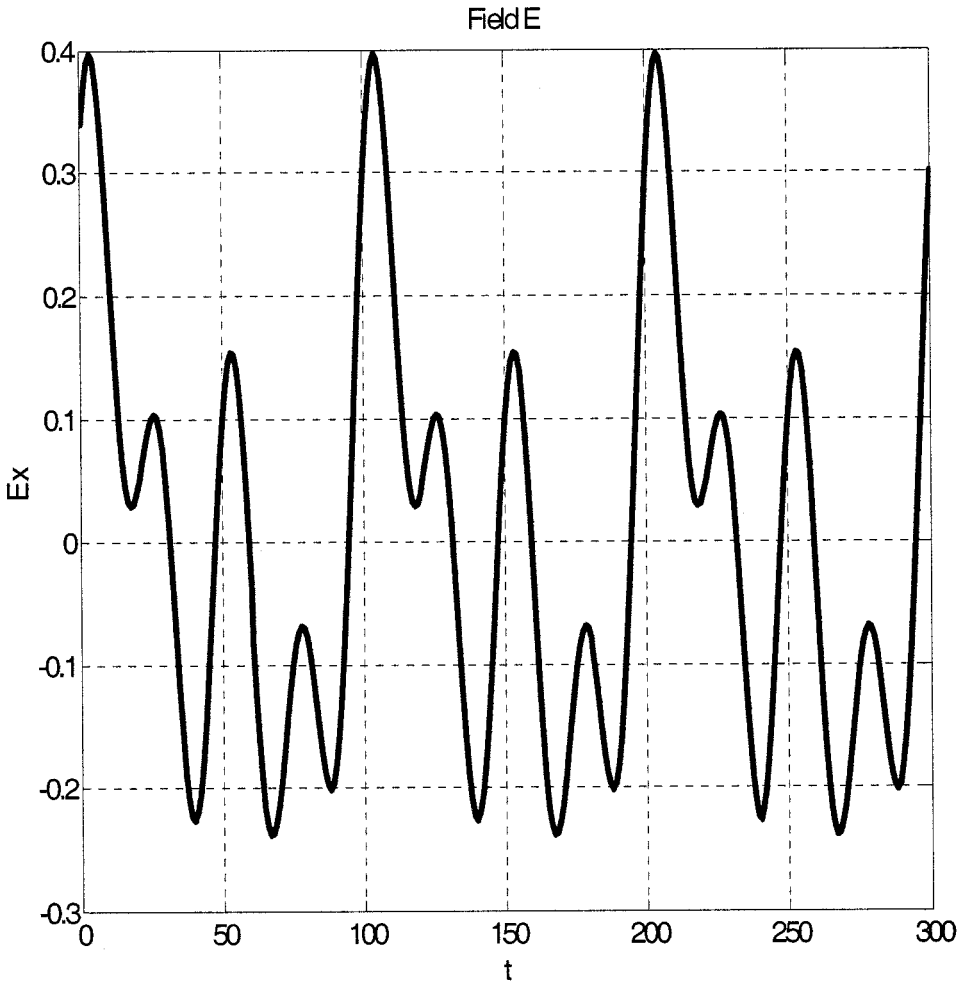

Figure A.5 Distorted sinusoid III in E

(c) Square wave

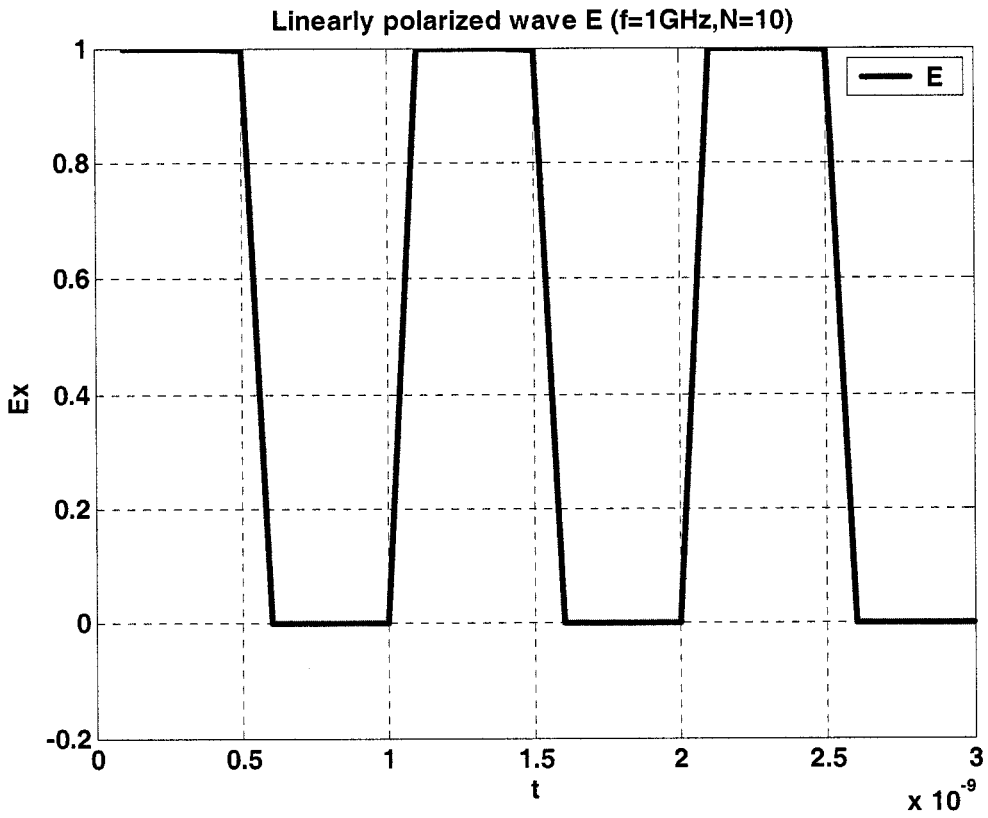

Figure A.6 Square wave in E (N=10, z=0.001).

(d) Trianglular wave

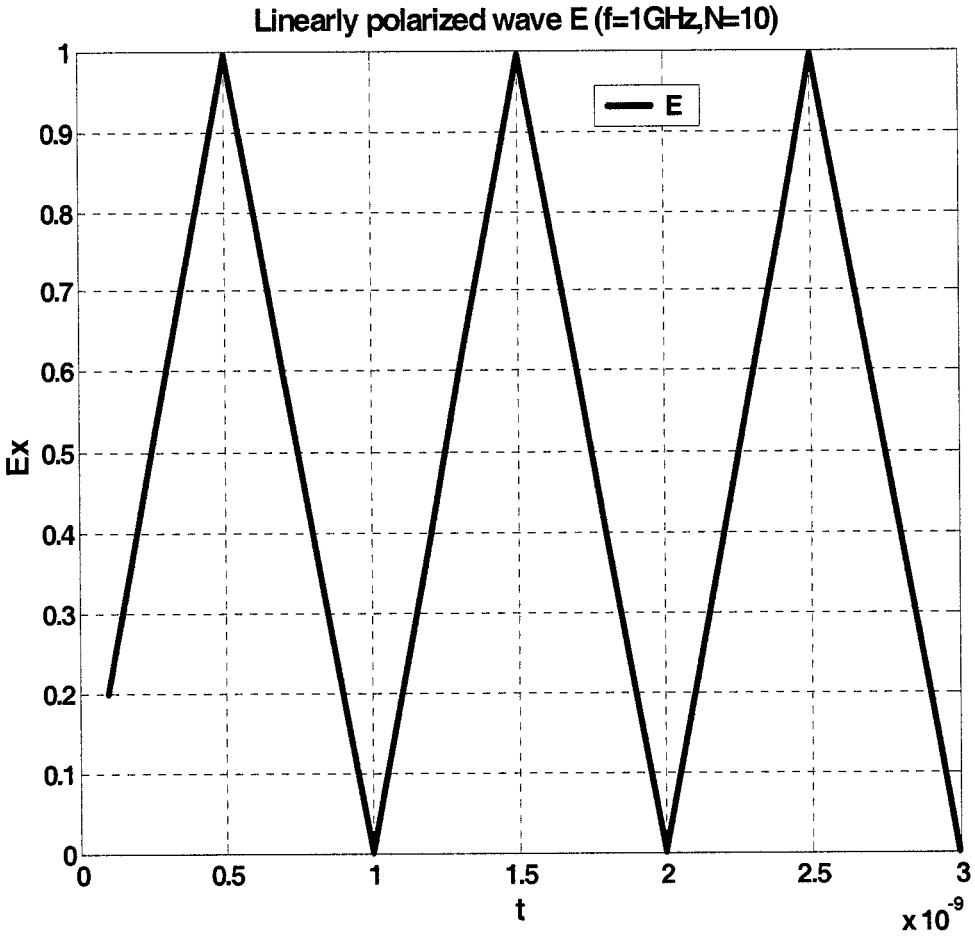

Figure A.7 Trianglular wave E (N=10, z=0.001)

A.3 Polarized Plane Waves

Now we consider an $\hat{x}$ and a $\hat{y}$ linearly polarized plane wave with amplitude vectors E_1 and E_2, which are traveling in the positive z-axis direction. The superposition of two waves can be written as

$$\vec{E} = T_e \exp(-j\vec{\Lambda}_z z).*(\vec{E}_1\hat{x} + \vec{E}_2\hat{y}). \tag{A.3}$$

Case I. $\vec{E}_1 \neq 0, \vec{E}_2 = 0$ (or $\vec{E}_2 \neq 0, \vec{E}_1 = 0$). It is a linearly polarized plane wave in $\hat{x}$ (or

$\hat{y}$) direction.

Case II. $\vec{E}_1.*\vec{E}_2 \neq 0$, and both $\vec{E}_1$ and $\vec{E}_2$ are real. We have a linearly polarized plane wave at the angle

$$\phi_i = \tan^{-1}\left(\vec{E}_2./\vec{E}_1\right)_i \tag{A.4}$$

Example A.1 Suppose that E_1=E_2, f=1GHz, N=100, Assume excitation is pulse at the origin. The polarized plane waves in Figure A.8 will be shown in graph Fig A. with $\phi_i = 45^\circ$ for all i.

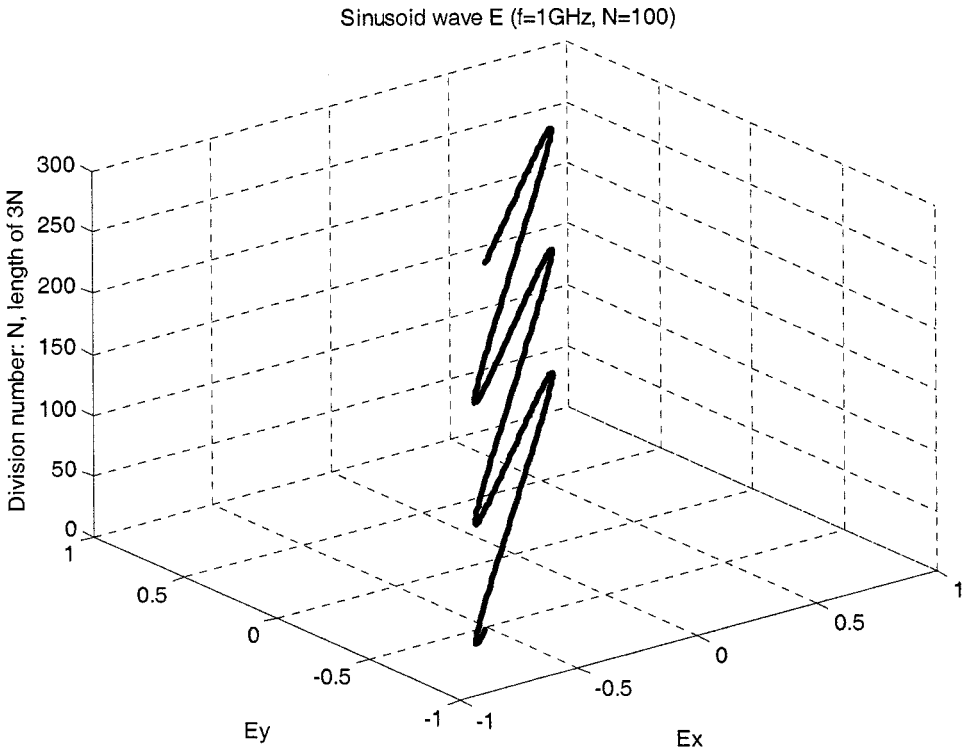

Figure A.8 Sinusoidal wave E with $\phi = 45^\circ$.

Case III. $\vec{E}_2 = j\vec{E}_1 = \vec{E}_0$, E_0 is real. We have

$$\vec{E} = T_e \exp(-j\vec{K}_z z).*\vec{E}_0(\hat{x} + j\hat{y}). \tag{A.5}$$

This wave is called **right hand circularly polarized wave** (or left hand circularly polarized wave if $\vec{E}_2 = -j\vec{E}_1 = \vec{E}_0$. It is plotted in Figure A.9. The incident wave in field

$\vec{e}$ is a pulse with f=1GHz, N=100 and z=0. We consider the time domain. The angle from the x-axis of the electric field vector at n is

$$\phi_i = \tan^{-1}\left(\vec{E}_2./\vec{E}_1\right)_i = \frac{nT}{N} \tag{A.6}$$

which shows that the polarization rotates at the uniform angular velocity ω .

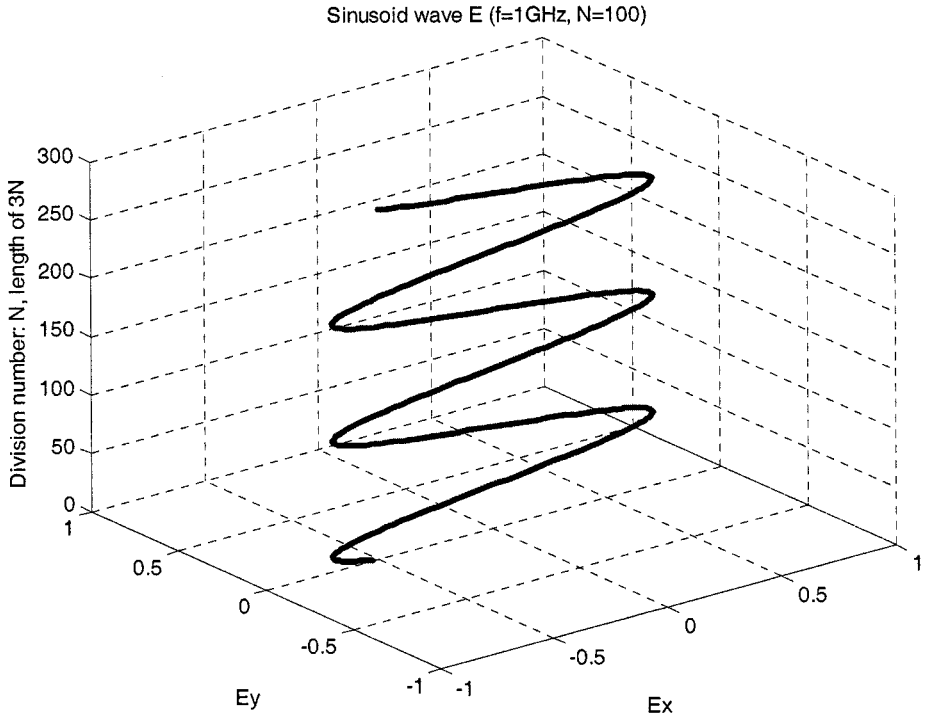

Figure A.9 Circularly polarized wave in E